ELECTROMAGNETIC WAVES IN STRATIFIED MEDIA

Being a thesis submitted for the degree of

Doctor of Philosophy, in the Faculty of Science,

of the University of London.

By

Heather Mary Liddell, B.Sc.
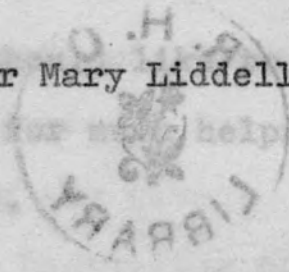
Department of Physics,

Royal Holloway College,

University of London

FEBRUARY 1966

ProQuest Number: 10096721

All rights reserved

INFORMATION TO ALL USERS
The quality of this reproduction is dependent upon the quality of the copy submitted.

In the unlikely event that the author did not send a complete manuscript
and there are missing pages, these will be noted. Also, if material had to be removed,
a note will indicate the deletion.

ProQuest 10096721

Published by ProQuest LLC(2016). Copyright of the Dissertation is held by the Author.

ProQuest LLC
789 East Eisenhower Parkway
P.O. Box 1346
Ann Arbor, MI 48106-1346

ACKNOWLEDGEMENTS

I wish to thank my supervisor, Professor O.S. Heavens, for suggesting the research topic and for his continued help and encouragement throughout the work.

Thanks are also due to Professor Tolansky for the use of facilities in the Physics department, Royal Holloway College; to Professor Buckingham and the staff of the University of London Institute of Computer Science for help with computations; and to Royal Holloway College for a research scholarship.

Finally, I should like to thank Dr. J.S. Seeley of Queen Mary College for much helpful discussion during the course of the work.

ABSTRACT

Some problems which arise in the analysis and design of multilayer filters are discussed in this thesis. The filters consist of sequences of parallel-sided media which reflect and transmit electromagnetic radiation. The cases considered are those appropriate to the optical region of the spectrum although the analysis is quite general.

In the optical region, the refractive index of a thin film is generally measured by the Abeles method, which entails determining the angle of incidence at which the film and the bare substrate have the same value of R_p. The presence of a small amount of absorption can produce errors in measurements of this kind. Two ways of estimating the magnitude of this error are given.

Considerable broadening of the reflectance band of a multilayer may be obtained by 'staggering' the layer thicknesses in such a way that they form either an arithmetic or geometric progression. Results are shown for fifteen, twenty-five and thirty-five layers. The presence of the narrow band transmission peaks exhibited by the symmetric filters is explained, and the advantages of the use of this type of filter as an interference filter are

discussed. A closed form expression for the matrix product of staggered layers is obtained for the case when the difference in thickness is small.

A 'least squares' method of filter design is introduced. This method may be used either to design a filter automatically if no initial design is available, or to 'refine' an existing design. The method is applied to the design of antireflection coatings, beam splitters, low- and high-pass filters and broad-band high reflectance coatings. In addition, one or two well-known filter designs are used to test the method.

CONTENTS

6

Page

Chapter III: Broad-band high-reflecting multilayers

3.1. Use of dielectric high reflecting films in interferometry ... 52

3.2. The 'classical' stack and previous work on broad-band reflecting filters ... 55

3.3. Reflectance characteristics of the staggered multilayers ... 62

3.4. Phase characteristics of the staggered multilayers ... 71

3.5. Closed form expression for staggered multilayers ... 79

Chapter IV: Review of design methods used in optical filter production

4.1. Basic methods of filter design ... 85

4.2. Design techniques for low-reflecting coatings ... 87

4.3. Use of equivalent index in thin film design ... 97

4.4. Application of circuit theory methods ... 102

4.5. The method of successive iterations ... 110

4.6. Automatic design methods ... 114

Chapter V: Least squares method of filter design

5.1. Discussion of design considerations ... 122

CHAPTER I. BASIC THEORY OF THE PROPAGATION OF LIGHT WAVES THROUGH THIN FILMS

§1.1. Introduction

In this thesis we shall consider some problems in the propagation of plane-polarised monochromatic light waves through thin dielectric films. This is one particular aspect of the subject of Electromagnetic waves in stratified media. We restrict ourselves to homogeneous, isotropic films. Mathematically, a 'thin' film is one whose thickness is of the order of the wavelength of light and whose extent is infinite compared to its thickness. The film is characterised by its refractive index, its absorption coefficient (if the film is absorbing) and its thickness. A combination of a number of thin films is sometimes called a 'multilayer'. The branch of optics which deals with the propagation of light waves through single films and multilayers is known as Thin Film Optics. Several books and reviews on the subject derive the basic formulae for thin film calculations. (See, for example, Baumeister, 1963; Berning, 1963; Heavens, 1955; Heavens, 1960; Vašíček, 1960; Weinstein, 1954.)

There are two distinct basic problems in thin film optics; the first is that of computing the spectral charac-

teristics of a multilayer in which the thicknesses and optical constants of the component films are known - this is a problem of _analysis_ and its solution is fairly straightforward. The second problem is vastly more complicated and consists of determining the optical constants and thicknesses of the component films in order that the multilayer will have specified spectral characteristics. This is the problem of _synthesis_. In practice, only a limited number of materials is available for use in optical filters, unlike the cases of electrical and microwave filters. The problem is therefore to design a multilayer, consisting of some or all of these available materials, which gives the best approximation to the required spectral curve.

In Chapter II, the effect of absorption on the measurement of refractive index of a single film by the Abelès method (Abelès, 1949) will be considered. This is an example of the method of analysis applied to a basically simple problem. The work in later chapters deals with transparent, non-dispersive media only, although the calculations could be generalised to include the effects of absorption and dispersion. The results in Chapter III for staggered broad-band reflecting multilayers were obtained by a method which could be considered as a combination of analysis and synthesis. The aim was to produce filters with a very wide reflection band, which specifies the

spectral characteristics to a certain extent. However, the results were obtained by changing the thicknesses of the films in the multilayer from those of a quarter-wave stack in a specific, partly intuitive, way and computing the spectral characteristics from the basic equations. Thus the method is mainly one of analysis. The general problem of Optical filter synthesis will be discussed in Chapter IV, which will also include a review of the current methods of design for optical filters. A 'least squares' method for filter design will be given in Chapter V and some of the results obtained from the method will be discussed. The final chapter, Chapter VI, will consist of an analysis of the results obtained in the previous chapters, and plans for future work based on the results reported in this thesis will be outlined. Some of the flow diagrams and Programs used in the computations will be included in the Appendix. Before starting on the original work to be presented in this thesis, the notation will be defined and some of the basic formulae to be used in the single film and multilayer calculations will be derived. These are mainly standard known results, except where otherwise indicated.

$$E_m = E_m^+ + E_m^-$$
$$H_m = \mu_m (E_m^+ - E_m^-)$$

§1.2. Notation

Several different methods have been used to evaluate the properties of a multilayer and thus several different notations have evolved as a result. The notation to be used here is similar to that used by Heavens (1955), following Abelès (1948a).

For the case of normal incidence on an isotropic medium it is unnecessary to show the direction of polarisation, so we can denote the electric and magnetic vectors of the positive-going wave in the mth layer by E_m^+, H_m^+ and those of the negative-going wave by E_m^-, H_m^-. The only case where non-normal incidence will be considered is the Abelès condition work (Chapter II) in which the light is polarised with the electric vector parallel the plane of incidence throughout, so no confusion need arise as we shall therefore need to use only the p-component of polarisation.

An alternative notation more generally used in multilayer theory is one in which the resulting equations are analogous to the equations for the electrical properties of transmission lines. E_m^-, E_m^+ are expressed in terms of the components of $\underline{E}$, $\underline{H}$, the electric and magnetic vectors by

$$E_m = E_m^+ + E_m^-$$
$$H_m = \mu_m (E_m^+ - E_m^-)$$

(1.2.1)

where $\mu_m = n_m/\cos\theta_m$ for the p-component of polarisation

and $\mu_m = n_m\cos\theta_m$ for the s-component of polarisation.

Clearly, $\mu_m = n_m$ for normal incidence.

n_m is the refractive index of, and θ_m is the angle of incidence in the mth layer.

The change of phase of the beam on traversing the mth layer is given by

$$\delta_m = 2\pi\sigma n_m d_m \cos\theta_m \qquad (1.2.2)$$

where σ is the wavenumber of the light and d_m is the geometrical thickness of the layer. The quantity $n_m d_m$ is called the 'optical thickness' of the layer. The index of the incident medium is n_o and the films are numbered sequentially to the substrate which has refractive index n_s (see Figure 1.1).

The equation of propagation of a wave entering an absorbing medium may be expressed in a similar form to that for a transparent medium if the refractive index, n, is replaced by a complex quantity $\underline{n} = n-iK$. K is a measure of the energy absorption; the attenuation of the amplitude of the wave in a path of one vacuum wavelength is $\exp(-2\pi K)$. The Fresnel coefficients for reflection and transmission are denoted by r_m and t_m respectively; for the case of a single absorbing film they are replaced by $l^{1/2}\exp(-\phi_{01})$ (0/1 interface), $m^{1/2}\exp(-\phi_{12})$ (1/2 interface).

n_o

E_o^+ θ_o E_o^-

n_1

E_1^+ θ_1 E_1^-

d_1

n_2

E_2^+ θ_2 E_2^-

d_2

n_m

E_m^+ θ_m E_m^-

d_m

n_N

E_N^+ θ_N E_N^-

E_{N+1}^+

d_N
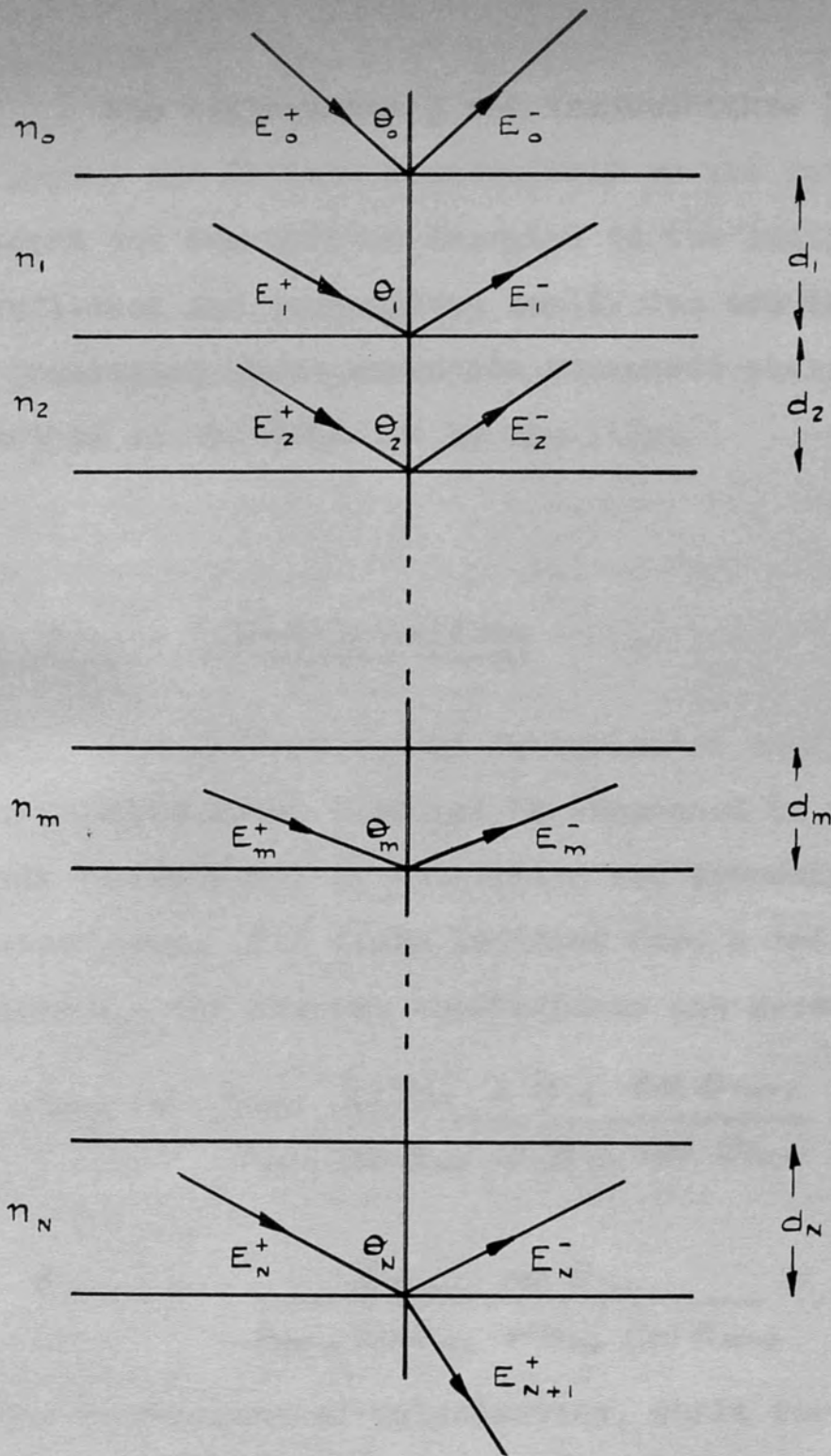
Fig. 1.1   Multilayer Notation

The reflectance $\underline{R}$ and transmittance $\underline{T}$ of a thin
film system are defined respectively as the ratio of the
reflected and transmitted energies to the incident energy.
The reflected and transmitted amplitudes are in general com-
plex quantities whose arguments represent phase changes on
reflection or transmission by the film.

§1.3. Single Film Calculations

The reflection and transmission coefficients for
a single transparent film may be expressed in terms of the
Fresnel coefficients of reflection and transmission for the
two interfaces. For light incident from a medium n_{m-1} onto
a medium n_m, the Fresnel coefficients are given by

$$r_{mp} = \frac{n_{m-1} \cos \theta_m - n_m \cos \theta_{m-1}}{n_{m-1} \cos \theta_m + n_m \cos \theta_{m-1}} \tag{1.3.1}$$

$$t_{mp} = \frac{2 n_{m-1} \cos \theta_{m-1}}{n_{m-1} \cos \theta_m + n_m \cos \theta_{m-1}} \tag{1.3.2}$$

for the p-component of polarisation, while for the s-
component we have

$$r_{ms} = \frac{n_{m-1} \cos \theta_{m-1} - n_m \cos \theta_m}{n_{m-1} \cos \theta_{m-1} + n_m \cos \theta_m} \tag{1.3.3}$$

$$t_{ms} = \frac{2 n_{m-1} \cos \theta_{m-1}}{n_{m-1} \cos \theta_{m-1} + n_m \cos \theta_m} \qquad (1.3.4)$$

Consider now a parallel beam of light of unit amplitude and wavenumber σ, incident on a plane, parallel-sided, homogeneous, isotropic film of thickness d_1, index n_1, bounded by semi-infinite, non-absorbing layers, indices n_0, n_2. The reflected and transmitted amplitudes are obtained by summing the multiply-reflected and transmitted beams. (See Figure 1.2.) We neglect the polarisation subscript as the results are valid for either direction of polarisation, provided r and t are given the appropriate values.

The reflected amplitude is given by

$$R = \frac{r_1 + r_2 e^{-2i\delta_1}}{1 + r_1 r_2 e^{-2i\delta_1}} \qquad (1.3.5)$$

where

$$\delta_1 = 2\pi \sigma n_1 d_1 \cos \theta_1 \qquad (1.3.6)$$

and the transmitted amplitude is given by

$$T = \frac{t_1 t_2 e^{-i\delta_1}}{1 + r_1 r_2 e^{-2i\delta_1}} \qquad (1.3.7)$$

The energies of the corresponding beams are $n_0 RR^*$, $n_2 TT^*$ respectively (* denotes complex conjugate) so the
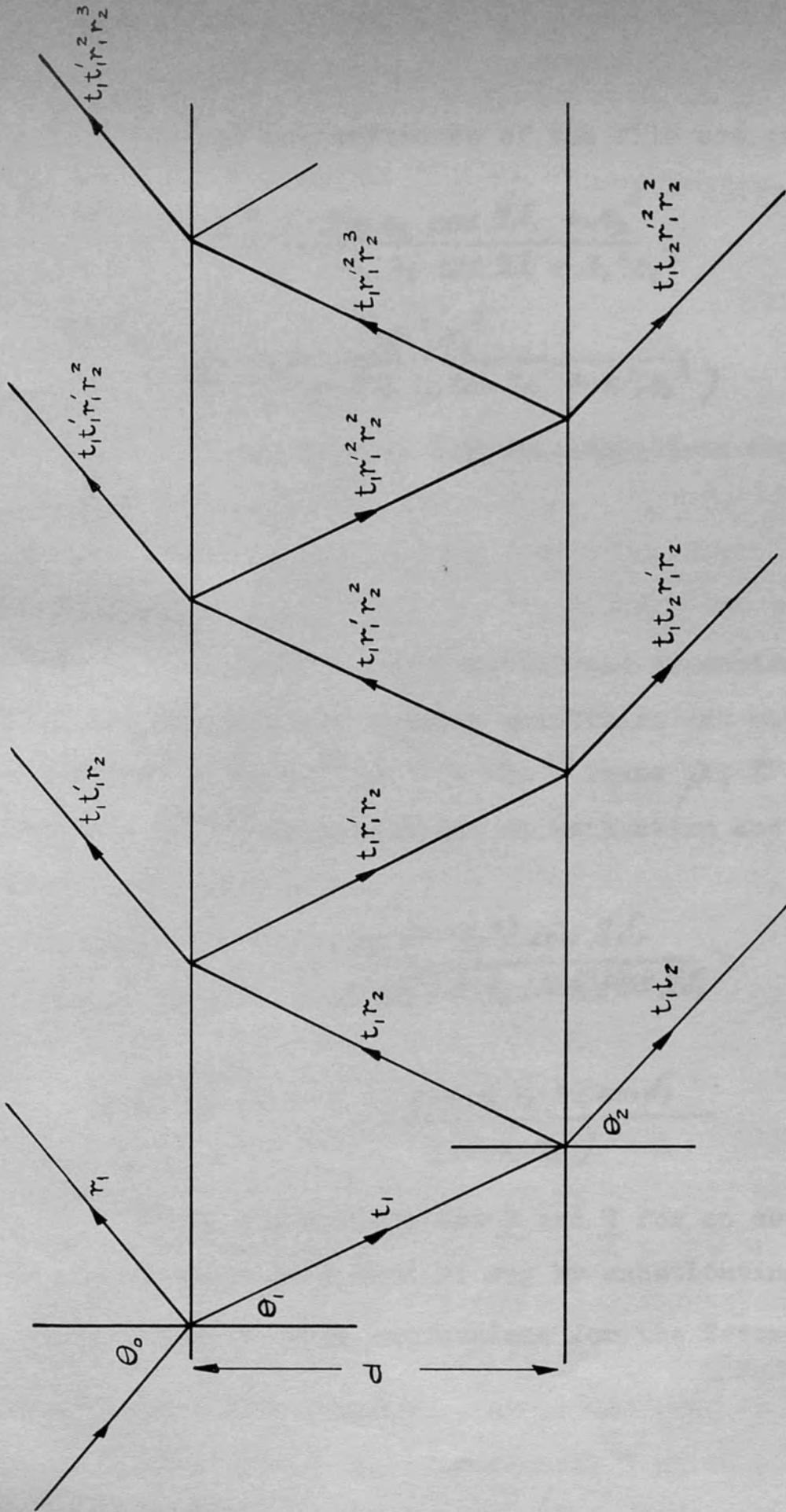
FIG. 1.2 SUMMATION OF MULTIPLE BEAMS FOR A SINGLE FILM

reflectance and transmittance of the film are given by

$$R = \frac{r_1{}^2 + 2r_1 r_2 \cos 2\delta_1 + r_2{}^2}{1 + 2r_1 r_2 \cos 2\delta_1 + r_1{}^2 r_2{}^2} \qquad (1.3.8)$$

$$T = \frac{n_2}{n_0} \frac{t_1{}^2 t_2{}^2}{(1 + 2r_1 r_2 \cos 2\delta_1 + r_1{}^2 r_2{}^2)} \qquad (1.3.9)$$

We know from energy considerations that for non-absorbing media

$$R + T = 1 \qquad (1.3.10)$$

The amplitude reflection and transmission coefficients, R and T are complex quantities and may therefore be written $R = \rho e^{i\psi}$ and $T = \tau e^{i\delta}$ where ρ, τ are real. Then ψ, δ the phase changes on reflection and transmission are given by

$$\tan \psi = \frac{- r_2 (1 - r_1{}^2) \sin 2\delta_1}{r_1 (1 + r_2{}^2) + r_2 (1 + r_1{}^2) \cos 2\delta_1} \qquad (1.3.11)$$

$$\tan \delta = \frac{-(1 - r_1 r_2) \tan \delta_1}{(1 + r_1 r_2)} \qquad (1.3.12)$$

The expressions for R and T for an absorbing film may be obtained in a similar way by substituting the corresponding complex expressions for the Fresnel coeffi-

cients. The latter are obtained by putting $\underline{n}$ instead of n
in equations (1.3.1) to (1.3.4). In this case, Snell's law
becomes

$$\sin \psi_1 = \frac{n_0 \sin \theta_0}{n_1 - i K_1}$$

(1.3.13)

so that ψ_1 is a complex quantity, not an angle, except for
the case of normal incidence, $\theta_0 = \psi_1 = 0$. A discussion
of refraction in an absorbing medium is given in Ditchburn,
1963, p.590. The expressions for $\underline{R}$ and $\underline{T}$ are rather cumber-
some, so will not be given explicitly here. (For explicit
expressions, see Born and Wolf, 1959.) The expression for
reflectance for the p-component of polarisation will be
given in Chapter II.

§1.4. Multilayer Theory

Several methods have been used to compute the
reflectance and phase change of a system of thin films.
Crook (1948) extended the method of multiple summation,
which was outlined above for a single film, to two layers
and indicated the procedure for a further extension to N
layers. However, this method quickly becomes very complica-
ted. Rouard (1937) and Vasicek (1950) used the fact that
since a single film may be represented by an effective

reflection coefficient and phase change, so also may a thin film system be represented by an effective single surface. They perform the calculations using a step-wise procedure. Rouard's method is slightly more tractable than that of Vašiček; Rouard starts with the layer next to the substrate and works to the top of the system whereas Vašiček starts with the top layer and moves downwards to the substrate.

The most convenient method for computation both by hand and by digital computer is the matrix method (see Heavens, 1960). Application of the boundary conditions to the equations of wave propagation at the interface between the (m-1)th and mth layers yields the following relationship between $E_m^{\pm}$, $E_{m-1}^{\pm}$:

$$E_{m-1}^{+} = \frac{1}{t_m}\left[E_m^{+} e^{i\delta_m} + r_m E_m^{-} e^{-i\delta_m}\right]$$

$$E_{m-1}^{-} = \frac{1}{t_m}\left[r_m E_m^{+} e^{i\delta_m} + E_m^{-} e^{-i\delta_m}\right]$$

(1.4.1)

An alternative recurrence relation in terms of the components of $\underline{E}$, and $\underline{H}$ is obtained from equations (1.2.1), giving

$$\begin{pmatrix} E_{m-1} \\ H_{m-1} \end{pmatrix} = \begin{pmatrix} \cos\delta_m & \frac{i}{\mu_m}\sin\delta_m \\ i\mu_m\sin\delta_m & \cos\delta_m \end{pmatrix}\begin{pmatrix} E_m \\ H_m \end{pmatrix}$$

(1.4.2)

so that for an N-layer combination

$$\begin{pmatrix} E_0 \\ H_0 \end{pmatrix} = \prod_{m=1}^{N} M_m \begin{pmatrix} E_N \\ H_N \end{pmatrix} \qquad (1.4.3)$$

where

$$M_m = \begin{pmatrix} \cos \delta_m & \dfrac{i}{\mu_m} \sin \delta_m \\ i \mu_m \sin \delta_m & \cos \delta_m \end{pmatrix} \qquad (1.4.4)$$

Applying boundary conditions to the substrate surface, remembering the negative-going wave in the substrate vanishes, it can be shown

$$\begin{pmatrix} E_N \\ H_N \end{pmatrix} = \begin{pmatrix} 1 \\ \mu_{sub} \end{pmatrix} E_{sub}^{+} \qquad (1.4.5)$$

The reflectance and phase change of the multi-layer are then given by

$$R = \left| \frac{\mu_0 E_0 - H_0}{\mu_0 E_0 + H_0} \right|^2 \qquad (1.4.6)$$

$$\psi = \arg \left(\frac{\mu_0 E_0 - H_0}{\mu_0 E_0 + H_0} \right) \qquad (1.4.7)$$

There are two main advantages of using the formulation given by (1.4.3) rather than that of (1.4.1). The first is that in the former case, each matrix contains

quantities characteristic of one layer only, whereas in the (1.4.7) formulation indices of two layers are involved. This is particularly important if it is desired to change the characteristics of one layer of the multilayer during the computations. (See, for example, Baumeister, 1962). The second advantage is that the matrices M_m have unity determinant. Not only does this provide a useful numerical check at any stage but it also enables simple closed formulae for 'periodic' multilayers to be obtained (Mielenz, 1959).

A 'periodic' multilayer is one in which the same sequence of films is repeated twice or more. According to Herpin (1947a), any sequence of films may be represented by a fictitious bi-layer $M_a M_b$. Then if this sequence occurs q times

$$\begin{pmatrix} E_o \\ H_o \end{pmatrix} = \left(M_a M_b \right)^q \begin{pmatrix} 1 \\ \mu_{sub} \end{pmatrix} E_{sub}^+ \qquad (1.4.8)$$

Sometimes, one considers a 'periodic symmetrical' multilayer which is of the form

$$\begin{pmatrix} E_o \\ H_o \end{pmatrix} = \left(M_a M_b \right)^q M_a \begin{pmatrix} 1 \\ \mu_{sub} \end{pmatrix} E_{sub}^+ \qquad (1.4.9)$$

In both cases the basic matrix is represented by

$$\left(M_a M_b \right) = \begin{pmatrix} a_{11} & a_{12} \\ a_{21} & a_{22} \end{pmatrix} \qquad (1.4.10)$$

Herpin (1947b) showed that the product $(M_a M_b)^q$ may be
expressed in terms of Lucas polynomials and Abelès (1948b)
observed that these may be reduced to Tschebyscheff poly-
nomials when the basic matrix is of unity determinant.
Writing

$$X = a_{11} + a_{22} \tag{1.4.11}$$

$$\left(M_a M_b \right)^q = S_{q-1}(X)\left(M_a M_b \right) - S_{q-2}(X)\left(I \right) \tag{1.4.12}$$

where $\left(I \right)$ is the unit matrix. The Tschebyscheff polynomials
$S_q(X)$ are defined by

$$S_q(X) = X S_{q-1}(X) - S_{q-2}(X) \tag{1.4.13}$$

where

$$S_0(X) = 1 \quad , \quad S_1(X) = X$$

or, alternatively,

$$S_q(X) = \frac{\sin(q+1)\textcircled{H}}{\sin \textcircled{H}} \quad , \quad X = 2\cos\textcircled{H}, \quad |X| < 2$$

$$\tag{1.4.14}$$

$$S_q(X) = \frac{\sinh(q+1)\overline{\Phi}}{\sinh \overline{\Phi}} \quad , \quad X = 2\cosh \overline{\Phi}, \quad |X| > 2$$

This method is particularly useful for computing the properties of quarter wave stacks. A quarter wave stack consists of alternate high- and low-index quarter wave layers $(\frac{\lambda_0}{4} = \frac{1}{4}\frac{1}{\sigma_0})$. In this case M_a, M_b represent individual layers and hence, if the films are non absorbing, the Tschebyscheff polynomials will have real arguments. This greatly simplifies the calculations. Thus, for normal incidence on a quarter wave stack, we have

$$\mu_a = n_H \, , \quad \mu_b = n_L$$

and

$$\delta_a = \delta_b = \beta = \frac{\pi}{2}\frac{\lambda_0}{\lambda} = \frac{\pi}{2}\frac{\sigma}{\sigma_0} \qquad (1.4.15)$$

Thus

$$X = 2 - \frac{(n_H + n_L)^2}{n_H \, n_L} \sin^2\beta \qquad (1.4.16)$$

An example of a numerical calculation performed using this method will be given in the Appendix.

§1.5. The concept of 'Equivalent' index

According to Herpin's theorem, any multilayer is equivalent, at one wavelength, to a two film combination. Each film in this equivalent bi-layer may be represented by matrices of the type M_m. Thus, four equations are obtained,

from which the two equivalent indices and the two thick-
nesses of the films in the bi-layer can be determined.
However, the matrices are unitary so in fact there are only
three independent parameters. For symmetric multilayers,
Epstein (1952) has shown that the 'Herpin equivalent' is a
single film characterised by an equivalent index N and an
equivalent thickness γ . He shows further how this kind
of analysis may be used in the design of optical filters,
particularly in Antireflection coatings. The use of these
symmetrical thin film combinations has also been studied by
Weinstein (1954) and Berning (1962). These applications to
filter design will be discussed more fully in Chapter IV.

Returning to the general case where there are
three independent parameters, it is clear that one of the
four parameters of the equivalent bi-layer may be chosen
arbitarily. Epstein suggests that one of the indices is
chosen to be that of its neighbouring surrounding medium,
so that the final matrix product for the mutlilayer may be
written

$$M = \begin{pmatrix} A & iB \\ iC & D \end{pmatrix} = \begin{pmatrix} \cos\alpha & \dfrac{i}{N'}\sin\alpha \\ iN'\sin\alpha & \cos\alpha \end{pmatrix} \begin{pmatrix} \cos\beta & \dfrac{i}{\eta_{sub}}\sin\beta \\ i\eta_{sub}\sin\beta & \cos\beta \end{pmatrix}$$

$$(1.5.1)$$

where N' is the equivalent index of the first layer and α , β

are the equivalent phase thicknesses. We have extended the
analysis to include this general case and evolved fairly
simple expressions for N', α, β in terms of the final
matrix product. These expressions are useful for numerical
computations of equivalent index and thickness. Writing
$x = \cos \alpha$, $y = \cos \beta$ for simplicity, we obtain from
(1.5.1).

$$A = xy - \frac{n_{sub}}{N'}(1-x^2)^{\frac{1}{2}}(1-y^2)^{\frac{1}{2}} \tag{1.5.2}$$

$$B = \frac{1}{n_{sub}}(1-y^2)^{\frac{1}{2}}x + \frac{1}{N'}y(1-x^2)^{\frac{1}{2}} \tag{1.5.3}$$

$$C = n_{sub}x(1-y^2)^{\frac{1}{2}} + N'y(1-x^2)^{\frac{1}{2}} \tag{1.5.4}$$

Substituting from (1.5.2) into (1.5.3) and (1.5.4)

$$n_{sub}^2 N'^2 B^2 = N'^2 x^2 + n_{sub}^2 y^2 - n_{sub}^2 x^2 y^2 + x^2 y^2 N'^2 - 2xy N'^2 A \tag{1.5.5}$$

$$C = n_{sub}^2 x^2 - n_{sub}^2 x^2 y^2 + N'^2 y^2 + x^2 y^2 N'^2 - 2xy N'^2 A \tag{1.5.6}$$

and, squaring (1.5.2)

$$n_{sub}^2 (1-x^2)(1-y^2) = N'^2 (x^2 y^2 - 2Axy + A^2) \tag{1.5.7}$$

Subtracting (1.5.7) from (1.5.5) and (1.5.6) in turn, we

obtain

$$x^2 = \frac{N'^2 (n_{sub}^2 B^2 + A^2) - n_{sub}^2}{(N'^2 - n_{sub}^2)} \tag{1.5.8}$$

$$y^2 = \frac{c^2 - n_{sub}^2 + A^2 N'^2}{(N'^2 - n_{sub}^2)} \tag{1.5.9}$$

From (1.5.4) and (1.5.3) we have

$$n_{sub}^2 (N'^2 B - c)^2 = x^2 (1 - y^2)(N'^2 - n_{sub}^2)^2 \tag{1.5.10}$$

and, using (1.5.9) and (1.5.10)

$$N'^2 = \frac{n_{sub}^2 (1 - Bc)^2 - n_{sub}^2 A^2 + A^2 c^2}{A^2 (1 - B^2 n_{sub}^2 - A^2)} \tag{1.5.11}$$

However, since M is unitary, $AD + BC = 1$ so (1.5.11) becomes

$$N'^2 = \frac{n_{sub}^2 (B^2 - 1) + c^2}{(1 - B^2 n_{sub}^2 - A^2)} \tag{1.5.12}$$

Finally, α, β may be found by substituting this value of N'^2 in (1.5.8), (1.5.9). For a symmetrical combination $A^2 = D^2 = 1 - BC$, so we obtain

$$\beta = 0, \quad \cos \alpha = A, \quad N'^2 = +\frac{c}{B} \tag{1.5.13}$$

which agree with equations (4) and (5) in Epstein's paper.

§1.6. Graphical methods

When the Fresnel coefficients for a single film are small, we can approximate the denominator of (1.3.8) by unity, so the reflectance is given by (Heavens 1955):

$$\underline{R} \, approx. = r_1^2 + 2 r_1 r_2 \cos 2\delta_1 + r_2^2 \qquad (1.6.1)$$

Physically, this means we are neglecting multiple reflections and considering only "two beam interference" in which the amplitudes of the beams are given by the Fresnel reflection coefficients r_1, r_2 with a phase difference δ, which is, of course, dependent on the film thickness (see Figure 1.3(a)). The resultant amplitude R is given by the vector sum of r_1 and r_2 (see Figure 1.3(b))

$$R = r_1 + r_2 \, exp \, (-2i\delta_1) \qquad (1.6.2)$$

For two films, approximating in the same manner as above

$$R = r_1 + r_2 \, exp \, (-2i\delta_1) + r_3 \, exp \, [-2i(\delta_1+\delta_2)] \qquad (1.6.3)$$

and again R is determined by the vector sum of the coefficients. This can be extended to include any number of films, provided the reflection coefficients r_1, r_2, ...r_{N+1} are small compared with unity. Although this latter condition severely limits the range of application of this method, there are many cases of practical interest, espe-
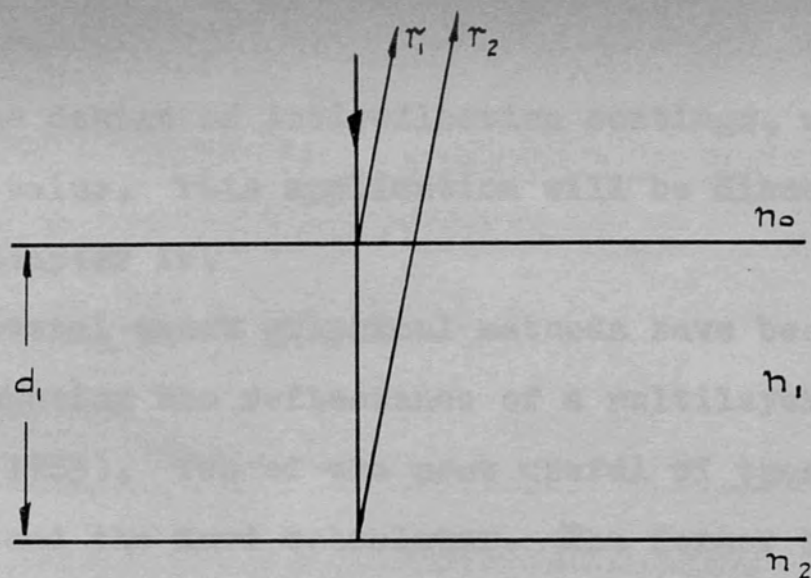
(a) REFLECTIONS AT A SINGLE FILM.
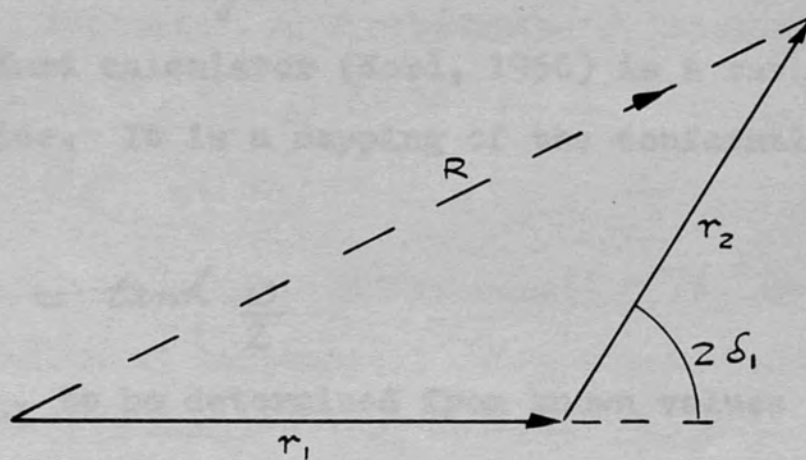
(b) VECTOR ADDITION OF AMPLITUDE FOR A SINGLE FILM.

FIG. 1.3. GRAPHICAL METHOD FOR A SINGLE FILM

cially in the design of Antireflection coatings, where it is of great value. This application will be discussed further in Chapter IV.

Several exact graphical methods have been developed for computing the reflectance of a multilayer (see Baumeister, 1963). Two of the most useful of these are the Smith chart and the Kard calculator. The former has been widely used in Electrical transmission line theory (details of its use are given in Potter and Fich, 1963) and makes use of the continuity of 'Optical Admittance' across any interface. The optical admittance is defined by

$$Y = \frac{H \text{ tangential}}{E \text{ tangential}} \qquad (1.6.4)$$

The Kard calculator (Kard, 1956) is a rather more convenient device. It is a mapping of the conformal transformation

$$Z = \tanh \frac{\omega}{2} \qquad (1.6.5)$$

and enables R_{m+1} to be determined from known values of r_{m+1}, R_m, δ_m.

CHAPTER II. INFLUENCE OF ABSORPTION ON MEASUREMENT OF THE REFRACTIVE INDEX OF FILMS BY THE ABELES METHOD

§2.1. Theory of the Abeles method for measurement of refractive index of transparent films

One of the simplest yet most reliable methods for measuring the refractive index of thin transparent films is that introduced by Abeles (1949). This method makes use of the fact that for light polarised with the electric vector parallel to the plane of incidence, the reflectance of a film, index n_1, deposited on a substrate of index n_2 at an angle of incidence $\theta_o = \theta_A$, given by

$$\tan \theta_A = \frac{n_1}{n_o} \tag{2.1.1}$$

is equal to that of the uncoated substrate. (n_o is the index of the medium of incidence.) This relationship is easily proven. From Snell's law, we have

$$n_1 \sin \theta_1 = n_o \sin \theta_o \tag{2.1.2}$$

For $\theta_o = \theta_A$, we obtain from (2.1.1)

$$\theta_o + \theta_1 = \frac{\pi}{2} \tag{2.1.3}$$

Using (2.1.2) equation (1.3.1) may be written

$$r_{mp} = \frac{\tan(\theta_m - \theta_{m-1})}{\tan(\theta_m + \theta_{m-1})} \qquad (2.1.4)$$

so that

$$R_{sub} = \frac{\tan^2(\theta_2 - \theta_0)}{\tan^2(\theta_2 + \theta_0)} \qquad (2.1.5)$$

$$r_1 = 0 \qquad (2.1.6)$$

$$r_2 = \frac{\tan(\theta_2 - \theta_1)}{\tan(\theta_2 + \theta_1)} \qquad (2.1.7)$$

Hence, from (2.1.3)

$$r_2 = \frac{\tan(\theta_2 - \theta_0)}{\tan(\theta_2 + \theta_0)} \qquad (2.1.8)$$

The reflectance of the film is given by

$$R_f = \frac{r_1^2 + 2r_1 r_2 \cos 2\delta + r_2^2}{1 + 2r_1 r_2 \cos 2\delta + r_1^2 r_2^2}$$

so for $\theta_0 = \theta_A$

$$R_f = r_2^2 = \frac{\tan^2(\theta_2 - \theta_0)}{\tan^2(\theta_2 + \theta_0)} \qquad (2.1.9)$$

which is the value of R_{sub}.

However, the value θ_A is not the only value of θ_0 for which the reflectance of the uncoated substrate

and the film on the substrate are equal. The condition for
equal reflectivity was obtained by Catalan (1964) as

$$(\mu_2 - \mu_0)^2 \left[\frac{\mu_0 \mu_2}{\mu_1} + \mu_1\right]^2 \sin^2\delta = (\mu_2 + \mu_0)^2 \left[\frac{\mu_0 \mu_2}{\mu_1} - \mu_1\right]^2 \sin^2\delta$$

(2.1.10)

The first solution given by this equation is

$$\mu_0 = \mu_1$$

(2.1.11)

For the s-component of polarisation, one obtains the
trivial solution that the index of the film is equal to that
of the incident medium; i.e. there is no film present. For
the p-component, an angle of incidence α_0 may be found to
satisfy (2.1.11), given by

$$\tan \alpha_0 = \frac{n_1}{n_0}$$

(2.1.12)

This means that α_0 is the Abelès angle. Another solution
is given by

$$\mu_2 = \mu_1$$

(2.1.13)

which again gives a trivial solution $n_2 = n_1$ for the s-
component of polarisation, but for the p-component the angle
of incidence β_0 for equal reflection is given by

$$\tan \beta_0 = \frac{n_2 n_1}{[n_0^2(n_2^2 + n_1^2) - n_2^2 n_1^2]^{\frac{1}{2}}}$$

(2.1.14)

However, in the usual case when the incident medium is air,
index 1.0, for β_0 to be real we must have

$$(n_2^2 - 1)(n_1^2 - 1) < 1 \qquad (2.1.15)$$

For a glass substrate, $n_2 = 1.50$, say, and condition (2.1.15) requires the index n_1 to be less than 1.32, so that $\beta_o > 80°$. These rather impractical values have led to this solution being neglected in most literature on the subject. A third solution of (2.1.10) is given by

$$\sin \delta = 0 \qquad (2.1.16)$$

which means $\delta = \frac{k\pi}{2}$. This is in fact the well-known result that for an optical path difference of an integral number of half-wavelengths the optical properties of the film are precisely those of the substrate (Heavens, 1964). This is true for both states of polarisation.

A word about the nomenclature should perhaps be mentioned here. In much of the literature on the subject, the term 'Brewster angle' is used for θ_A. However, Catalan (1964) points out that as the p-component of polarisation does not actually vanish, this term is rather misleading, so here it will be called the 'Abelès angle' instead, to avoid confusion.

The Abelès angle solution does not depend on the film thickness, nor on the refractive index of the substrate. However, the sensitivity of the method does depend
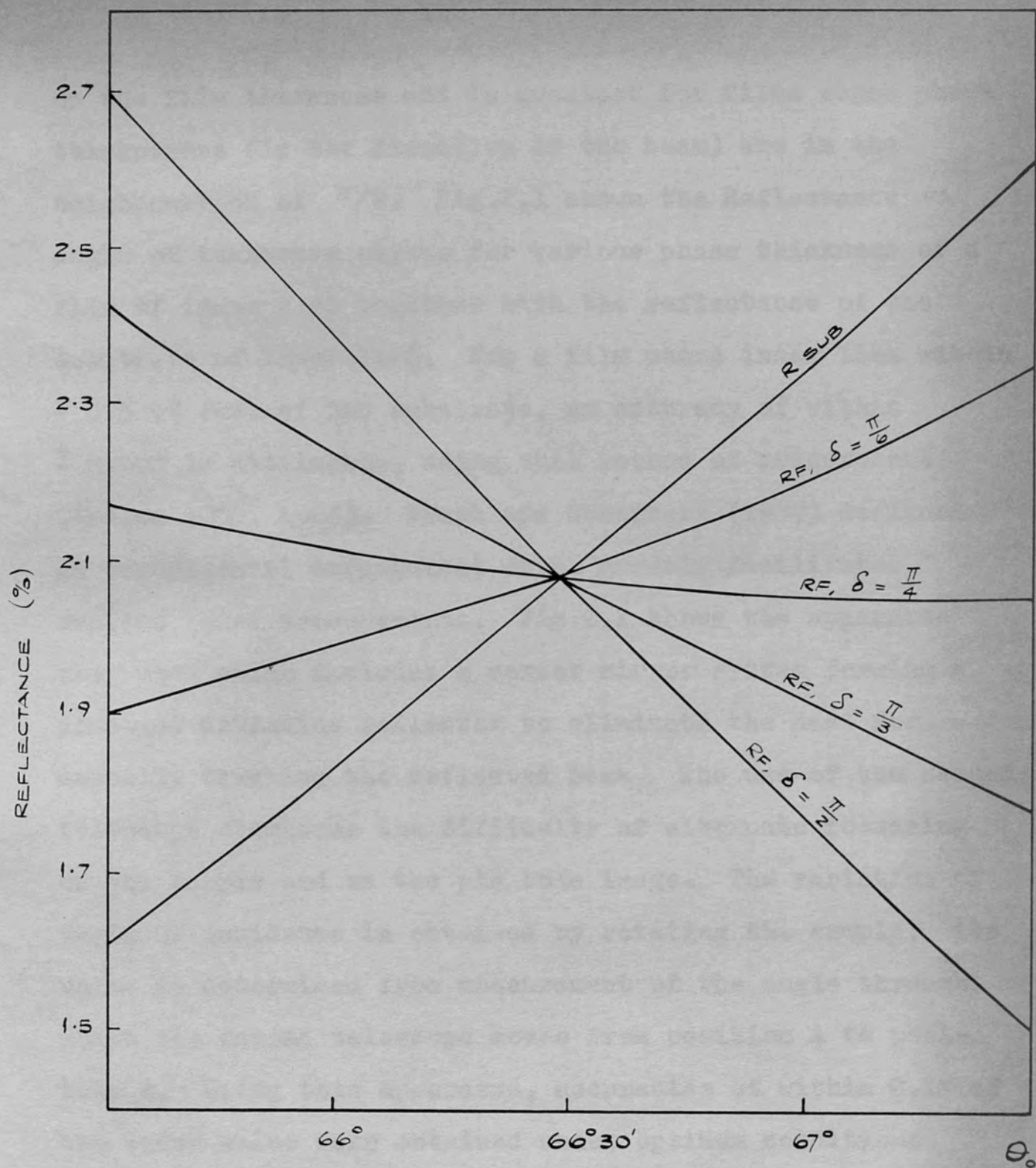
FIG. 2.1 VARIATION OF R_{SUB} AND R_F WITH θ_0
FOR DIFFERENT FILM THICKNESSES.

on the film thickness and is greatest for films whose phase

thicknesses (in the direction of the beam) are in the

neighbourhood of $\pi/2$. Fig.2.1 shows the Reflectance vs.

angle of incidence curves for various phase thickness of a

film of index 2.30 together with the reflectance of the

substrate of index 1.46. For a film whose index lies within

$\pm$ 0.3 of that of the substrate, an accuracy of within

$\pm$ 0.002 is attainable, using this method of measurement

(Abeles 1950, 1963). Traub and Osterberg (1957) designed

an experimental arrangement which greatly facilitates

routine index measurements. Fig.2.2 shows the apparatus

they used which included a corner mirror system forming a

constant deviation reflector to eliminate the need for

manually tracking the reflected beam. The use of the second

telescope overcomes the difficulty of alternate focussing

on the sample and on the pin hole image. The variation of

angle of incidence is obtained by rotating the sample; its

value is determined from measurement of the angle through

which the second telescope moves from position A to posi-

tion B. Using this apparatus, accuracies of within 0.1% of

the index value were obtained under optimum conditions.

For films whose indices were in the region of 2.3, deposi-

ted on a glass substrate, the accuracy was not quite so

good, but measurements within a probable error of $\pm$ 0.005

were obtained.
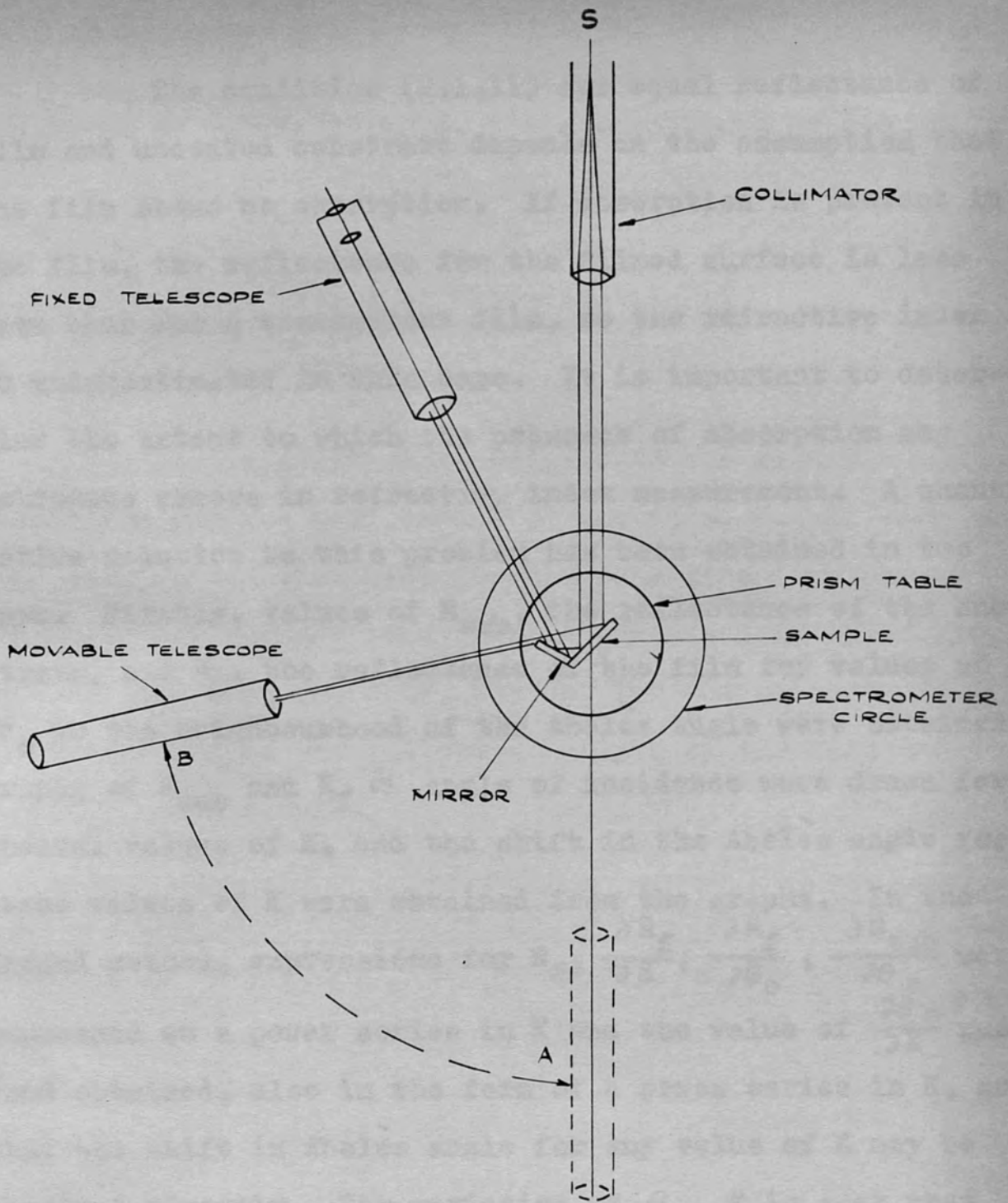
FIG. 2.2 APPARATUS USED BY TRAUB AND OSTERBERG

The condition (2.1.11) for equal reflectance of film and uncoated substrate depends on the assumption that the film shows no absorption. If absorption is present in the film, the reflectance for the filmed surface is less than that for a transparent film, so the refractive index is underestimated in this case. It is important to determine the extent to which the presence of absorption may introduce errors in refractive index measurement. A quantitative solution to this problem has been obtained in two ways. Firstly, values of R_{sub}, the reflectance of the substrate, and R_f, the reflectance of the film for values of θ_o in the neighbourhood of the Abelès angle were obtained. Graphs of R_{sub} and R_f *vs.* angle of incidence were drawn for several values of K, and the shift in the Abelès angle for these values of K were obtained from the graphs. In the second method, expressions for R_f, $\frac{\partial R_f}{\partial K}$, $\frac{\partial R_f}{\partial \theta_o}$, $\frac{\partial R_{sub}}{\partial \theta_o}$ were expressed as a power series in K and the value of $\frac{\partial \theta_o}{\partial K}$ was then obtained, also in the form of a power series in K, so that the shift in Abelès angle for any value of K may be obtained directly. The variation of θ_o, K is such that the reflectances of the filmed surfaces and substrate are maintained equal. Hence $\theta_o = \theta_A$ when no absorption is present. In both cases, a film of index 2.30 on a substrate of index 1.46 was considered, the medium of incidence

being air ($n_o = 1.0$). This corresponds to Cerium Dioxide deposited on quartz at $50^\circ C$, for a wavelength of 440 nm.

§2.2. Graphical method of determination of

error due to absorption

When absorption is present in the film the expression for the reflectance of the film, R_f, is very much more complicated than that for the case of a transparent film. It may be most conveniently expressed in the following way (see Born and Wolf, 1959). For convenience, we drop the subscripts on the optical constants of the film and denote $\underline{n}_1$ by $\underline{n} = n-iK$.

$$R_f = \frac{l e^{2v\eta} + m e^{-2v\eta} + 2l^{\frac{1}{2}} m^{\frac{1}{2}} \cos(\phi_{12} - \phi_{01} + 2u\eta)}{e^{2v\eta} + lm\, e^{-2v\eta} + 2l^{\frac{1}{2}} m^{\frac{1}{2}} \cos(\phi_{12} + \phi_{01} + 2u\eta)} \tag{2.2.1}$$

where

$$l = \frac{[(n^2-K^2)\cos\theta_0 - n_0 u]^2 + [2nK\cos\theta_0 - n_0 v]^2}{[(n^2-K^2)\cos\theta_0 + n_0 u]^2 + [2nK\cos\theta_0 + n_0 v]^2} \tag{2.2.2}$$

$$m = \frac{[(n^2-K^2)\cos\theta_2 - n_2 u]^2 + [2nK\cos\theta_2 - n_2 v]^2}{[(n^2-K^2)\cos\theta_2 + n_2 u]^2 + [2nK\cos\theta_2 + n_2 v]^2} \tag{2.2.3}$$

$$\eta = \frac{\pi}{2 (n^2 - n_0^2 \sin^2 \theta_0)^{1/2}} \tag{2.2.4}$$

$$\tan \phi_{01} = \frac{2 n_0 \cos \theta_0 [2nKu - (n^2 - K^2)v]}{(n^2 + K^2)^2 \cos^2 \theta_0 - n_0^2 (u^2 + v^2)} \tag{2.2.5}$$

$$\tan \phi_{12} = \frac{2 n_2 \cos \theta_2 [2nKu - (n^2 - K^2)v]}{(n^2 + K^2)^2 \cos^2 \theta_2 - n_2^2 (u^2 + v^2)} \tag{2.2.6}$$

and u, v are obtained from the relations

$$\left. \begin{array}{c} u^2 - v^2 = n^2 - K^2 - n_0^2 \sin^2 \theta_0 \\ uv = nK \end{array} \right\} \tag{2.2.7}$$

θ_2 and θ_0 are related by Snell's law, so the value of R_f may be calculated from the above equations for any value of K, θ_0 for a given film. For the film we are considering here, n = 2.30, so in the absence of absorption the Abelès angle is given by

$$\theta_A = \arctan (2.30) = 66° \, 30.1' \tag{2.2.8}$$

The values of R_f for several angles of incidence in the range 65° 30' to 67° 30' were calculated for values of K = 0.00, 0.005, 0.01, 0.02, 0.03, 0.05. The value for K = 0.00 corresponds to the value of R_f given by equation

(1.3.18). The value of R_{sub}, the reflectance of the sub-
strate, was also calculated for these angles of incidence.
The calculations could be performed on a desk calculator,
but it was more convenient to obtain the results using a
digital computer. This latter method had the additional
advantage that, once the program was written, values for
other films could be obtained fairly easily if desired.
Further details about the program, which was written in
Extended Mercury Autocode and run on the London University
Atlas computer, will be given in the Appendix. The results
are given in Table 2.1.

TABLE 2.1

θ	R_{SUB} %	R_F %					
		K=0.00	K=0.005	K=0.01	K=0.02	K=0.03	K=0.05
65°30'	1.619	2.698	2.660	2.623	2.554	2.489	2.372
66°0'	1.837	2.381	2.345	2.311	2.246	2.185	2.077
66°15'	1.953	2.227	2.193	2.160	2.097	2.039	1.935
66°30'	2.075	2.076	2.043	2.011	1.951	1.896	1.798
66°45'	2.202	1.929	1.897	1.867	1.809	1.755	1.661
67°0'	2.337	1.785	1.755	1.726	1.670	1.619	1.529
67°30'	2.616	1.510	1.482	1.455	1.405	1.358	1.278
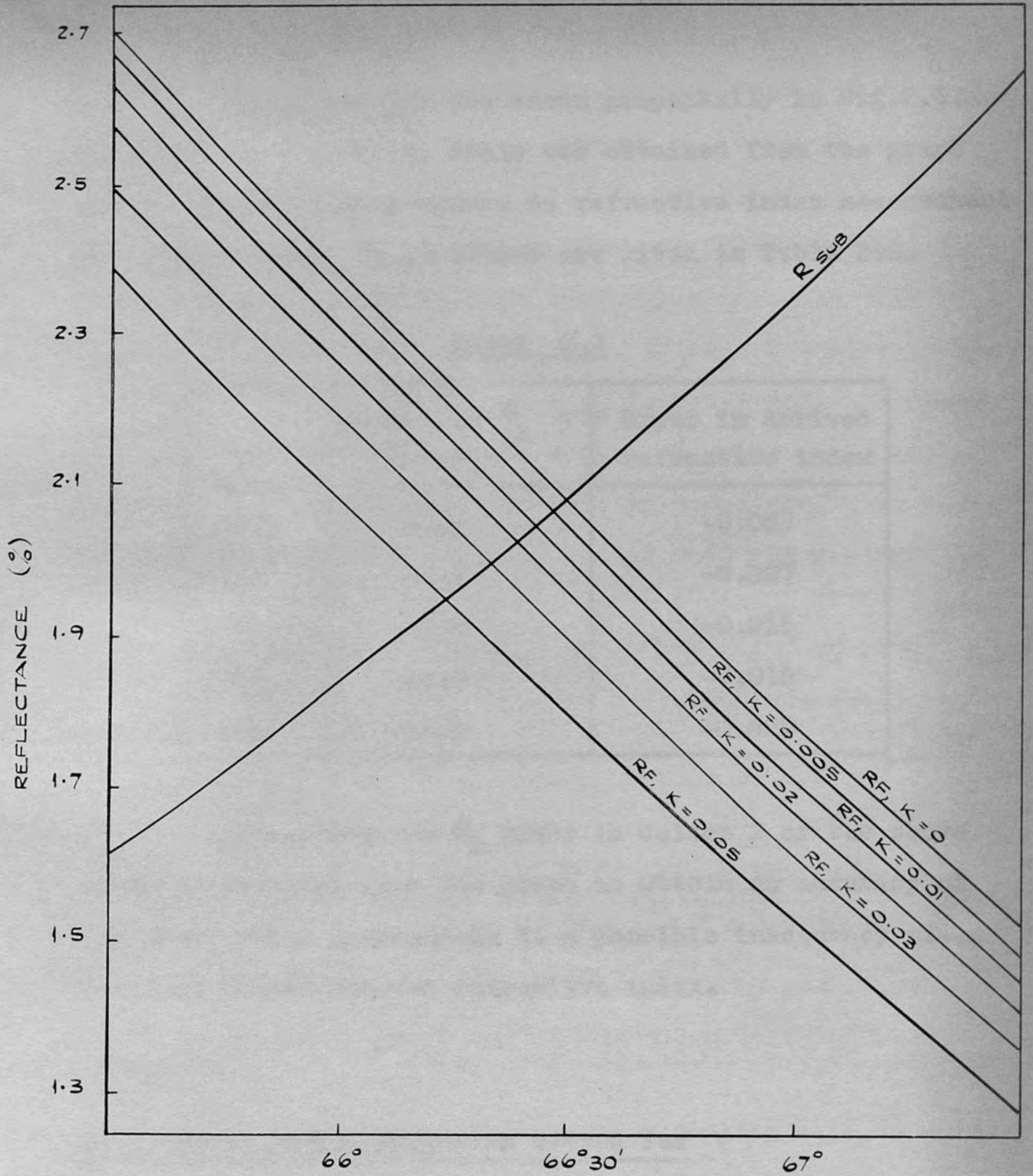
FIG. 2.3   GRAPHICAL ESTIMATE OF ERROR

These results are shown graphically in Fig.2.3. The shift in the Abeles angle was obtained from the graph and the corresponding errors in refractive index measurement were calculated. These values are given in Table 2.2.

TABLE 2.2

K	Change in θ_A (mins)	Error in derived refractive index
0.005	-1.5	-0.003
0.01	-3.5	-0.007
0.02	-7.0	-0.013
0.03	-10.0	-0.018
0.05	-16.0	-0.029

The change in θ_A given in column 2 of the above table is obtained from the graph to within an accuracy of 0.5 mins. This corresponds to a possible inaccuracy of $\pm$ 0.0006 in the derived refractive index.

§23. Power series expansion method for determining error

The method for determining error in measurement due to absorption, described above, is very convenient if

estimates of error for several different films are required and if a digital computer is available. However, if only one film is to be considered, it is sometimes more useful to obtain a value for $\frac{\partial\theta_0}{\partial K}$ in terms of K, so that a direct estimate of the error can be made for any K. In this section we consider only variation of θ_0 and K such that the equality of reflectance $R_f = R_{sub}$ is preserved. In order to work only in terms of one angle, θ_0, the angle of incidence, θ_2, must be expressed in terms of θ_0 by means of Snell's law. Then (2.2.3) and (2.2.6) are replaced by

$$m = \frac{[(n^2-K^2)(n_2^2-n_0^2\sin^2\theta_0)^{1/2}-n_2^2 u]^2+[2nK(n_2^2-n_0^2\sin^2\theta_0)^{1/2}-n_2^2 v]^2}{[(n^2-K^2)(n_2^2-n_0^2\sin^2\theta_0)^{1/2}+n_2^2 u]^2+[2nK(n_2^2-n_0^2\sin^2\theta_0)^{1/2}+n_2^2 v]} \quad (2.3.1)$$

$$\tan\phi_{12} = \frac{2n_2^2(n_2^2-n_0^2\sin^2\theta_0)^{1/2}[2nKu-(n^2-K^2)v]}{(n^2+K^2)^2(n_2^2-n_0^2\sin^2\theta_0)-n_2^4(u^2+v^2)} \quad (2.3.2)$$

For equality of reflectance to be preserved

$$R_f(\theta, K) - R_{sub}(\theta_0) = 0 \quad (2.3.3)$$

Considering only values of θ_0 which satisfy (2.3.3) we have

$$\frac{\partial\theta_0}{\partial K} = \frac{-\frac{\partial R_f}{\partial K}}{\left(\frac{\partial R_f}{\partial\theta_0}-\frac{\partial R_{sub}}{\partial\theta_0}\right)} \quad (2.3.4)$$

We therefore have to obtain expressions for $\dfrac{\partial R_{sub}}{\partial \theta_0}$, $\dfrac{\partial R_f}{\partial \theta_0}$ and $\dfrac{\partial R_f}{\partial K}$. As the expressions for R_f and R_{sub} are rather cumbersome those for their derivatives are even more so, so it is most convenient to obtain them in a stepwise method.

Letting

$$R_{sub} = \frac{pq}{rs} \tag{2.3.5}$$

where

$$
\begin{aligned}
p &= \left[n_0 \sin \theta_0 - \tan \theta_0 \, (n_2^2 - n_0^2 \sin^2 \theta_0)^{\frac{1}{2}} \right]^2 \\
q &= \left[(n_2^2 - n_0^2 \sin^2 \theta_0)^{\frac{1}{2}} - n_0 \sin \theta_0 \tan \theta_0 \right]^2 \\
r &= \left[n_0 \sin \theta_0 + \tan \theta_0 \, (n_2^2 - n_0^2 \sin^2 \theta_0)^{\frac{1}{2}} \right]^2 \\
s &= \left[(n_2^2 - n_0^2 \sin^2 \theta_0)^{\frac{1}{2}} + n_0 \sin \theta_0 \tan \theta_0 \right]^2
\end{aligned} \tag{2.3.6}
$$

we have

$$\frac{\partial R_{sub}}{\partial \theta_0} = \frac{1}{rs} \left\{ \left[p \frac{dq}{d\theta_0} + q \frac{dp}{d\theta_0} \right] - R_{sub} \left[r \frac{ds}{d\theta_0} + s \frac{dr}{d\theta_0} \right] \right\} \tag{2.3.7}$$

and from (2.3.6)

$$\frac{dp}{d\theta_0} = 2 \left[n_0 \sin \theta_0 - \tan \theta_0 (n_2^2 - n_0^2 \sin^2 \theta_0)^{\frac{1}{2}} \right] \left[n_0 \cos \theta_0 - \sec^2 \theta_0 (n_2^2 - n_0^2 \sin^2 \theta_0)^{\frac{1}{2}} + n_0^2 \sin^2 \theta_0 (n_2^2 - n_0^2 \sin^2 \theta_0)^{-\frac{1}{2}} \right]$$

$$\frac{dq}{d\theta_0} = -2 \sin \theta_0 \left[(n_2^2 - n_0^2 \sin^2 \theta_0)^{\frac{1}{2}} - n_0 \tan \theta_0 \sin \theta_0 \right] \left[n_0^2 \cos \theta_0 (n_2^2 - n_0^2 \sin^2 \theta_0)^{-\frac{1}{2}} + n_0 (\sec^2 \theta_0 + 1) \right]$$

$$\frac{dr}{d\theta_0} = 2 \left[n_0 \sin \theta_0 + \tan \theta_0 (n_2^2 - n_0^2 \sin^2 \theta_0)^{\frac{1}{2}} \right] \left[n_0 \cos \theta_0 + \sec^2 \theta_0 (n_2^2 - n_0^2 \sin^2 \theta_0)^{\frac{1}{2}} - n_0^2 \sin^2 \theta_0 (n_2^2 - n_0^2 \sin^2 \theta_0)^{-\frac{1}{2}} \right]$$

$$\frac{ds}{d\theta_0} = 2 \sin \theta_0 \left[(n_2^2 - n_0^2 \sin^2 \theta_0)^{\frac{1}{2}} + n_0 \tan \theta_0 \sin \theta_0 \right] \left[n_0 (\sec^2 \theta_0 + 1) - n_0^2 \cos \theta_0 (n_2^2 - n_0^2 \sin^2 \theta_0)^{-\frac{1}{2}} \right] \tag{2.3.8}$$

R_{sub} is obviously independent of the optical properties of the film so R_{sub}, $\dfrac{\partial R_{sub}}{\partial \theta_o}$ can be calculated directly from equations (2.3.5) to (2.3.8) if n_o, n_2, θ_o are known. We may similarly break down the expression (2.2.1) to obtain values for R_f, $\dfrac{\partial R_f}{\partial \theta_o}$, $\dfrac{\partial R_f}{\partial K}$ as follows.

Let

$$R_f = \frac{f}{g} \tag{2.3.9}$$

Then

$$\frac{\partial R_f}{\partial \theta_o} = \frac{1}{g}\left[\frac{\partial f}{\partial \theta_o} - R_f \frac{\partial g}{\partial \theta_o}\right] \tag{2.3.10}$$

$$\frac{\partial R_f}{\partial K} = \frac{1}{g}\left[\frac{\partial f}{\partial K} - R_f \frac{\partial g}{\partial K}\right] \tag{2.3.11}$$

where

$$f = l e^{2v\eta} + m e^{-2v\eta} + 2 l^{\frac{1}{2}} m^{\frac{1}{2}} \cos(\phi_{12} - \phi_{01} + 2u\eta) \tag{2.3.12}$$

$$g = e^{2v\eta} + l m e^{-2v\eta} + 2 l^{\frac{1}{2}} m^{\frac{1}{2}} \cos(\phi_{12} + \phi_{01} + 2u\eta) \tag{2.3.13}$$

Then

$$\frac{\partial f}{\partial \theta_o} = \frac{\partial}{\partial \theta_o}\left[l e^{2v\eta}\right] + \frac{\partial}{\partial \theta_o}\left[m e^{-2v\eta}\right] + \frac{\partial}{\partial \theta_o}\left[2 l^{\frac{1}{2}} m^{\frac{1}{2}} \cos(\phi_{12} - \phi_{01} + 2u\eta)\right] \tag{2.3.14}$$

where

$$\frac{\partial}{\partial \theta_0} \left[l e^{2v\eta} \right] = \left\{ \frac{\partial l}{\partial \theta_0} + 2l \left[\eta \frac{\partial v}{\partial \theta_0} + v \frac{\partial \eta}{\partial \theta_0} \right] \right\} e^{2v\eta}$$

$$\frac{\partial}{\partial \theta_0} \left[m e^{-2v\eta} \right] = \left\{ \frac{\partial m}{\partial \theta_0} - 2m \left[\eta \frac{\partial v}{\partial \theta_0} + v \frac{\partial \eta}{\partial \theta_0} \right] \right\} e^{-2v\eta}$$

$$\frac{\partial}{\partial \theta_0} \left[2 l^{\frac{1}{2}} m^{\frac{1}{2}} \cos(\phi_{12} - \phi_{01} + 2u\eta) \right] = \left\{ \frac{m^{\frac{1}{2}}}{l^{\frac{1}{2}}} \frac{\partial l}{\partial \theta_0} + \frac{l^{\frac{1}{2}}}{m^{\frac{1}{2}}} \frac{\partial m}{\partial \theta_0} \right\} \cos(\phi_{12} - \phi_{01} + 2u\eta)$$
$$- 2 l^{\frac{1}{2}} m^{\frac{1}{2}} \sin(\phi_{12} - \phi_{01} + 2u\eta) \left[\frac{\partial \phi_{12}}{\partial \theta_0} - \frac{\partial \phi_{01}}{\partial \theta_0} + 2 \left(u \frac{\partial \eta}{\partial \theta_0} + \eta \frac{\partial u}{\partial \theta_0} \right) \right]$$

and

$$\frac{\partial q}{\partial \theta_0} = \frac{\partial}{\partial \theta_0} \left[e^{2v\eta} \right] + \frac{\partial}{\partial \theta_0} \left[l m e^{-2v\eta} \right] + \frac{\partial}{\partial \theta_0} \left[2 l^{\frac{1}{2}} m^{\frac{1}{2}} \cos(\phi_{12} + \phi_{01} + 2u\eta) \right]$$

$$(2.3.15)$$

where

$$\frac{\partial}{\partial \theta_0} \left[e^{2v\eta} \right] = 2 e^{2v\eta} \left[\eta \frac{\partial v}{\partial \theta_0} + v \frac{\partial \eta}{\partial \theta_0} \right]$$

$$\frac{\partial}{\partial \theta_0} \left[l m e^{-2v\eta} \right] = \left\{ l \frac{\partial m}{\partial \theta_0} + m \frac{\partial l}{\partial \theta_0} - 2 l m \left(\eta \frac{\partial v}{\partial \theta_0} + v \frac{\partial \eta}{\partial \theta_0} \right) \right\} e^{-2v\eta}$$

$$\frac{\partial}{\partial \theta_0} \left[2 l^{\frac{1}{2}} m^{\frac{1}{2}} \cos(\phi_{12} + \phi_{01} + 2u\eta) \right] = \left\{ \frac{m^{\frac{1}{2}}}{l^{\frac{1}{2}}} \frac{\partial l}{\partial \theta_0} + \frac{l^{\frac{1}{2}}}{m^{\frac{1}{2}}} \frac{\partial m}{\partial \theta_0} \right\} \cos(\phi_{12} + \phi_{01} + 2u\eta)$$
$$- 2 l^{\frac{1}{2}} m^{\frac{1}{2}} \sin(\phi_{12} + \phi_{01} + 2u\eta) \left[\frac{\partial \phi_{12}}{\partial \theta_0} + \frac{\partial \phi_{01}}{\partial \theta_0} + 2 \left(u \frac{\partial \eta}{\partial \theta_0} + \eta \frac{\partial u}{\partial \theta_0} \right) \right]$$

Similar expressions may be obtained for $\frac{\partial f}{\partial K}$, $\frac{\partial g}{\partial K}$ by replacing $\frac{\partial}{\partial \theta_0}$ by $\frac{\partial}{\partial K}$. We must now obtain expressions

for $\dfrac{\partial l}{\partial \theta_0}$, $\dfrac{\partial m}{\partial \theta_0}$, $\dfrac{\partial u}{\partial \theta_0}$, $\dfrac{\partial v}{\partial \theta_0}$, $\dfrac{\partial \eta}{\partial \theta_0}$, $\dfrac{\partial \phi_{01}}{\partial \theta_0}$, $\dfrac{\partial \phi_{12}}{\partial \theta_0}$ and the

corresponding partial derivatives with respect to K.

From (2.2.7) we obtain

$$\frac{\partial u}{\partial \theta_0} = \frac{n_0^2 \sin\theta_0 \cos\theta_0}{(n^2 - k^2 - n_0^2 \sin^2\theta_0)^{1/2}} \left[\frac{3 n^2 k^2}{2(n^2 - k^2 - n_0^2 \sin^2\theta_0)^2} - 1 \right]$$

$$\frac{\partial v}{\partial \theta_0} = \frac{nk\, n_0^2 \sin\theta_0 \cos\theta_0}{(n^2 - k^2 - n_0^2 \sin^2\theta_0)^{3/2}} \left[1 - \frac{5 n^2 k^2}{2(n^2 - k^2 - n_0^2 \sin^2\theta_0)^2} \right]$$

$$(2.3.16)$$

and from (2.2.4)

$$\frac{\partial \eta}{\partial \theta_0} = \frac{\pi \sin\theta_0 \cos\theta_0}{2(n^2 - n_0^2 \sin^2\theta_0)^{3/2}} \qquad (2.3.17)$$

To find expressions for $\dfrac{\partial l}{\partial \theta_0}$, $\dfrac{\partial m}{\partial \theta_0}$, we let

$l = \dfrac{a}{b}$, $m = \dfrac{c}{d}$ so that

$$\frac{\partial l}{\partial \theta_0} = \frac{1}{b}\left[\frac{\partial a}{\partial \theta_0} - l \frac{\partial b}{\partial \theta_0} \right]$$

$$(2.3.18)$$

$$\frac{\partial m}{\partial \theta_0} = \frac{1}{d}\left[\frac{\partial c}{\partial \theta_0} - m \frac{\partial d}{\partial \theta_0} \right]$$

and here again we obtain similar expressions for $\dfrac{\partial l}{\partial K}$, $\dfrac{\partial m}{\partial K}$ simply by substituting $\dfrac{\partial}{\partial K}$ for $\dfrac{\partial}{\partial \theta_0}$.

Then

$$\frac{\partial a}{\partial \theta_0} = -2\left\{ \left[(n^2 - k^2)\cos\theta_0 - n_0 u \right]\left[(n^2 - k^2)\sin\theta_0 + n_0 \frac{\partial u}{\partial \theta_0} \right] \right.$$
$$\left. + \left[2nk\cos\theta_0 - n_0 v \right]\left[2nk\sin\theta_0 + n_0 \frac{\partial v}{\partial \theta_0} \right] \right\}$$

$$\frac{\partial b}{\partial \theta_0} = 2\left\{ \left[(n^2 - k^2)\cos\theta_0 + n_0 u \right]\left[n_0 \frac{\partial u}{\partial \theta_0} - (n^2 - k^2)\sin\theta_0 \right] \right.$$
$$\left. + \left[2nk\cos\theta_0 + n_0 v \right]\left[-2nk\sin\theta_0 + n_0 \frac{\partial v}{\partial \theta_0} \right] \right.$$

$$\frac{\partial c}{\partial \theta_0} = -2\left\{[(n^2-k^2)(n_2^2-n_0^2\sin^2\theta_0)^{\frac{1}{2}} - n_2^2 u][(n^2-k^2)(n_2^2-n_0^2\sin^2\theta_0)^{-\frac{1}{2}} n_0^2\sin\theta_0\cos\theta_0 + n_2^2\frac{\partial u}{\partial\theta_0}] \right. $$
$$\left. + [2nk(n_2^2-n_0^2\sin^2\theta_0)^{\frac{1}{2}} - n_2^2 v][n_2^2\frac{\partial v}{\partial\theta_0} + 2nk(n_2^2-n_0^2\sin^2\theta_0)^{-\frac{1}{2}} n_0^2\sin\theta_0\cos\theta_0]\right\}$$

$$\frac{\partial d}{\partial \theta_0} = 2\left\{[(n^2-k^2)(n_2^2-n_0^2\sin^2\theta_0)^{\frac{1}{2}} + n_2^2 u][n_2^2\frac{\partial u}{\partial\theta_0} - (n^2-k^2)(n_2^2-n_0^2\sin^2\theta_0)^{-\frac{1}{2}} n_0^2\sin\theta_0\cos\theta_0] \right.$$
$$\left. + [2nk(n_2^2-n_0^2\sin^2\theta_0)^{\frac{1}{2}} - n_2^2 v][n_2^2\frac{\partial v}{\partial\theta_0} - 2nk(n_2^2-n_0^2\sin^2\theta_0)^{-\frac{1}{2}} n_0^2\sin\theta_0\cos\theta_0]\right\}$$

$$(2.3.19)$$

To obtain expressions for $\dfrac{\partial\phi_{01}}{\partial\theta_0}$, $\dfrac{\partial\phi_{12}}{\partial\theta_0}$ we make the following substitutions

$$x = \tan\phi_{01}$$
$$y = \tan\phi_{12}$$

$$(2.3.20)$$

so that

$$\frac{\partial\phi_{01}}{\partial\theta_0} = \frac{1}{(1+x^2)}\frac{\partial x}{\partial\theta_0}$$

$$\frac{\partial\phi_{12}}{\partial\theta_0} = \frac{1}{(1+y^2)}\frac{\partial y}{\partial\theta_0}$$

$$(2.3.21)$$

where

$$\frac{\partial x}{\partial\theta_0} = \frac{-2\left\{n_0\sin\theta_0[2nku-(n^2-k^2)v] + n_0\cos\theta_0[(n^2-k^2)\frac{\partial v}{\partial\theta_0} - 2nk\frac{\partial u}{\partial\theta_0}] - x[(n^2+k^2)^2\cos\theta_0\sin\theta_0 + n_0^2(u\frac{\partial u}{\partial\theta_0}+v\frac{\partial v}{\partial\theta_0})]\right\}}{(n^2+k^2)^2\cos^2\theta_0 - n_0^2(u^2+v^2)}$$

$$\frac{\partial y}{\partial\theta_0} = \frac{2\left\{n_2^2(n_2^2-n_0^2\sin^2\theta_0)^{\frac{1}{2}}[2nk\frac{\partial u}{\partial\theta_0}-(n^2-k^2)\frac{\partial v}{\partial\theta_0}] - n_2^2 n_0^2\sin\theta_0\cos\theta_0(n_2^2-n_0^2\sin^2\theta_0)^{-\frac{1}{2}}[2nku-(n^2-k^2)v] + y[n_0^2(n^2+k^2)^2\sin\theta_0\cos\theta_0 + n_2^4(u\frac{\partial u}{\partial\theta_0}+v\frac{\partial v}{\partial\theta_0})]\right\}}{(n^2+k^2)^2(n_2^2-n_0^2\sin^2\theta_0) - n_2^4(u^2+v^2)}$$

$$(2.3.22)$$

Returning to (2.2.2) through (2.2.7) we obtain the following expressions for partial derivatives with

respect to K to obtain a value for $\frac{\partial R_f}{\partial K}$ from (2.3.11) et seq.

$$\frac{\partial \eta}{\partial K} = 0 \tag{2.3.23}$$

$$2u\,\frac{\partial u}{\partial K} = K\left\{\frac{[2n^2-(n^2-n_0^2\sin^2\theta_0-K^2)]}{[(n^2-K^2-n_0^2\sin^2\theta_0)^2+4n^2K^2]^{\frac{1}{2}}}-1\right\}$$

$$2v\,\frac{\partial v}{\partial K} = K\left\{\frac{[2n^2-(n^2-n_0^2\sin^2\theta_0-K^2)]}{[(n^2-K^2-n_0^2\sin^2\theta_0)^2+4n^2K^2]^{\frac{1}{2}}}+1\right\} \tag{2.3.24}$$

and

$$\frac{\partial a}{\partial K} = 2\left\{[2nK\cos\theta_0-n_0 v][2n\cos\theta_0-n_0\frac{\partial v}{\partial K}]\right.$$
$$\left.-[(n^2-K^2)\cos\theta_0-n_0 u][2K\cos\theta_0+n_0\frac{\partial u}{\partial K}]\right\}$$

$$\frac{\partial b}{\partial K} = 2\left\{[2nK\cos\theta_0+n_0 v][2n\cos\theta_0+n_0\frac{\partial v}{\partial K}]\right.$$
$$\left.-[(n^2-K^2)\cos\theta_0+n_0 u][2K\cos\theta_0-n_0\frac{\partial u}{\partial K}]\right\}$$

$$\frac{\partial c}{\partial K} = 2\left\{[2nK(n_2^2-n_0^2\sin^2\theta_0)^{\frac{1}{2}}-n_2^2 v][2n(n_2^2-n_0^2\sin^2\theta_0)^{\frac{1}{2}}-n_2^2\frac{\partial v}{\partial K}]\right.$$
$$\left.-[(n^2-K^2)(n_2^2-n_0^2\sin^2\theta_0)^{\frac{1}{2}}-n_2^2 u][2K(n_2^2-n_0^2\sin^2\theta_0)^{\frac{1}{2}}+n_2^2\frac{\partial u}{\partial K}]\right\}$$

$$\frac{\partial d}{\partial K} = 2\left\{[2nK(n_2^2-n_0^2\sin^2\theta_0)^{\frac{1}{2}}+n_2^2 v][2n(n_2^2-n_0^2\sin^2\theta_0)^{\frac{1}{2}}+n_2^2\frac{\partial v}{\partial K}]\right.$$
$$\left.-[(n^2-K^2)(n_2^2-n_0^2\sin^2\theta_0)^{\frac{1}{2}}+n_2^2 u][2K(n_2^2-n_0^2\sin^2\theta_0)^{\frac{1}{2}}-n_2^2\frac{\partial u}{\partial K}]\right\} \tag{2.3.25}$$

Also

$$\frac{\partial x}{\partial K} = \frac{\left\{2n_0\cos\theta_0[2nu+2nK\frac{\partial u}{\partial K}+2Kv-(n^2-K^2)\frac{\partial v}{\partial K}]-x[4K(n^2+K^2)\cos^2\theta_0-2n_0^2(u\frac{\partial u}{\partial K}+v\frac{\partial v}{\partial K})]\right\}}{[(n^2+K^2)^2\cos^2\theta_0-n_0^2(u^2+v^2)]}$$

$$\frac{\partial y}{\partial K} = \frac{\left\{2n_2^2(n_2^2-n_0^2\sin^2\theta_0)^{\frac{1}{2}}[2nu+2nK\frac{\partial u}{\partial K}+2Kv-(n^2-K^2)\frac{\partial v}{\partial K}]-y[4K(n^2+K^2)(n_2^2-n_0^2\sin^2\theta_0)-2n_2^4(u\frac{\partial u}{\partial K}+v\frac{\partial v}{\partial K})]\right\}}{[(n^2+K^2)(n_2^2-n_0^2\sin^2\theta_0)-n_2^4(u^2+v^2)]}$$

$$\tag{2.3.26}$$

We are now in a position to be able to calculate $\frac{\partial R_f}{\partial \theta_o}$ and $\frac{\partial R_f}{\partial K}$ using the above equations. For any given film these expressions may be calculated in the form of a power series in K. For values of K up to K = 0.05 it was found unnecessary to include terms of $O(K^4)$. The coefficients in the power series for R_f, $\frac{\partial R_f}{\partial K}$, $\frac{\partial R_f}{\partial \theta_o}$ were evaluated for the case mentioned above in which n = 2.3, n_o = 1.0, n_2 = 1.46, θ_o = 66° 30.1'. From the expressions given above, the following results were obtained (Heavens and Liddell, 1965)

$$R_{film} = 0.020755 - 0.067418K + 0.243401K^2$$

$$\frac{\partial R_f}{\partial \theta_o} = -0.341265 + 0.567719K - 0.510771K^2$$

$$\frac{\partial R_f}{\partial K} = -0.067418 + 0.486825K - 1.002804K^2$$

From (2.3.6) it was found

$$\frac{\partial R_{sub}}{\partial \theta_o} = +0.284557$$

We can now obtain $\frac{\partial \theta_o}{\partial K}$ from (2.3.3), giving

$$\frac{\partial \theta_o}{\partial K} = -0.107727 + 0.680172K - 0.899434K^2$$

The above expression may be integrated to give the shift in the Abelès angle in terms of K

$$\Delta \theta_A = -0.107727K + 0.340086K^2 - 0.299145K^3$$

This formula may be used to calculate the change in θ_A and resulting error in measured refractive index for K = 0.005, 0.01, 0.02, 0.03, 0.05. We see from Table 2.3 below, that these results agree very well with the values obtained by the graphical method.

TABLE 2.3

K	Change in θ_A (mins)	Error in derived refractive index	
		Power series method	Graphical method
0.005	-1.82	-0.004	-0.003
0.01	-3.59	-0.007	-0.007
0.02	-6.95	-0.013	-0.013
0.03	-10.1	-0.019	-0.018
0.05	-15.7	-0.029	-0.029

CHAPTER III: BROAD BAND HIGH-REFLECTING

MULTILAYERS

§3.1. Use of dielectric high reflecting

films in interferometry

The transmission at normal incidence of the Fabry-Perot interferometer is given by (Baumeister, 1963):-

$$T = \frac{T_{max}}{1 + F \sin^2 \eta} \qquad (3.1.1)$$

where

$$T_{max} = \frac{T_1 T_2}{(1 - R)^2} \qquad (3.1.2)$$

$$F = \frac{4R}{(1-R)^2} \quad , \quad R = \sqrt{R_1 R_2} \qquad (3.1.3)$$

R_1, R_2 and T_1, T_2 are the reflectances and transmittances of the mirror coatings.

$$\eta = 2\pi nd\sigma - \psi(\sigma) \qquad (3.1.4)$$

where n, d are the refractive index and the thickness of the spacer and $\psi(\sigma)$ is the average value of the phase changes on reflection in the spacer at the spacer/mirror boundaries for wavenumber σ. Suppose a light wave whose electric vector is represented by

$$E = E_0 \exp i(\omega t - 2\pi x \sigma) \qquad (3.1.5)$$

is incident on boundary 1; then the electric vector of the reflected wave may be represented by

$$E_h = R_1^{\frac{1}{2}} E_0 \exp i(\omega t + 2\pi x \sigma + \psi_1) \qquad (3.1.6)$$

where ψ_1 is the phase change on reflection at boundary 1.

We see from (3.1.1) that transmission bands will occur when $\eta = m\pi$. The integer m is called the 'order number'. If the transmittance and absorptance of the coatings are T, A respectively

$$T + A + R = 1 \qquad (3.1.7)$$

and the maximum transmittance is given by

$$T_{max} = \frac{1}{(1 + \frac{A}{T})^2} \qquad (3.1.8)$$

Thus, it is important that the absorption should be as low as possible. Typical values for silver coatings (Heavens, 1955) are R = 0.95, T = 0.01, A = 0.04 so from (3.1.8) we see that the maximum transmittance is only 4%. A much better performance is achieved by the use of dielectric multilayers, for which maximum transmittances of more than 90% may be obtained (Baumeister, 1963).

The method of analysis of the performance of the Fabry-Perot interferometer outlined above may be used to

analyse other multilayer filters. The filter may be con-
sidered as a Fabry-Perot system by selecting one layer and
treating it as a spacer layer and then treating the layers
between this layer and the substrate as one 'effective
interface' and those between the spacer layer and the medium
of incidence as the other 'effective interface'. This idea
was developed by Smith (1958).

The width at half-maximum (sometimes referred to
as the 'half-width') of the pass-band of an interference
filter is given by (Baumeister and Jenkins, 1957):-

$$\Delta\sigma = \frac{(1-R)}{R^{\frac{1}{2}}\left[2\pi n d - \frac{\partial \psi}{\partial \sigma}\right]} \tag{3.1.9}$$

For metal films, the dispersion of phase change is negligible
so that (3.1.9) becomes

$$\frac{\Delta\sigma}{\sigma} = \frac{(1-R)}{m\pi R^{\frac{1}{2}}} \tag{3.1.10}$$

since $\psi \doteq \pi$ in this case. For dielectric films, the
dispersion of phase change is significant and its sign in
the high-reflecting region is such as to decrease $\Delta\sigma$.
Much narrower pass-bands may therefore be obtained by the
use of dielectric films in place of silver. Later in the
chapter we shall discuss several types of broad-band reflec-
tor which exhibit extremely rapid variation of the phase
change on reflection with wavenumber. The broad-band
reflectors have the additional advantage that their high-

reflecting region covers the whole of the visible spectrum, whereas that of the 'classical' quarter wave stack covers only about one half of this range. This is the one big disadvantage of using quarter-wave stacks rather than the conventional silver coatings for the Fabry-Perot system, but this can be overcome by use of broad-band reflectors.

§3.2. The 'classical' stack and previous work
on broad-band reflecting filters

The classical quarter-wave stack consists of a number of alternating high-and low-index layers which have an 'optical thickness' of $\frac{\lambda_o}{4}$. Then at the wavenumber $\sigma_o = 1/\lambda_o$, the beams reflected from the various interfaces between the layers will all be in phase so that the reflectance obtained is a maximum. Fig. 3.1 shows the computed reflectance vs. relative wavenumber of 1, 5, 9, 13-layer stacks of CeO_2 ($n_H = 2.36$) and M_gF_2 ($n_L = 1.39$). From the graphs it is seen that the maximum reflectance (which is the value of the reflectance at $\sigma/\sigma_o = 1.0$ for this type of filter) increases with increase of the number of layers, whereas the total width of the high-reflectance band remains substantially constant. In fact, the limiting width of the high-reflectance band of a classical stack is determined solely by the ratio n_H/n_L. Following the analysis outlined
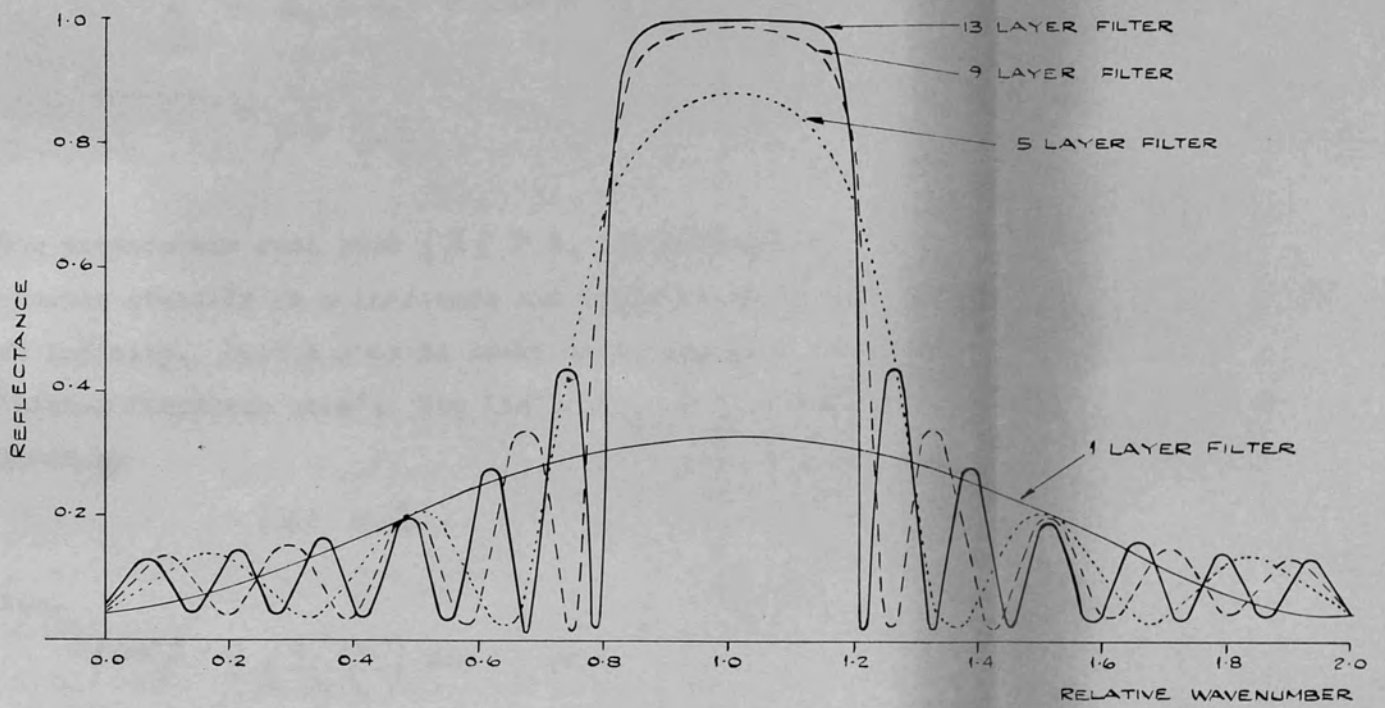
FIG. 3.1   CLASSICAL MULTILAYER STACKS

by Weinstein (1954) and from (1.4.12), we see

$$[A]^m = S_{m-1}(X)[A] - S_{m-2}(X)[I] \qquad (3.2.1)$$

where

$$[A] = \begin{pmatrix} a_{11} & a_{12} \\ a_{21} & a_{22} \end{pmatrix} = \begin{pmatrix} \cos\beta & \frac{i}{n_H}\sin\beta \\ in_H\sin\beta & \cos\beta \end{pmatrix} \begin{pmatrix} \cos\beta & \frac{i}{n_L}\sin\beta \\ in_L\sin\beta & \cos\beta \end{pmatrix}$$

$$X = a_{11} + a_{22} = 2\cos^2\beta - \left(\frac{n_H^2 + n_L^2}{n_H n_L}\right)\sin^2\beta$$

$$\beta = \frac{\pi}{2}\frac{\sigma}{\sigma_o}$$

For wavenumbers such that $|X| > 2$, the reflectance increases steadily as m increases and tends to unity as m tends to infinity. Such a zone is known as a 'stopping zone' or 'high-reflectance zone'. The limit σ_L of this zone is given by

$$|X| = 2 \qquad (3.2.2)$$

i.e.

$$\left| \cos^2\beta - \frac{1}{2}\left(\frac{n_H^2 + n_L^2}{n_H n_L}\right)\sin^2\beta \right| = 1$$

$$\frac{\pi}{2}\frac{\sigma_L}{\sigma} = \arcsin\left[\frac{2\sqrt{n_H n_L}}{n_H + n_L}\right] \qquad (3.2.3)$$

The high-reflectance zone is symmetrical about $\sigma/\sigma_o = 1.0$. The expression for the distance $\Delta\left(\frac{\sigma}{\sigma_o}\right)$ from

the centre of the zone, $\sigma = \sigma_0$ to the edge $\sigma = \sigma_L$ is given by

$$\Delta \left(\frac{\sigma}{\sigma_0} \right) = \left| \frac{\sigma_0 - \sigma_L}{\sigma_0} \right| = \frac{2}{\pi} \left| \arcsin(1) - \arcsin \left(\frac{2\sqrt{n_H n_L}}{n_H + n_L} \right) \right|$$

Hence, we have

$$\Delta \left(\frac{\sigma}{\sigma_0} \right) = \frac{2}{\pi} \arcsin \left| \frac{n_H - n_L}{n_H + n_L} \right| \tag{3.2.4}$$

The bandwidth may, in principle, be increased by using a very high ratio of n_H/n_L, but there are severe practical limitations to this procedure. For the visible region, it is difficult to find materials to give n_H/n_L greater than 2. In the near infra-red, semiconducting materials of high index may be used, giving a ratio of n_H/n_L up to 3.65, which corresponds to a total bandwidth of $0.77\sigma/\sigma_0$.

A possible approach to the problem of obtaining greater bandwidths than those given by (3.2.4) for the classical stack, is to assume practical values for the refractive indices of the layers and to evolve suitable com-binations of layer thicknesses to produce a specified band-width. This method has been used by Baumeister and Stone (1956) and by Penselin and Steudel (1955).

Baumeister and Stone computed the reflectance curve for a system of N layers with optical thicknesses $\frac{\lambda_j}{4}$ and con-sidered variations $\delta\lambda_j$ in thickness which produced varia-tions $\delta R(\lambda)$ in reflectance, and expanded in a Taylor series

LAYER	λ_i (nm)
1	690·8
2	690·8
3	690·8
4	666·7
5	575·7
6	701·3
7	626·2
8	517·0
9	520·5
10	463·7
11	463·7
12	434·8
13	414·0
14	414·0
15	414·0
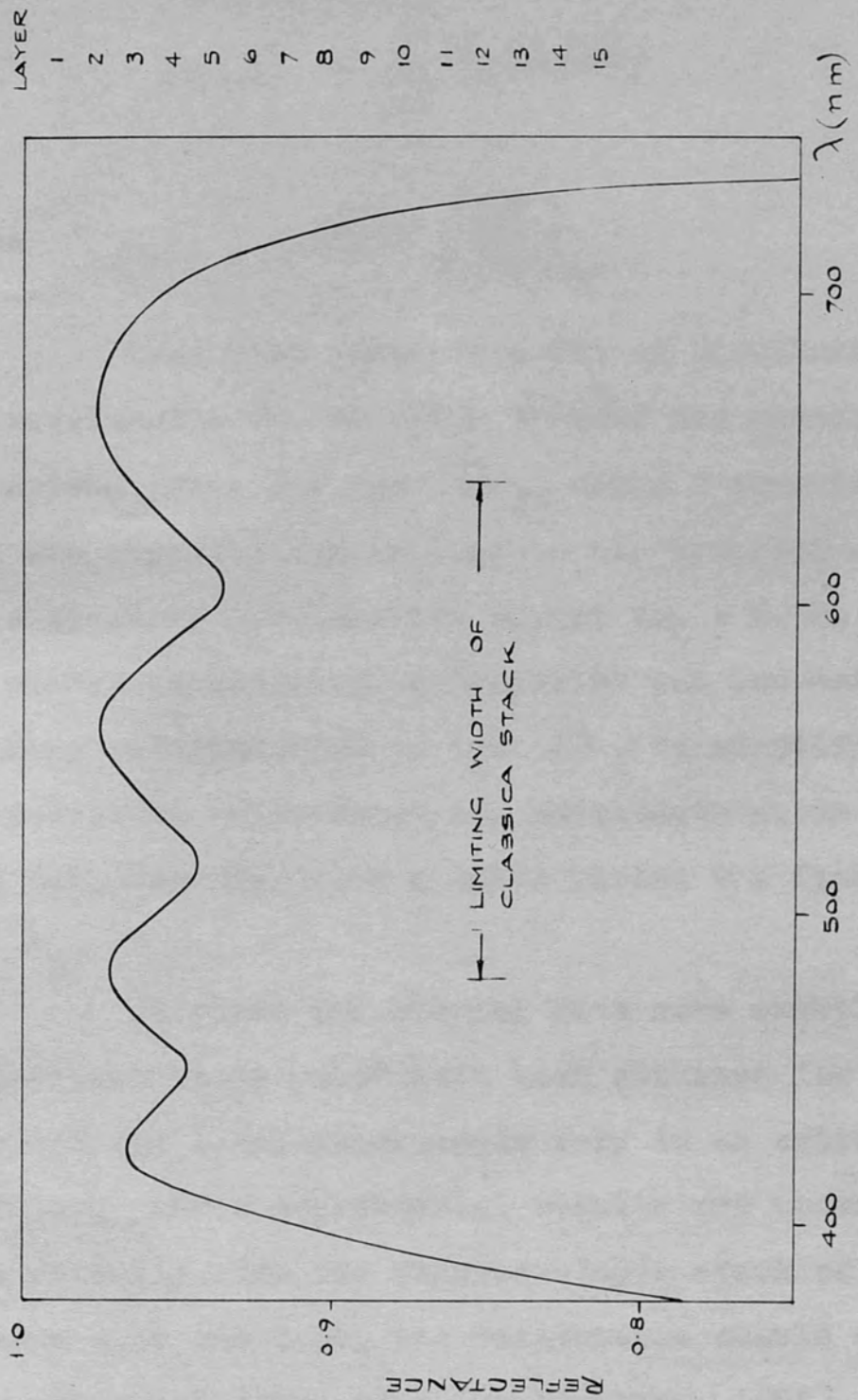
FIG. 3.2. BAUMEISTER AND STONE'S RESULT.

$$\delta R(\lambda) = \sum_{j=1}^{N} A_j(\lambda)\,\delta\lambda_j \qquad\qquad (3.2.5)$$

where
$$A_j = \left(\frac{\partial R}{\partial \lambda}\right)_{\lambda_j}$$

      They thus obtained a set of simultaneous equations for wavelengths λ at which $\delta R(\lambda)$ has prescribed values and solved these for the $\delta\lambda_j$, using a computer. The process was repeated for as long as the computer was hired. For a 15-layer ZnS-Cryolite system ($n_H = 2.30$, $n_L = 1.35$), the number of independent variables was reduced by imposing arbitary relationships on the $\delta\lambda_j$ to simplify the problem. The resultant reflectance vs. wavelength curve is shown in Fig. 3.2, together with a table giving the final values of the λ_j.

      Penselin and Steudel give some examples of reflectance bands which have been obtained for a multilayer in which the layer-thicknesses vary in an arithmetic progression. Their experimental results are shown in Fig. 3.3. Theoretically, for the thirteen-layer stack of films with indices 2.30 and 1.38, the reflectance should exceed 90% over the range 380nm to 610nm (Jenkins, 1958). This work suggests that the use of staggered stacks may lead to a significant broadening of the high-reflectance band.
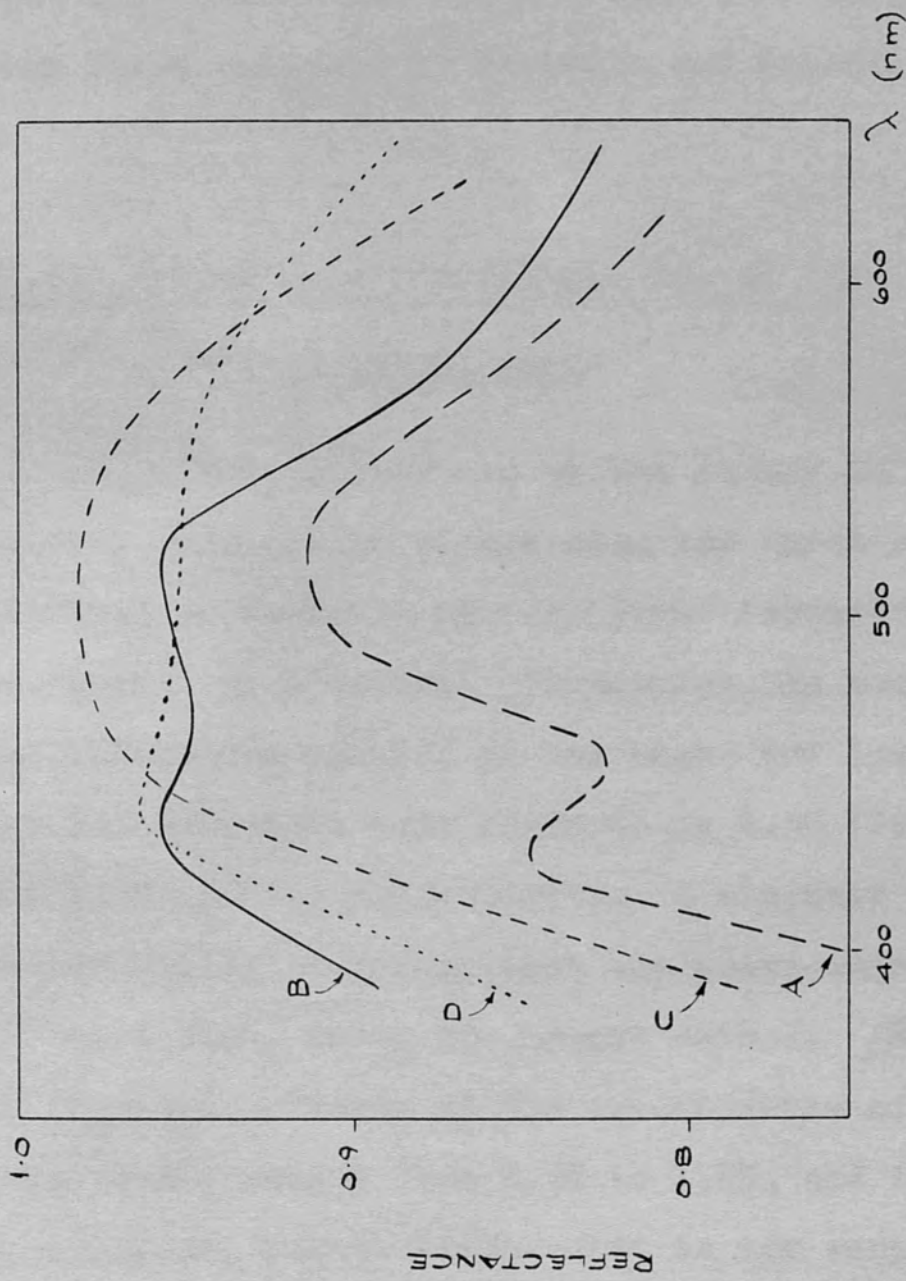
FIG. 3.3. PENSELIN AND STEUDELS' RESULTS

The results reported in the next section were obtained by staggering the layers in such a way as to form either an arithmetic or geometric progression. They show that this method can produce very much larger bandwidths than those obtained by Penselin and Steudel.

§3.3. Reflectance characteristics of the
staggered multilayers

The thicknesses of the layers in the systems studied were varied either from the first layer (asymmetric filters) or from the central layer (symmetric filters) in an arithmetic or geometric progression, as shown in Figure 3.4. The refractive indices of the high- and low-index materials and the substrate were taken to be 2.36 (CeO_2), 1.39 (MgF_2) and 1.53 (glass) respectively. A computer was programmed to obtain values of reflectance and phase change on reflection of the filter, using the matrix method. /Equations (1.4.2) to (1.4.7)/. Values of the common ratio of the geometric progression ranged from 0.95 to 1.05, and for the arithmetic progression, common differences in the range −0.05 to +0.05 were used. The initial calculations were made over a range of σ/σ_0 from 0.0 to 2.0 at an interval of σ/σ_0 = 0.1. The most favourable cases were then investigated in greater

L   t   t   L

H kt $t(1+k)$ H

L $k^{q-2}t$ $t[1+(q-2)k]$ L

H $k^{q-1}t$ $t[1+(q-1)k]$ H
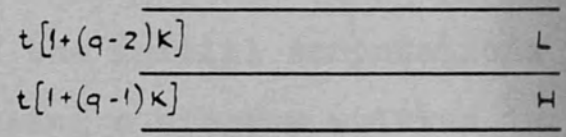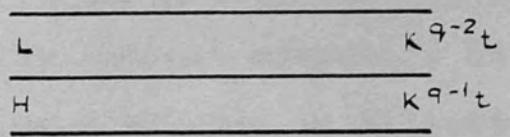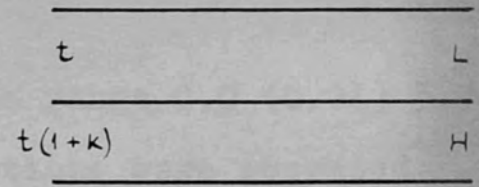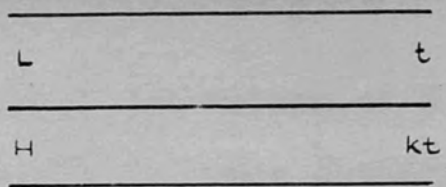
(a)   (b)

ASYMMETRIC GEOMETRIC   ASYMMETRIC ARITHMETIC

L $k^{\frac{q-1}{2}}t$ $t[1+(\frac{q-1}{2})k]$ L

H $k^{\frac{q-3}{2}}t$ $t[1+(\frac{q-3}{2})k]$ H

L kt $t(1+k)$ L

H t t H

L kt $t(1+k)$ L

H $k^{\frac{q-3}{2}}t$ $t[1+(\frac{q-3}{2})k]$ H

L $k^{\frac{q-1}{2}}t$ $t[1+(\frac{q-1}{2})k]$ L
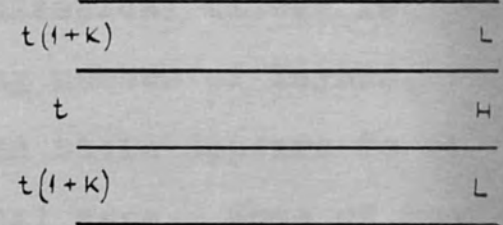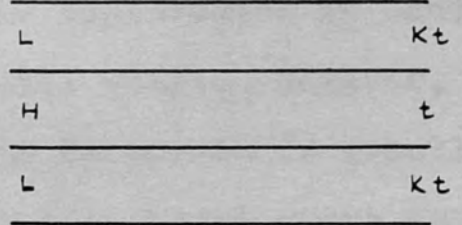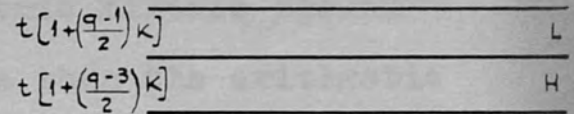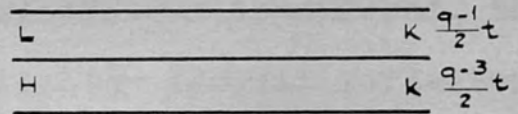
(c)   (d)

SYMMETRIC GEOMETRIC   SYMMETRIC ARITHMETIC

FIG. 3.4. STAGGERED MULTILAYERS

detail and values of R and ψ over the range 0.0 (0.01) 3.0

of σ/σ_0 were obtained. The calculations were repeated

for filters of different total numbers of layers (2q+1).

Most of the computations were carried out using a program

written in Extended Mercury Autocode on the London Univer-

sity 'Atlas' computer, but some of the initial computations

were performed on Elliott '803', using a program written in

Elliott Autocode.

In general, for the values of the ratios and

differences considered, the geometric filters showed

slightly broader reflectance bands than the arithmetic

filters with the same number of layers (see Table 3.1,

below). For filters consisting of fifteen films or less,

the improvement in bandwidth over a classical filter is

quite small. However, with increasing number of layers,

the bandwidth is greatly increased and there appears to be

no 'limiting' width as in the classical case. Some of the

results for the fifteen, twenty-five and thirty-five layer

asymmetric geometric filters are shown in Figs. 3.5 to 3.9.

It may be noted that the bandwidth appears to increase

as the ratio of the thickest to thinnest film in the

filter. A comparison of the bandwidths of various broad-

band reflecting multilayers is given in Table 3.1.
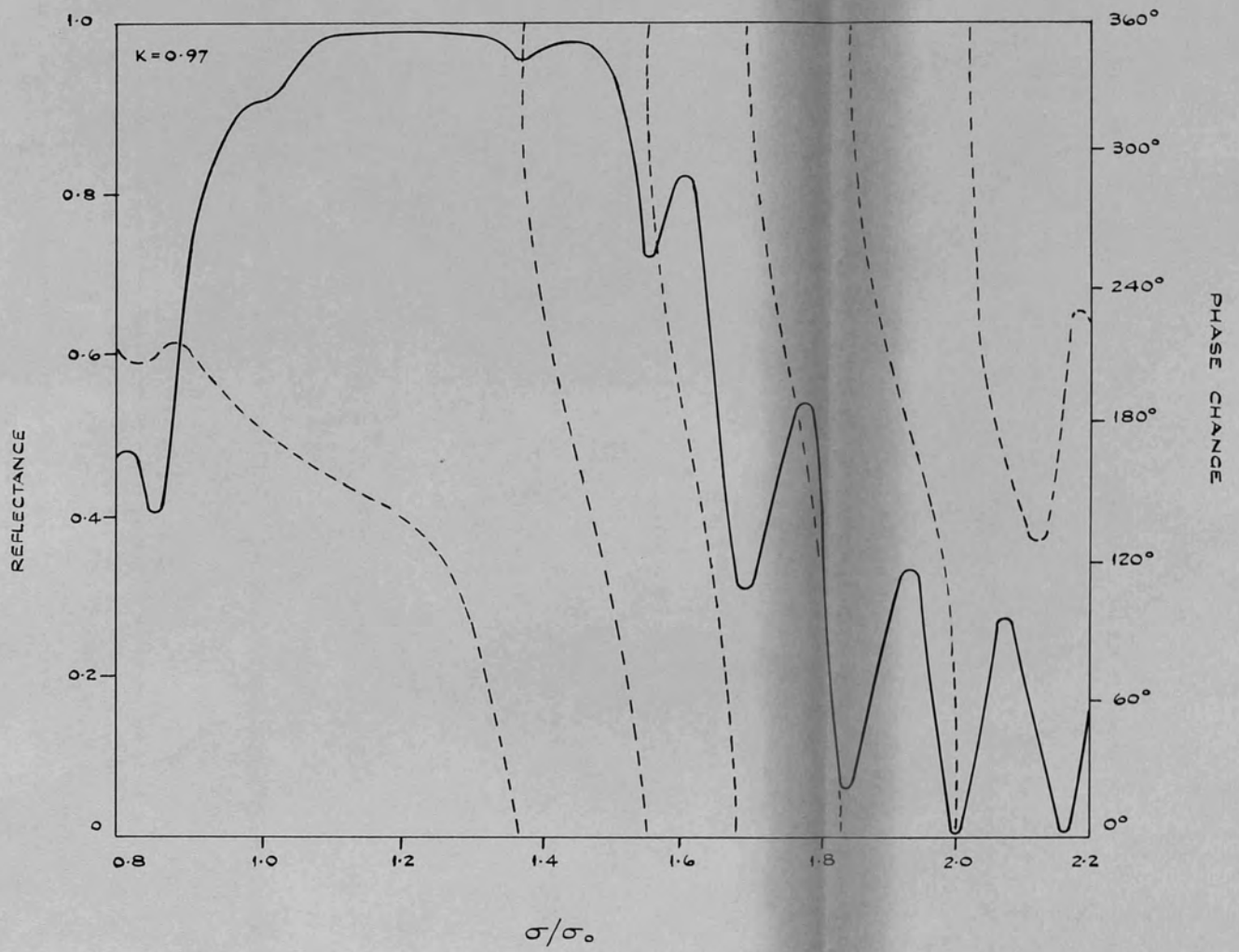
FIG. 3.5. 15-LAYER ASYMMETRIC GEOMETRIC FILTER.
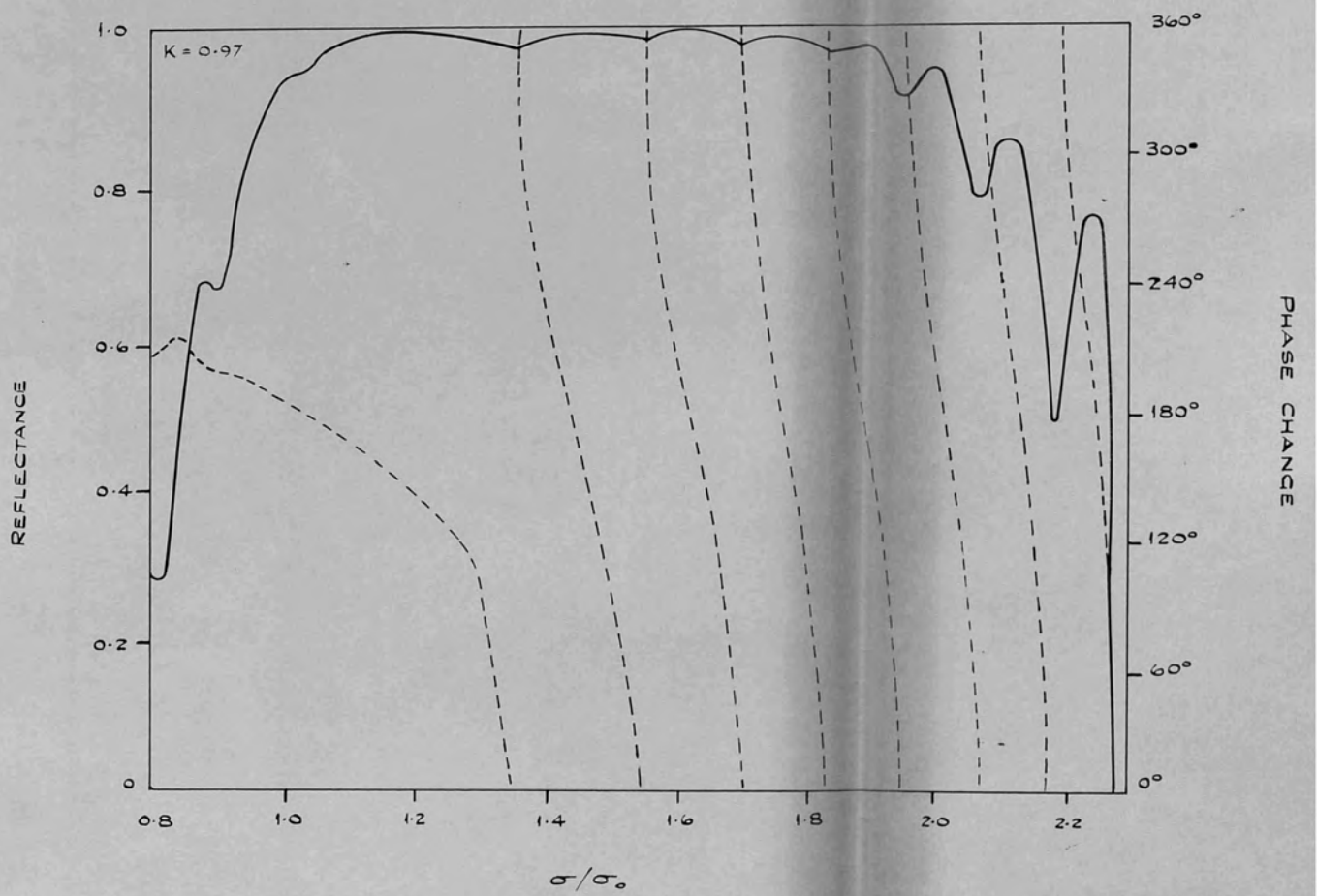
FIG. 3.6.   25-LAYER ASYMMETRIC GEOMETRIC FILTER
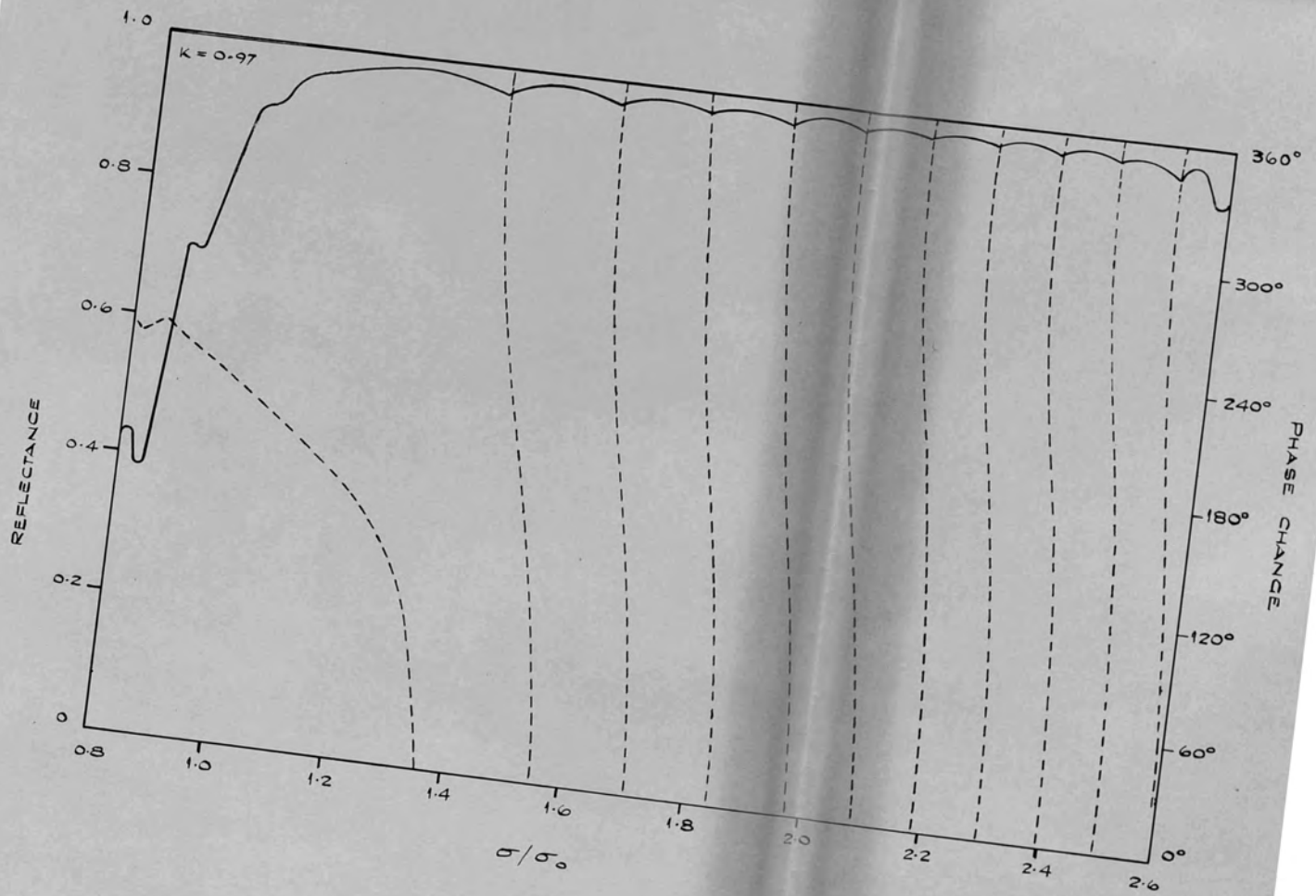
FIG. 3.7. 35-LAYER ASYMMETRIC GEOMETRIC FILTER

RATIO OF THICKNESS (K) = 1·03
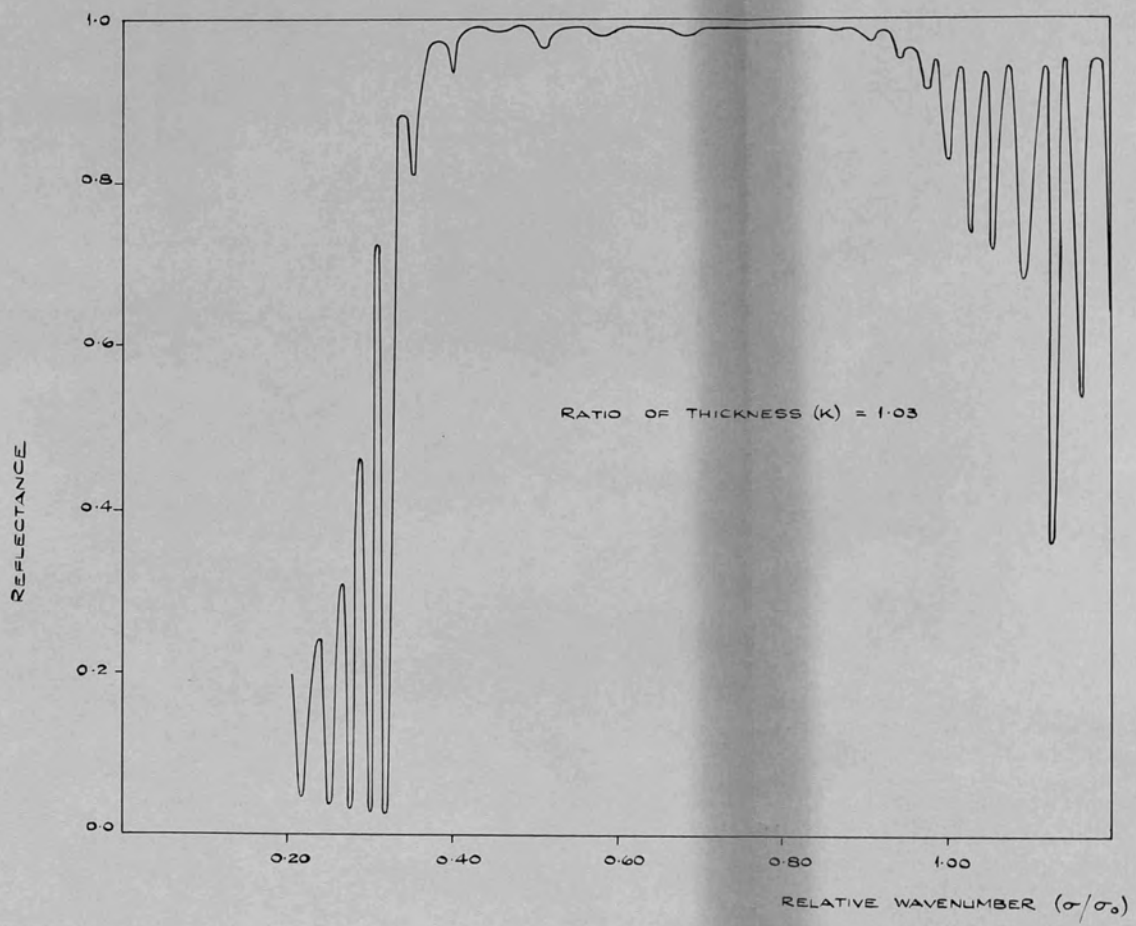
FIG. 3.9.   35-LAYER ASYMMETRIC GEOMETRIC FILTER
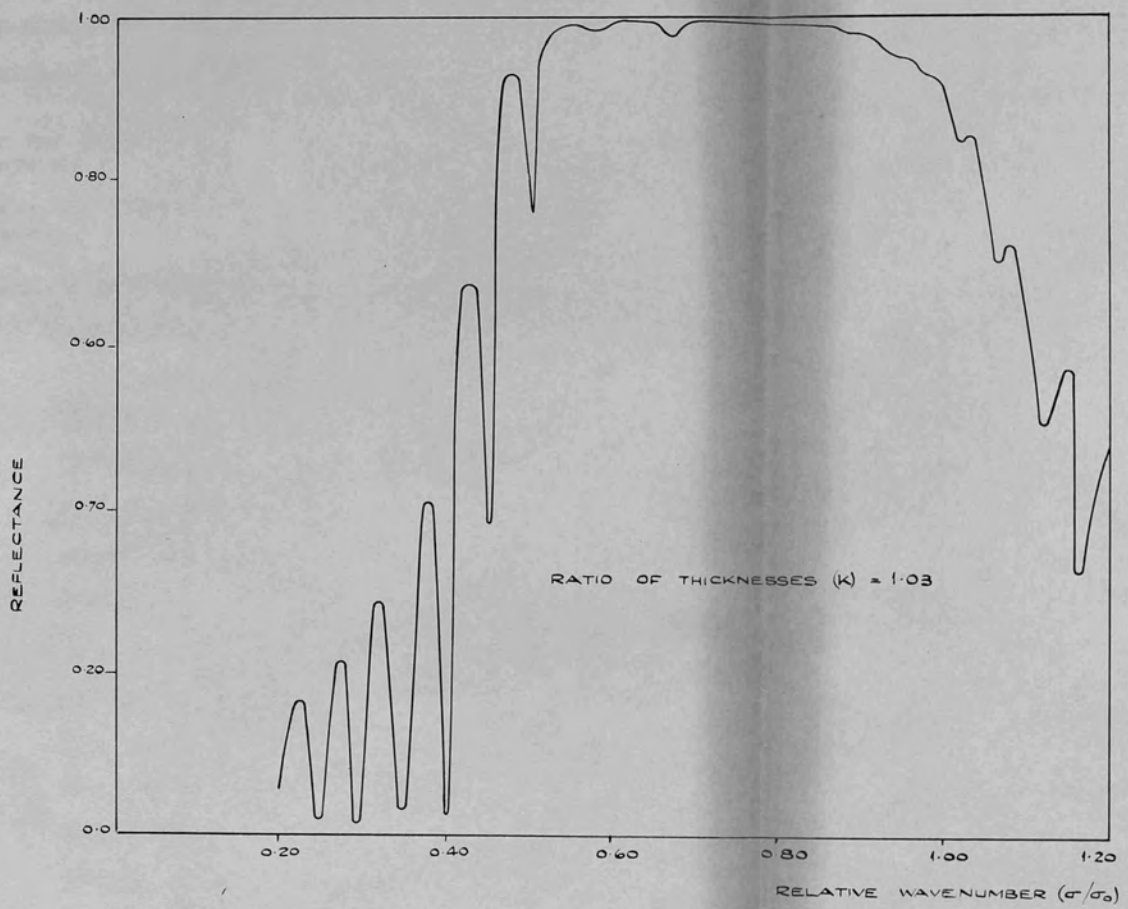
FIG. 3.8.   25-LAYER ASYMMETRIC GEOMETRIC FILTER.

TABLE 3.1

Type of Filter	Bandwidth for R > 90%	$\lambda_o = \frac{1}{\sigma_o}$
13 layer classical stack	430 nm - 610 nm	500 nm
Limiting value for infinite stack	425 nm - 620 nm	500 nm
Penselin and Steudel (13-layers)	380 nm - 610 nm	
Baumeister and Stone (15-layers)	410 nm - 740 nm	
Asymmetric Arithmetic Filters		
(K = -0.02)		
15-layers	419 nm - 625 nm	600 nm
25-layers	418 nm - 725 nm	700 nm
35-layers	330 nm - 840 nm	800 nm
(K = +0.02)		
15-layers	384 nm - 550 nm	400 nm
25-layers	377 nm - 655 nm	400 nm
35-layers	380 nm - 730 nm	400 nm
Asymmetric Geometric Filters		
K = 0.97		
15-layers	394 nm - 625 nm	600 nm
25-layers	342 nm - 730 nm	700 nm
35-layers	300 nm - 826 nm	800 nm
K = 1.03		
15-layers	400 nm - 580 nm	400 nm
25-layers	400 nm - 780 nm	400 nm
35-layers	305 nm - 790 nm	300 nm

The results for the symmetric filters (see Figs. 3.10, 3.11) are somewhat similar to those for the asymmetric ones, apart from the presence of a number of narrow band transmission peaks. The reason that these transmission bands occur will be explained in the next section when the phase characteristics of the multilayers are discussed. The regions of these bands were investigated more closely, at an interval of $\sigma/\sigma_o = 0.0005$. The bands were fairly narrow; in some cases their half-widths were smaller than $\frac{\Delta\sigma}{\sigma_o} = 0.002$.

§3.4. Phase characteristics of the

staggered multilayers

The phase change on reflection vs. wavenumber curves for some of the asymmetric goemetric filters are shown in Figs. 3.5 to 3.9, together with the reflectance curves. We see from these curves that the dispersion of phase change over most of the high-reflectance region is very large compared with that of a classical filter (see Table 3.2).

The $(2q + 1)$-layer symmetric filters can be considered as two q-layer asymmetric filters surrounding the central layer which acts as a spacer. We know from equations (3.1.1) and (3.1.4) that transmission bands will occur
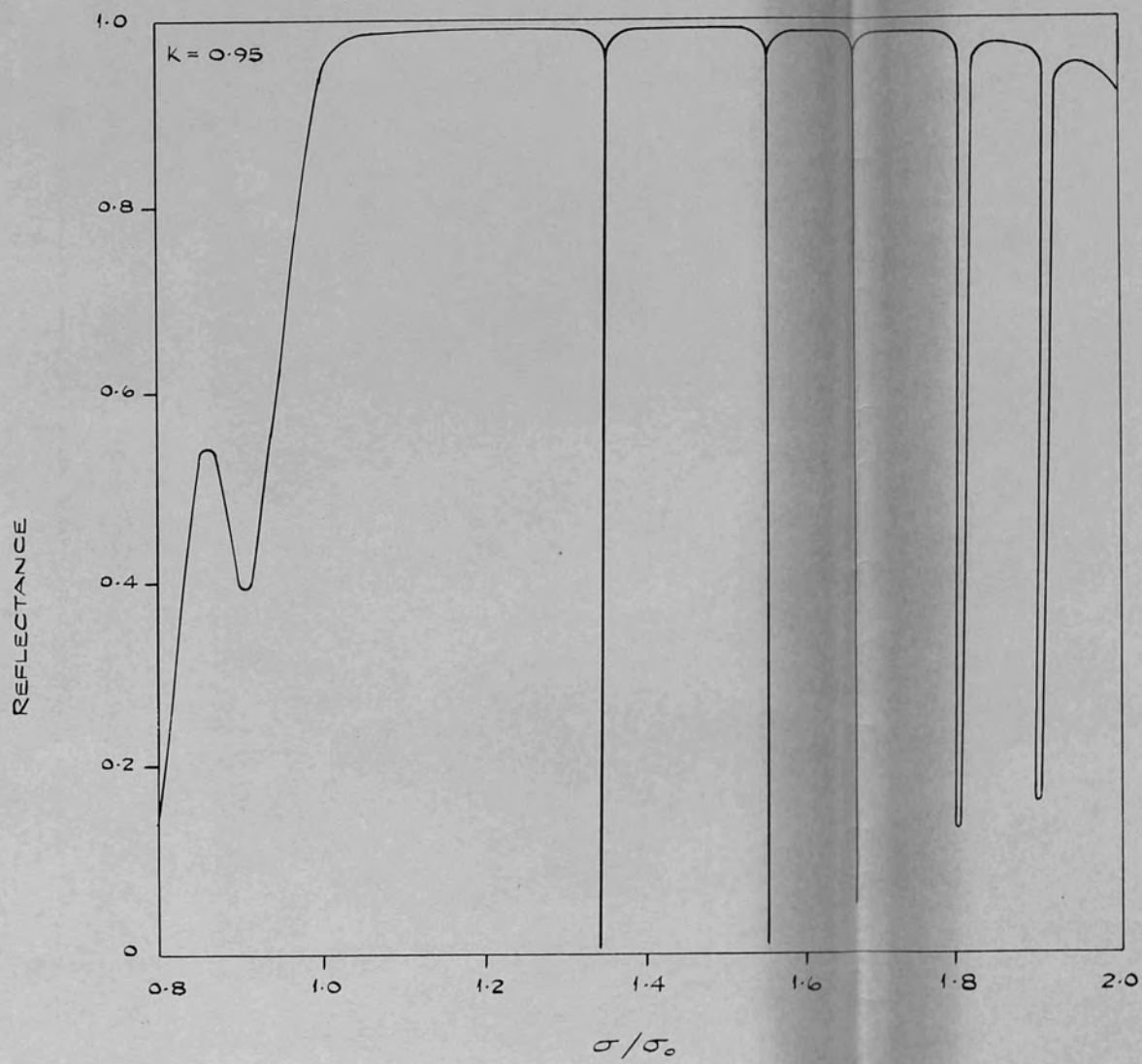
FIG. 3.10. 25-LAYER SYMMETRIC GEOMETRIC FILTER
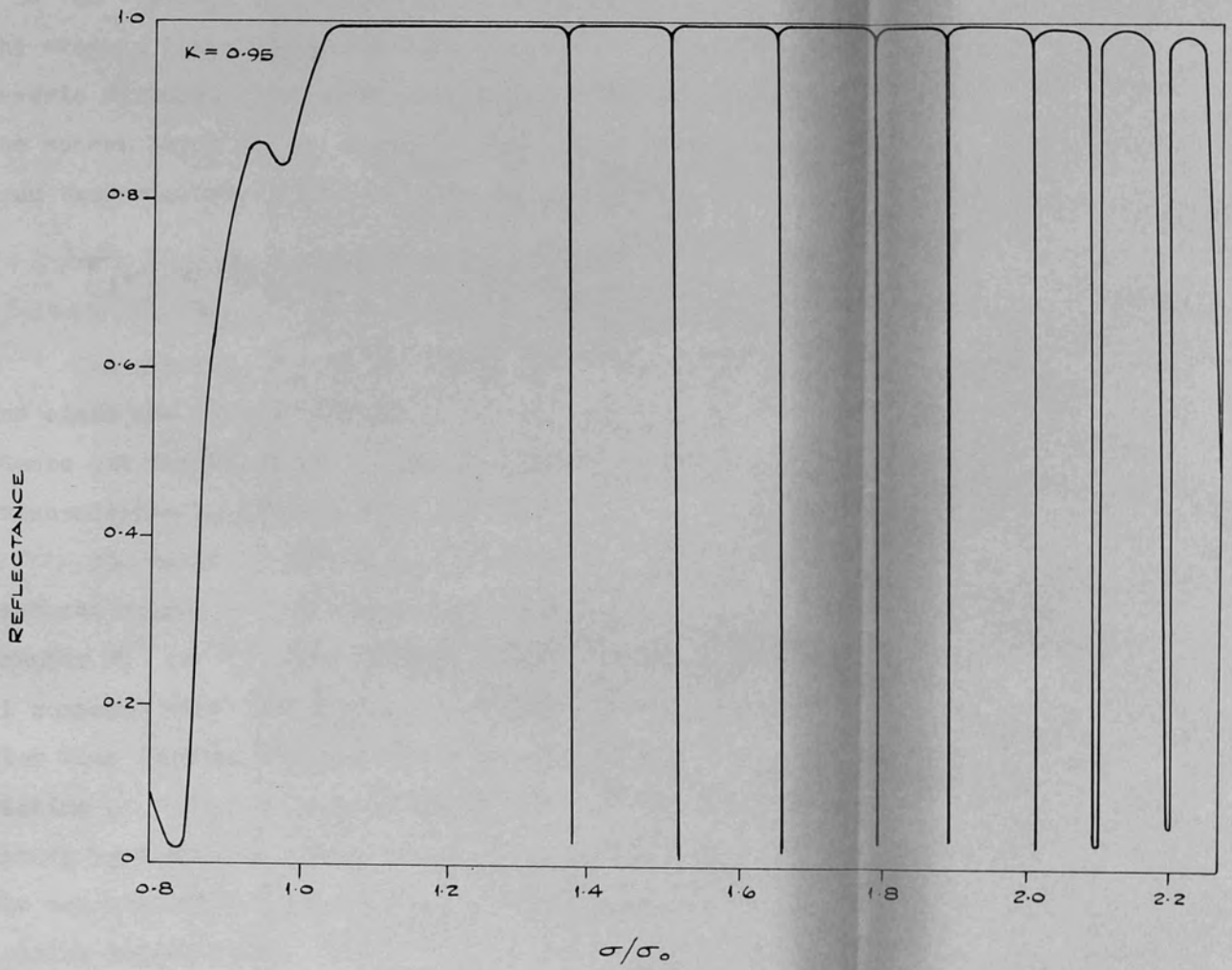
FIG. 3.11   35 - LAYER   SYMMETRIC   GEOMETRIC   FILTER

when

$$2\pi nd\sigma - \psi(\sigma) = \pm m\pi \qquad (3.4.1)$$

'nd' is the 'optical thickness' of the central layer, and $\psi(\sigma)$ is the average phase change on reflection of the two q-layer asymmetric filters. The phase changes are those occurring in the spacer layer at the spacer/filter boundaries. The maximum transmission at these points is given by

$$T(\sigma) = \frac{[1 - R_1(\sigma)][1 - R_2(\sigma)]}{[1 - R(\sigma)]^2} \qquad (3.4.2)$$

In general, R_1 and R_2 differ only by a small amount since one q-layer filter is bounded by the medium of incidence and the other by the substrate, so for the most part, the transmission is greater than 95% for these bands.

The value of ψ at the centre of the high-reflectance region of a classical stack (i.e. at the central wavenumber σ_0) is π. The phase dispersion for this case is small compared with that for the staggered stack, although greater than that of a metal reflector. Thus, for a filter consisting of two classical stacks (or two metal reflectors) separated by a spacer, condition (3.4.1) is satisfied only at the central wavenumber. However, if two broad-band reflecting multilayers are used in an interference filter, condition (3.4.1) is fulfilled at several points in the

high-reflectance region. This occurs for two reasons:
(i) the reflectance band is much wider than that of a
classical stack (ii) the phase dispersion is an order of
magnitude, or more, greater than in the classical case.
The phase dispersion characteristics of the Baumeister and
Stone filters are discussed by Baumeister and Jenkins (1957)
and Baumeister, Jenkins and Jeppesen (1959).

In the (2q+1)-layer symmetric filter, several
transmission bands would be expected in the high-reflectance
region as σ/σ_0 approaches 2.0, the point at which the
central layer has a phase thickness of π. Figs. 3.12,
3.13 show the graphs of $\psi(\sigma)$ and $2\pi nd\sigma$ as functions of
σ/σ_0 for the 25 and 35-layer filters respectively (ψ
is the average phase change of the component 12- or 17-layer
filters). The points of intersection give the positions of
the transmission bands. These points agree with the posi-
tions of the bands as shown in Figs. 3.10, 3.11.

The reflection characteristics of the asymmetric
filter may also be analysed in a similar manner to that
used above. In this case, the 'spacer' is again the layer
which has a phase thickness of π when $\sigma/\sigma_0 = 2.0$.
However, the spacer is now surrounded by a 2q-layer stag-
gered filter on one side and the medium of incidence on the
other. The reflectances of these 'effective interfaces'
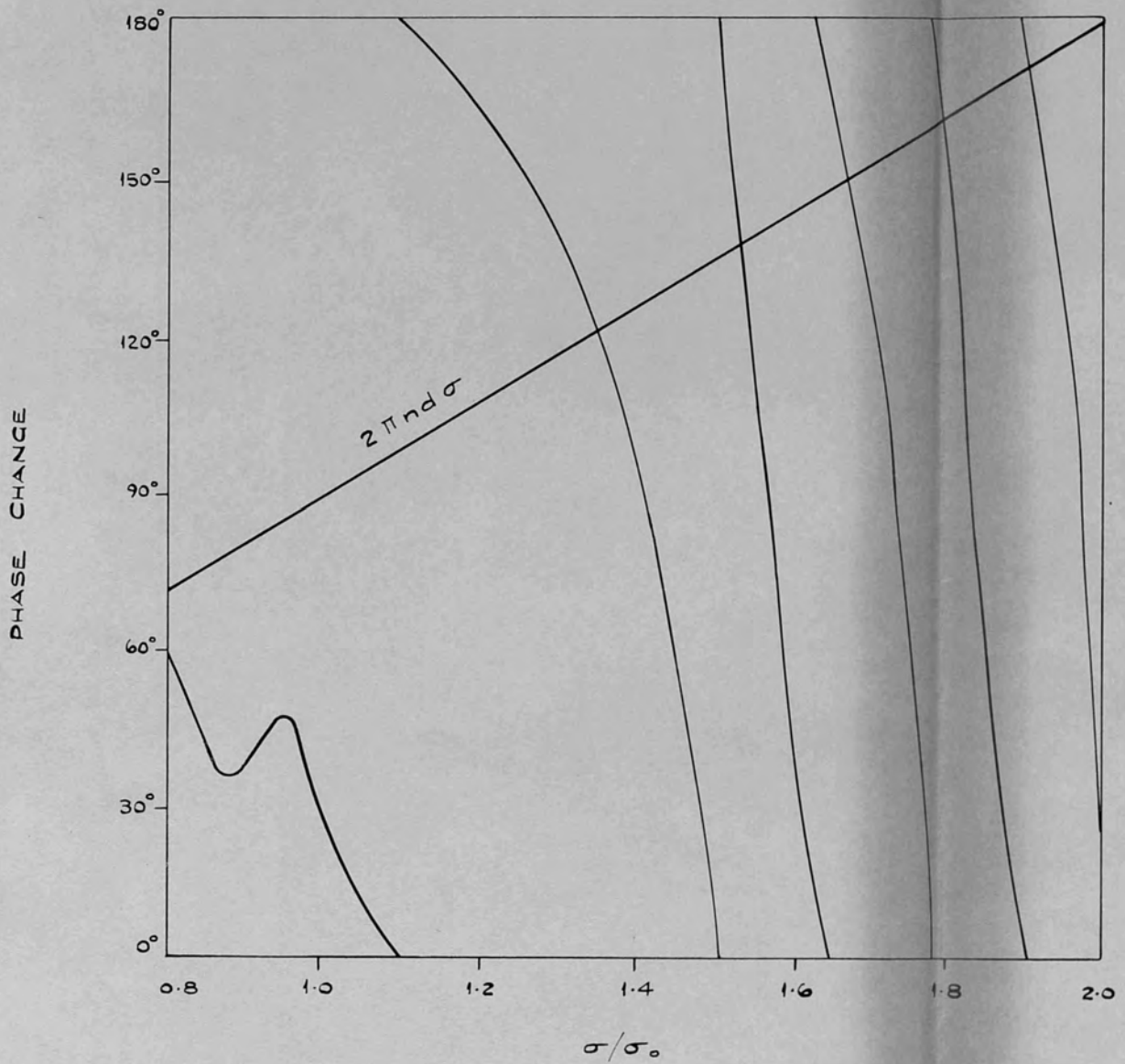
FIG. 3.12. GRAPHS OF $\gamma(\sigma)$ AND $2\pi nd\sigma$ FOR THE 25-LAYER SYMMETRIC GEOMETRIC FILTER.
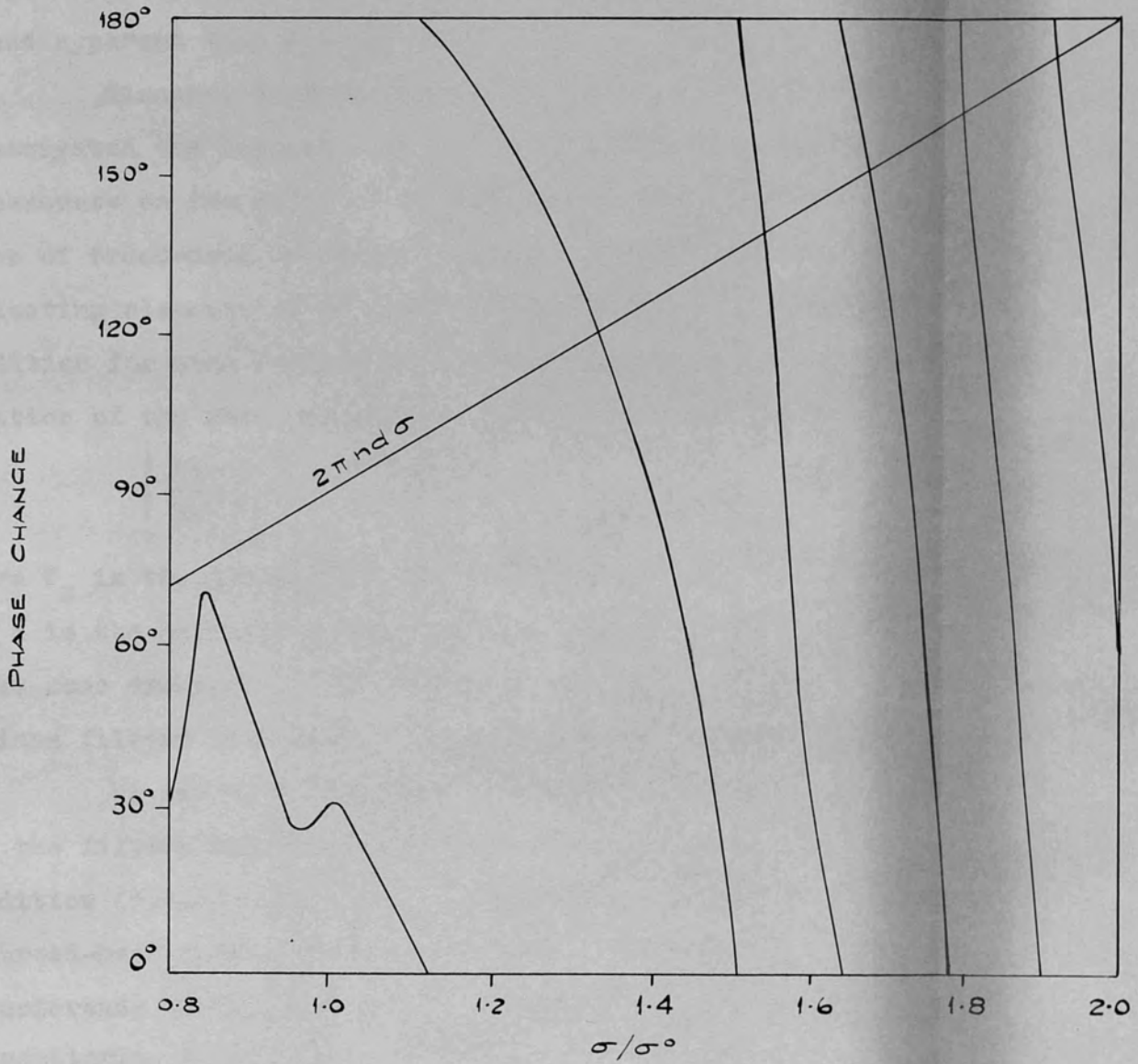
FIG. 3.13. GRAPHS OF $\gamma(\sigma)$ AND $2\pi nd\sigma$ FOR THE
35-LAYER SYMMETRIC GEOMETRIC FILTER.

will obviously be considerably different. Thus, we see
from equation (3.4.2) that the transmission peaks at wave-
numbers satisfying (3.4.1) will be very small, and this is
indeed apparent from Figs. 3.5 to 3.9.

Giacomo, Baumeister and Jenkins (1959) have
investigated the influence of random variations in layer
thicknesses on the width of the pass-band, when various
types of broad-band reflecting multilayers are used as the
reflecting elements of an interference filter. A necessary
condition for such variations to have minimum effect on the
position of the pass-band of an interference filter is

$$\left| \frac{\partial \psi}{\partial \sigma} \right| = 4 \pi n T_m$$

(3.4.3)

where T_m is the geometrical thickness of one of the mirrors
and n is the refractive index of the spacer. Table 3.2
gives some examples of the values of $4 \pi n T_m$ and $\left| \frac{\partial \psi}{\partial \sigma} \right|$ for
various filters used with a cryolite spacer of index 1.35.

We see that both the Baumeister and Stone filter
and the filters reported here come nearer to fulfilling
condition (3.4.3) than a classical filter. Thus, the use
of broad-band filters as the reflecting elements of an
interference filter renders the filter far less sensitive
to monitoring errors than if classical stacks are used.

TABLE 3.2

Type of filter	λ_o (nm.)	$4\pi n\, T_m$ (μm-radians)	Approx. value of $\left|\frac{\partial\psi}{\partial\sigma}\right|$ over the high-reflectance region (μm-radians)
Baumeister and Stone (15-layers)		20.4	10-23
15-layer Asymmetric Geometric	600	17.5	11-30
25-layer Asymmetric Geometric	700	29.9	13-55
35-layer Asymmetric Geometric	800	42.0	15-70
15-layer Classical Stack	550	20.8	1.8

§3.5. Closed Form expression for 'staggered'

multilayers

In Chapter I, the closed form expressions for periodic multilayers were obtained in terms of Tschebyscheff polynomials (of the second kind). For small variations in layer thicknesses from this classical form, the corresponding expressions for staggered reflectance filters may also be

obtained.

We consider multilayers of the form $\left[M_H \ M_L \right]^q M_H$ where the phase thicknesses of the layers are β, $\beta + \delta$, $\beta + 2\delta$, ... $\beta + 2q\delta$. We assume $2q\delta$ is small compared with β, so we can make the following approximation:-

$$\cos(\beta + m\delta) = \cos\beta - m\delta\sin\beta$$
$$\sin(\beta + m\delta) = \sin\beta + m\delta\cos\beta \qquad (3.5.1)$$

for $m = 1, 2, \ldots 2q$. For layers of equal thickness

$$[A] = [M_H \ M_L] = \begin{bmatrix} a_{11} & a_{12} \\ a_{21} & a_{22} \end{bmatrix} = \begin{bmatrix} \cos^2\beta - \dfrac{n_L}{n_H}\sin^2\beta & i\left(\dfrac{1}{n_H} + \dfrac{1}{n_L}\right)\sin\beta\cos\beta \\ i(n_H + n_L)\sin\beta\cos\beta & \cos^2\beta - \dfrac{n_H}{n_L}\sin^2\beta \end{bmatrix}$$

$$(3.5.2)$$

and for the staggered case /neglecting terms $O(\delta^2)$ 7

$$\left[M_{H_{2m-1}} M_{L_{2m}} \right] = \begin{bmatrix} \cos^2\beta - \dfrac{n_L}{n_H}\sin^2\beta - (4m-3)\delta\left(1 + \dfrac{n_L}{n_H}\right)\sin\beta\cos\beta \\ i\left[\left(\dfrac{1}{n_L} + \dfrac{1}{n_H}\right)\sin\beta\cos\beta + (4m-3)\delta\left(\dfrac{\cos^2\beta}{n_L} - \dfrac{\sin^2\beta}{n_H}\right) + (2m-2)\delta(n_H - n_L)\right] \\ i\left[(n_H + n_L)\sin\beta\cos\beta + (4m-3)\delta(n_L\cos^2\beta - n_H\sin^2\beta) + (2m-2)\delta(n_H - n_L)\right] \\ \cos^2\beta - \dfrac{n_H}{n_L}\sin^2\beta - (4m-3)\delta\left(1 + \dfrac{n_H}{n_L}\right)\cos\beta\sin\beta \end{bmatrix}$$

$$(3.5.3)$$

$$= A + (4m-3)i\delta B + (2m-2)i\delta C \qquad (3.5.4)$$

where

$$B = \begin{pmatrix} \dfrac{ia_{21}}{n_H} & \dfrac{a_{11}}{n_L} \\ n_L a_{22} & in_H a_{12} \end{pmatrix}, \qquad C = (n_H - n_L)\begin{pmatrix} 0 & \dfrac{-1}{n_H n_L} \\ 1 & 0 \end{pmatrix}$$

Then the matrix product for the staggered case is given by

$$\left[M_H \, M_L\right]^q = (A + i\delta B)(A + 5i\delta B + 2i\delta C) \cdots\cdots (A + [4q-3]i\delta B + [2q-2]i\delta C)$$

$$(3.5.5)$$

which may be written in the form

$$\left[M_H \, M_L\right]^q = A^q + i\delta\left\{BA^{q-1} + 5ABA^{q-2} + \cdots + (4q-3)A^q B + 2ACA^{q-2} + \cdots + (2q-2)A^q C\right\}$$

$$(3.5.6)$$

to first order in δ. We know from (1.4.12)

$$A^m = S_{m-1}(x)A - S_{m-2}(x)I$$

where

$$X = a_{11} + a_{22}$$

Thus in general,

$$A^{m-1}B\,A^{q-m} = \left[S_{m-2}(x)A - S_{m-3}(x)I\right]B\left[S_{q-m-1}(x)A - S_{q-m-2}(x)I\right]$$

$$= \left\{S_{m-2}S_{q-m-1}ABA - S_{m-3}S_{q-m-1}BA - S_{q-m-2}S_{m-2}AB + S_{m-3}S_{q-m-2}B\right\}$$

$$(3.5.7)$$

Then, using (3.5.6)

$$\left[M_H \, M_L\right]^q = \left[S_{q-1}(x)A - S_{q-2}(x)I\right] + i\delta\left\{ABA \sum_{m=2}^{q-1}(4m-3)S_{m-2}S_{q-m-1}\right.$$

$$- BA\left[\left(\sum_{m=2}^{q-1}(4m-3)S_{m-3}S_{q-m-1}\right) - S_{q-2}\right] - AB\left[\left(\sum_{m=2}^{q-1}(4m-3)S_{q-m-2}S_{m-2}\right) - (4q-3)S_{q-2}\right]$$

$$+ B\left[\left(\sum_{m=2}^{q-1}(4m-3)S_{q-m-2}S_{m-2}\right) - (4q-2)S_{q-3}\right]$$

$$(3.5.8)$$

$$+ ACA \sum_{m=2}^{q-1}(2m-2)S_{m-2}S_{q-m-1} - CA\sum_{m=2}^{q-1}(2m-2)S_{m-3}S_{q-m-1}$$

$$\left. - AC\left[\left(\sum_{m=2}^{q-1}(2m-2)S_{q-m-2}S_{m-2}\right) - (2q-2)S_{q-2}\right] + C\left[\sum_{m=2}^{q-1}(2m-2)S_{m-3}S_{q-m-2} - (2q-2)S_{q-3}\right]\right\}$$

Expressing $S_m(X)$ in the form given by (1.4.14)

$$S_m(X) = \frac{\sin(m+1)\,\textcircled{H}}{\sin\textcircled{H}}, \quad X = 2\cos\textcircled{H}, \text{ for } |X| \leq 2$$

$$S_m(X) = \frac{\sinh(m+1)\,\underline{\Phi}}{\sinh\underline{\Phi}}, \quad |X| = 2\cosh\underline{\Phi}, \text{ for } |X| > 2$$

and using

$$\sum_{m=2}^{q-1} \cos(p-2m)\,\textcircled{H} = \frac{\sin(2q-1-p)\textcircled{H} - \sin(3-p)\textcircled{H}}{2\sin\textcircled{H}} \quad (3.5.9)$$

$$\sum_{m=2}^{q-1} \sin(p-2m)\,\textcircled{H} = \frac{\cos(2q-p-1)\textcircled{H} - \cos(3-p)\textcircled{H}}{2\sin\textcircled{H}}$$

$$\sum_{m=2}^{q-1} (p-2m)\cos(p-2m)\,\textcircled{H} = \frac{d}{d\textcircled{H}}\left[\sum_{m=2}^{q-1} \sin(p-2m)\textcircled{H}\right]$$

$$= \frac{(p-2)\cos(p-4)\textcircled{H} - (p-4)\cos(p-2)\textcircled{H} + (2q-p-2)\cos(2q-p)\textcircled{H} - (2q-p)\cos(2q-p-2)\textcircled{H}}{2[1-\cos 2\textcircled{H}]}$$

$$(3.5.10)$$

For $|x| \leq 2$ we may express (3.5.8) in the form

$$[M_4 M_L]^q = \left[\frac{A\sin q\,\textcircled{H}}{\sin\textcircled{H}} - \frac{I\sin(q-1)\textcircled{H}}{\sin\textcircled{H}}\right] + i\delta\left\{\frac{1}{2\sin^2\textcircled{H}}\left[\frac{\sin(q-2)\textcircled{H}}{\sin\textcircled{H}} - (q-2)\cos(q-2)\textcircled{H}\right]\right.$$
$$\left. \times \left[(2q-1)\,ABA + (q-1)\,ACA\right]\right.$$

$$-\frac{1}{2\sin^2\theta}\left[\frac{\sin(q-2)\theta\,\cos\theta}{\sin\theta} - (q-2)\cos(q-2)\theta\right]\left[(2q+1)BA+qCA+(2q-3)AB+(q-2)AC\right]$$

$$+\frac{1}{2\sin^2\theta}\left[\frac{\sin(q-2)\theta}{\sin\theta} - (q-2)\cos(q-3)\theta\right]\left[(2q-1)B+(q-1)C\right]$$

$$\hspace{8cm}(3.5.11)$$

$$-\frac{\sin(q-2)\theta}{\sin\theta}\left[(4q-2)B+(2q-2)C\right] - \frac{\sin(q-1)\theta}{\sin\theta}\left[(2q-2)AC+BA+(4q-3)AB\right]\Big\}$$

For $|x| > 2$, the corresponding form is given by

$$(-1)^q\left[M_H M_L\right]^q = \left[\frac{A\sinh q\Phi}{\sinh\Phi} - \frac{I\sinh(q-1)\Phi}{\sinh\Phi}\right] + i\delta\left\{\frac{1}{2\sinh^2\Phi}\left[(q-2)\cosh(q-1)\Phi - \frac{\sinh(q-2)\Phi}{\sinh\Phi}\right]\right.$$
$$\times\left[(2q-1)ABA + (q-1)ACA\right]$$

$$+\frac{1}{2\sinh^2\Phi}\left[\frac{\sinh(q-2)\Phi\cosh\Phi}{\sinh\Phi} - (q-2)\cosh(q-2)\Phi\right]\left[(2q+1)BA+qCA+(2q-3)AB+(q-2)AC\right]$$

$$+\frac{1}{2\sinh^2\Phi}\left[(q-2)\cosh(q-3)\Phi - \frac{\sinh(q-2)\Phi}{\sinh\Phi}\right]\left[(2q-1)B+(q-1)C\right]$$
$$\hspace{9cm}(3.5.12)$$

$$\left. -\frac{\sinh(q-1)\Phi}{\sinh\Phi}\left[(2q-2)AC+BA+(4q-3)AB\right] - \frac{\sinh(q-2)\Phi}{\sinh\Phi}\left[(4q-2)B+(2q-2)C\right]\right\}$$

This analysis is immediately applicable to the arithmetic filters. Now, for small variations, the ratio of the geometric progression is of the form $(1 + \delta)$ where $|\delta| << 1$ Then we may approximate

$$(1+\delta)^q = 1 + q\delta + O(\delta^2) \doteq 1 + q\delta \hspace{3cm}(3.5.13)$$

for $|q\delta| << 1$. Thus the results for the geometric case

are similar to those for the arithmetic case for the values of δ for which we may use the above analysis; i.e. for very small variations.

CHAPTER IV: REVIEW OF DESIGN METHODS USED

IN OPTICAL FILTER PRODUCTION

§4.1.   Basic Methods of Filter Design

The problem of designing a multilayer combination
with specified properties is very complex and there is no
simple method of solution for all problems. In general
there is usually no means of obtaining the 'true' solution
although very good approximations may be obtained. The
advent of large, high-speed digital computers has proved a
great asset both to basic thin film calculations and to
approximate design methods. Several design methods have
evolved in the last few years, which owe their existence to
the availability of these computers. Until recently, the
design methods fell into one of two main types - namely,
analytic methods and successive iteration methods. In the
last year or so, one or two 'automatic' design methods have
appeared in the literature. These are automatic because,
unlike the successive iteration methods, they need no start-
ing design.

Theoretically, one might expect to achieve a
desired result by writing down the explicit expressions for
the reflectance R or transmittance T at different wavelengths

and solving them for the values of the design variables which give the required values of R and T at these wavelengths. However, in general, for more than one or two layers, the resulting equations are far too difficult to write down so their solution becomes almost impossible. In any case, the desired function is usually a continuous curve, so an infinite number of design variables would be needed to obtain an exact solution. In some cases, both the desired function and the explicit expressions for the inverse of transmittance may be expressed as a series expansion in terms of wavenumber. The coefficients of the power series may then be equated and the solution of the resulting simultaneous equations will yield the required construction parameters for the multi-layers. This method has been used by Pohlack (1960). In other cases, analytic methods which are used in electric filter synthesis may be applied. These electrical engineering techniques could prove extremely useful, but there is a minor problem of different language and training to be overcome in communication between Electrical Engineers and Opticists.

In the successive iteration methods one must start with a design which is a fairly good approximation to the required curve. Small changes are made in the design variables (usually the layer thicknesses) to improve the performance of the system and the process is repeated until

either a satisfactory approximation to the required design
is achieved or until no further improvement may be obtained.
An automatic design method chooses the best starting point
from a range of values of the design variables, so one need
not know an approximate design in this case.

Much of the early design work was applied to the
production of low-reflecting coatings, so initially, a brief
discussion of some of the methods used in this application
will be given.

§4.2. Design Techniques for Low-reflecting

coatings

From equation (1.3.8) it can be seen that for a
single layer to have zero reflectance at normal incidence
for some wavelength λ , such that the thickness of the layer
is $\frac{\lambda}{4}$, its index must be given by

$$n_1 = \sqrt{n_0 \, n_{sub}} \qquad\qquad (4.2.1)$$

i.e. its index must be the geometric mean of the indices of
the surrounding media. The film is then said to 'match' the
surrounding media for this wavelength. However, condition
(4.2.1) is often difficult to fulfill and it is usually
advantageous to use two or three layer coatings for this

purpose. The latter have low reflectance over a wider spectral range than that of a single-layer coating .

The thicknesses of the double-layer coatings have usually taken either the 'double quarter wave' form or the 'quarter-wave, half-wave' form, whereas the most common arrangements of thicknesses for the triple-layer coatings are 'triple quarter-wave' and 'quarter-wave, half-wave, quarter wave.' The spectral reflectivity for some of these coatings is given in Fig. 4.1. The exact formulae for zero reflectance were first given by Mooney (1945) and Lockhart and King (1946). For a double quarter-wave coating to have two positions of zero reflectance one must have

$$n_1 n_2 = n_0 n_{sub} \qquad (4.2.2)$$

and the condition for a triple quarter-wave filter to have three positions of zero reflectance is

$$n_1 n_3 = n_2^2 = n_0 n_{sub} \qquad (4.2.3)$$

One of the most useful methods for producing coatings which anti-reflect at one particular wavelength is by use of vector diagrams (see §1.6). This is an approximate method (it ignores multiple reflections) but nevertheless can produce results accurate enough to serve as a guide. We saw that the resultant reflectance, R, of a system of N films may be obtained from the vector sum of the Fresnel
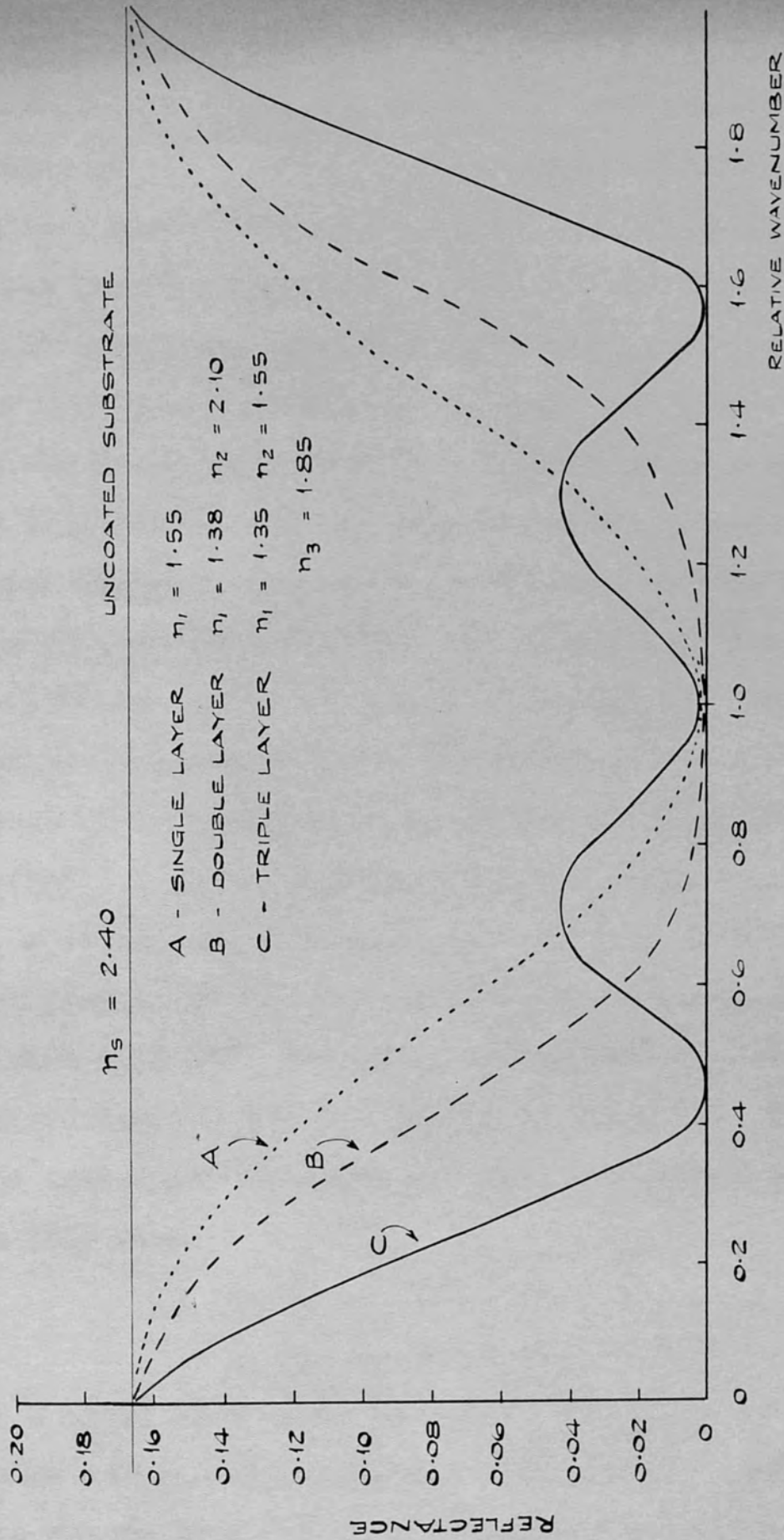
FIG. 4.1 COMPUTED REFLECTIVITY OF ANTIREFLECTION
MULTIPLE QUARTER-WAVE COATINGS
AT NORMAL INCIDENCE

coefficients r_1, r_2 ... r_{N+1}, of the layers $\underline{/}$Figure 1.3(b)$\underline{/}$.
Hence, if r_1, ... r_{N+1} form a closed polygon, the resultant
reflectance will be zero. Then for any given materials for
a two layer coating, it is possible to obtain the required
thicknesses such that the reflectance will be zero for a
particular wavelength, by applying the cosine and sine laws
to the triangle obtained by the vectors r_1, r_2, r_3. Thus,
in this method, the 'design variables' are chosen to be the
layer thicknesses - this can be particularly useful if one
has only one or two available materials. The method is best
illustrated by an example:- Consider the design of a low
reflecting coating using two layers, CeO_2 and MgF_2 on glass
which is to give zero reflectance at 632.8 nm. n_0(air) = 1.0,
n_1(MgF_2) = 1.38, n_2(CeO_2) = 2.30, n_{sub} = 1.52 so that
r_1 = -0.16, r_2 = -0.25, r_3 = +0.204. A triangle may be
constructed whose sides are proportional to r_1, r_2, r_3 (see
Figure 4.2) and from this, values for δ_1, δ_2, the phase
thicknesses of the two layers at 632.8 nm., may be obtained.
The optical thicknesses are then determined from (1.2.2).
In this case

$$n_1 d_1 = 110.3 \text{ nm.}$$
$$n_2 d_2 = 281.5 \text{ nm.}$$

As a check that these values of thickness gave a very low
value for $\underline{R}$, the reflectance was calculated exactly using
the matrix method and was found to be less than 0.0001.
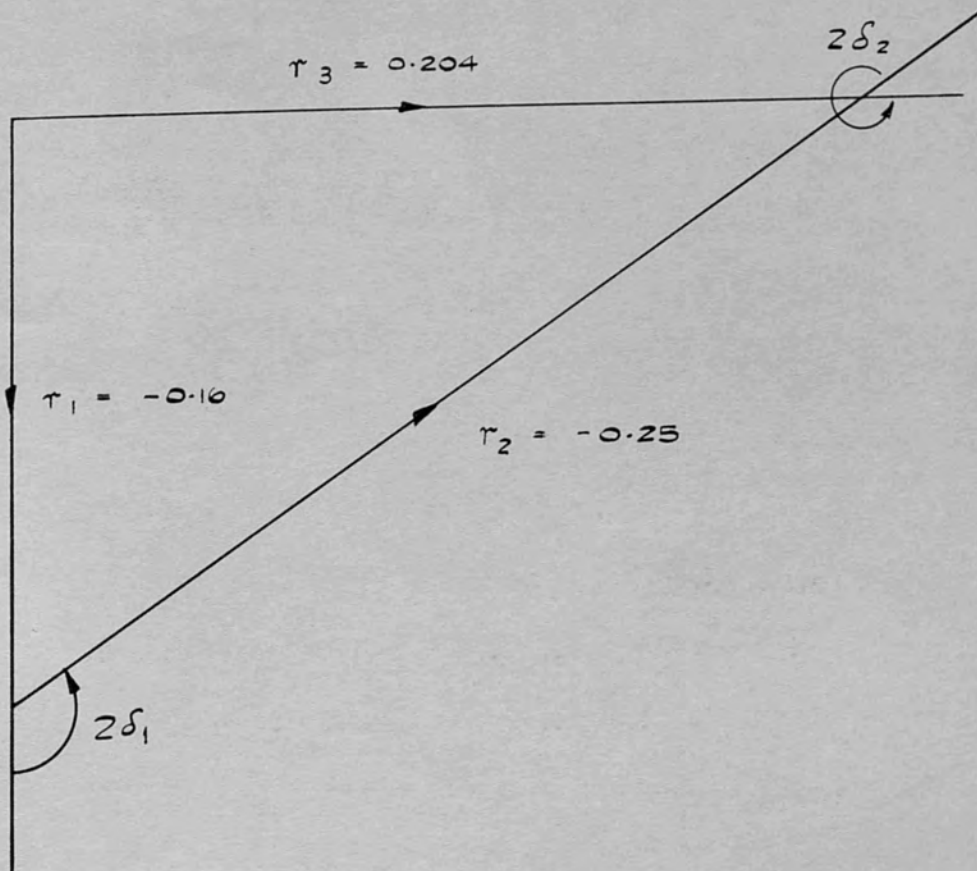
FIG. 4.2 TWO-LAYER ANTIREFLECTION COATING
FOR 632·8 nm

For some applications a coating is desired to anti-reflect at more than one wavelength. Such a coating is said to be achromatised. Methods of achromatising two and three films have been discussed by Vasicek (1953) and Turner (1950). In order that the coating be achromatised at two points the vector diagram must close in symmetric positions on either side of some reference phase position /Fig.4.3(a)7. For a three-layer coating to be achromatised at three wavelengths, the vector diagram must also close at the central phase position /Fig.4.3(b)7. This means that the algebraic sum of the Fresnel coefficients should be zero. Thus, the quadri-lateral formed by r_1, r_2, r_3, r_4 circumscribes a circle and this fact may be used to calculate $p = \dfrac{r_1}{r_2}$, $q = \dfrac{r_1}{r_3}$, $r = \dfrac{r_1}{r_4}$ so that the values of n_1, n_2, n_3 may be obtained for given phase thicknesses (Vasicek). Turner suggests using film thicknesses in the ratio $1 : 2 : \ldots : N$ for an N-layer filter, the thickness of the first layer being a quarter-wave at the centre of symmetry. Again the method is best illus-trated by a practical example:- The He-Ne laser may be made to operate at 3390 nm. and at 632.8 nm. If elements are to be inserted in the resonant cavity, it is convenient if they are anti-reflected at both these wavelengths. Consider a design of an anti-reflecting system for use on quartz (n_{sub} for quartz = 1.457 at 632.8 nm and 1.409 at 3390 nm). As the ratio of the wavelengths to be achromatised is 5.357,
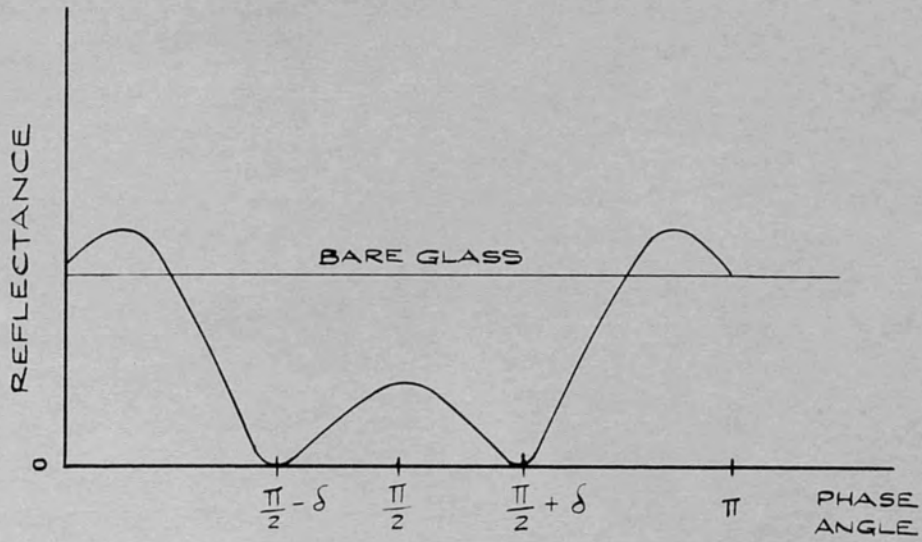
(a) COATING ACHROMATISED AT TWO POINTS
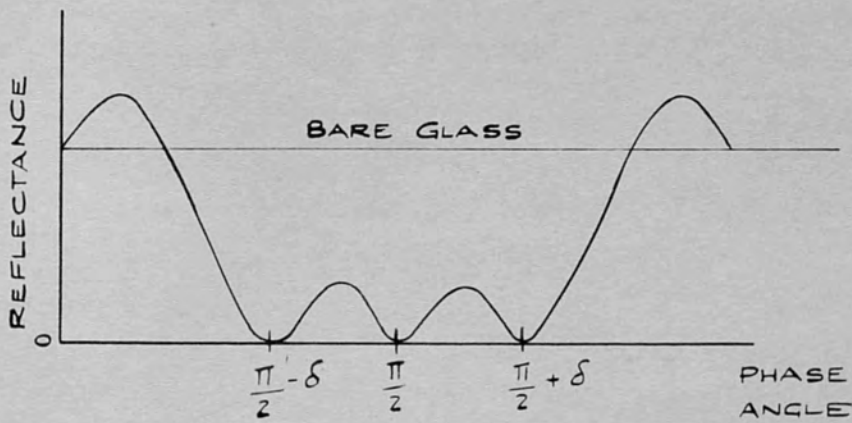
(b) COATING ACHROMATISED AT THREE POINTS

FIG. 4.3 ACHROMATISED COATINGS

the periodic property of reflectance may be used, so that
one considers reflectance zeros at $\frac{\pi}{2}$, $\frac{\pi}{2} \pm \delta$, and $\frac{5\pi}{2}$, $\frac{5\pi}{2} \pm \delta$.
For real refractive indices, values of $\delta \doteqdot 5°$, $6°$ and $7.5°$
will give exact achromatisation. However, it is seen from
Table 4.1, below, that the reflectivity is low at both wave-
lengths for values of δ up to $30°$. We may thus obtain
approximate achromatisation for any value of $0 < \delta < 30°$.
If x_1, x_2, x_3 are the phase thicknesses of the layers at
$\frac{\pi}{2} - \delta$ ($x_2 = 2x_1$, $x_3 = 3x_1$) a series of values of n_1, n_2, n_3
may be obtained for $60° < x_1 < 90°$. If n_1, n_2, n_3 are
plotted against x_1 (see Fig.4.4), then for any value of x_1,
a set of values n_1, n_2, n_3 is obtained which may be used as
an anti-reflecting coating achromatised at 632.8 nm. and
3390 nm.

TABLE 4.1

δ	$5°$	$7.5°$	$15°$	$20°$	$25°$	$27.5°$
x_1	$85°$	$82.5°$	$75°$	$70°$	$65°$	$62.5°$
p	0.5671	0.5823	0.6830	0.8440	1.2993	2.1567
q	-1.0313	-1.0731	-1.3660	-1.8794	-3.5016	-6.7959
r	-4.849	-4.6639	-3.7322	-2.8794	-1.9383	-1.4631
n_1	1.2641	1.2784	1.2903	1.3319	1.4716	1.8052
n_2	1.9634	1.9574	1.8783	1.8722	1.9782	2.3595
n_3	1.5288	1.5354	1.5594	1.6085	1.7752	2.1682
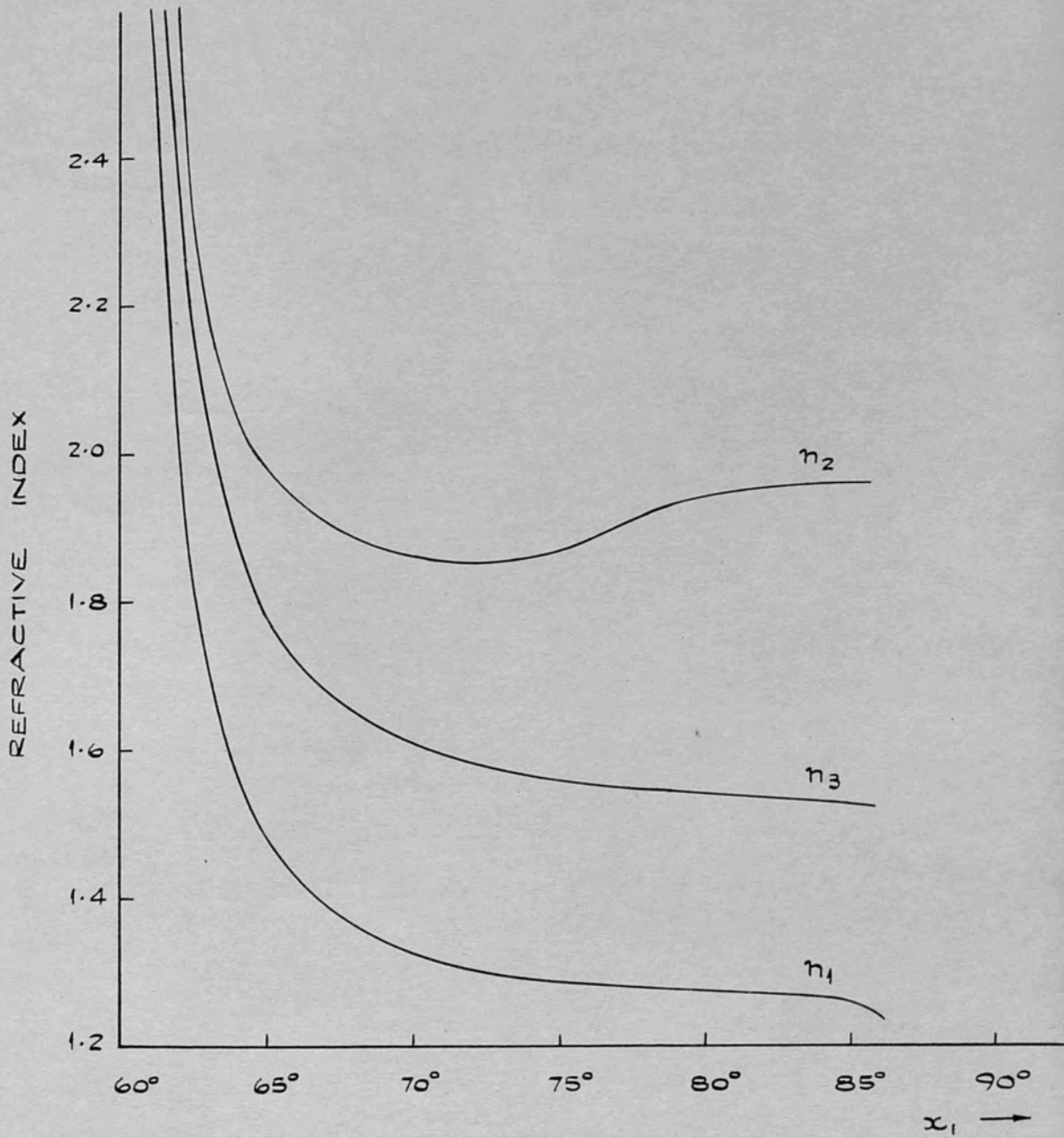
FIG. 4.4. INDICES FOR THE THREE LAYER
ACHROMATISED COATING.

Table 4.1 continued.

$R_{632.8\ nm}$%	0.0023	0.002	0.0098	0.0247	0.098	0.015
$R_{3390\ nm}$%	0.0257	0.0192	0.0573	0.066	0.0347	0.1696

The monitoring wavelength for any set of indices is given by

$$\lambda_0 = \frac{450}{450+\delta} \times 632.8\ nm. \qquad \delta \leq 5°$$

$$\lambda_0 = 632.8\ nm. \qquad 5° < \delta < 7.5°$$

$$\lambda_0 = \frac{450}{450-\delta} \times 632.8\ nm. \qquad \delta \geq 7.5°$$

As an example one may consider the result for $\delta = 25°$ for which an achromatised anti-reflecting coating may be produced for 632.8 nm. and 3390 nm by monitoring at $\lambda_0 = 669.4$ nm.:-

15 $\frac{\lambda_0}{4}$ layers of Lead Fluoride $\qquad (n_3 = 1.76)$

10 $\frac{\lambda_0}{4}$ layers of Tin Oxide $\qquad (n_2 = 1.96)$

5 $\frac{\lambda_0}{4}$ layers of Barium Fluoride $\qquad (n_1 = 1.47)$

The result may be checked by the matrix method, and for this coating it was found $R_{632.8\ nm} = 0.083\%$, $R_{3390\ nm} = 0.097\%$, showing that the graphical method gives an adequate result.

§4.3. Use of equivalent index in thin film design

In §1.5 the concept of 'equivalent index' was introduced. This can be very useful in filter design work, especially in the production of low-reflecting coatings (Epstein, 1952; Berning, 1962) and Band-pass filters (Baumeister, 1963; Epstein, 1952). Epstein showed that a symmetrical combination of thin films is equivalent at any wavelength to a single film, characterised by an equivalent index N and an equivalent thickness γ. It is seen from Figure 4.5 that for multilayers whose component thicknesses are small compared with wavelength, the equivalent index assumes a nearly constant value which lies between the values of the component film indices, and the equivalent thickness is nearly equal to the sum of the component thicknesses.

For the design of low-reflecting coatings, let us consider three layer symmetric combinations. Berning shows that for small thicknesses in this case

$$N \doteq n_1 \left(\frac{q + n_2/n_1}{q + n_1/n_2} \right)^{\frac{1}{2}} \tag{4.3.1}$$

$$\gamma \doteq \delta \left(1 + \frac{(n_1 - n_2)^2 q}{n_1 n_2 (1+q)^2} \right)^{\frac{1}{2}} \tag{4.3.2}$$
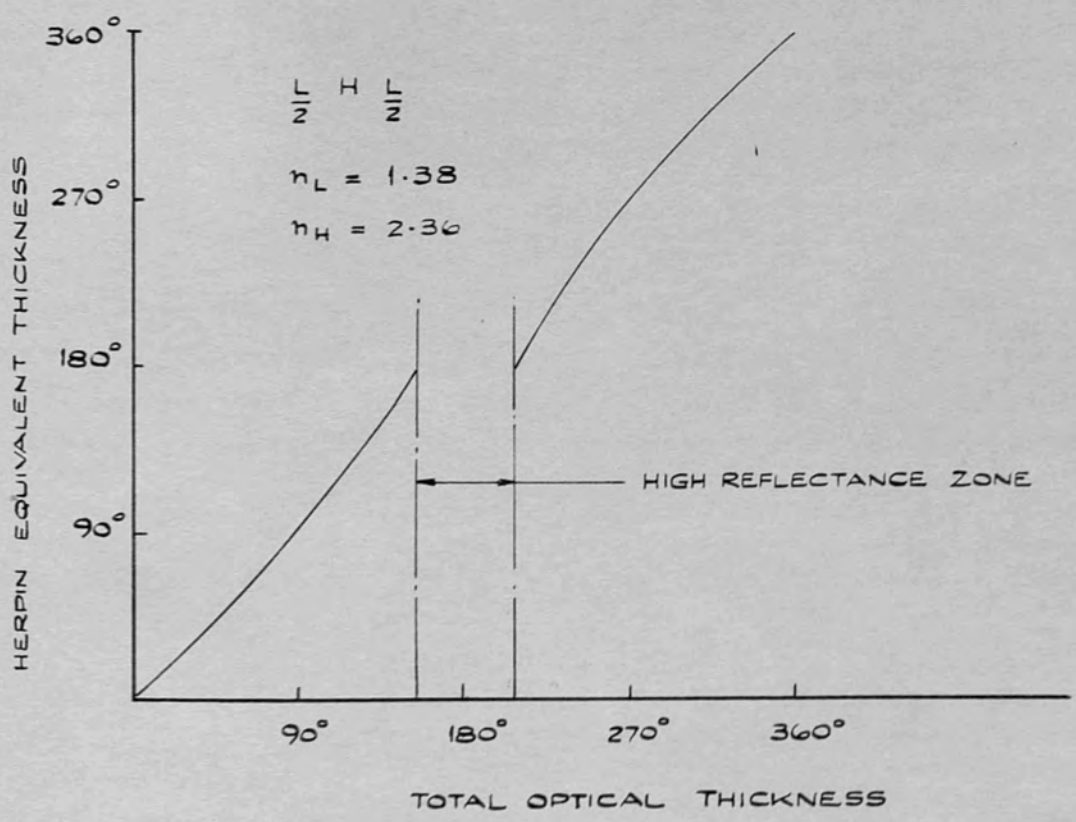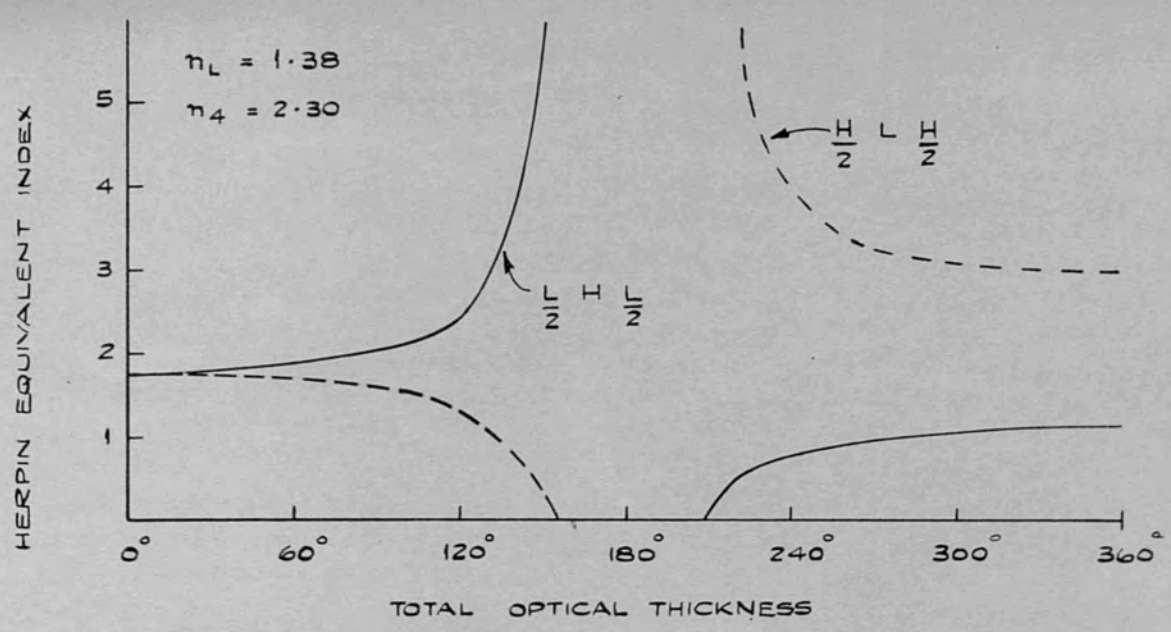
FIG. 4.5 EQUIVALENT INDEX AND THICKNESS

where q is the ratio of the thicknesses and $\delta = 2\delta_1 + \delta_2$, the total thickness of the layers in the combination. Then N is approximately a constant whose value lies between n_1 and n_2 and depends on the ratio of the component thicknesses. Thus any particular value for N may be obtained by varying q. These results are most useful if one wishes to 'match' two media, for in this case the index of the 'matching' layer should be the geometric mean of the indices of the two surrounding media. In fact the range of application of (4.3.1) & (4.3.2) is surprisingly large; equation (4.3.2) will hold for values of δ up to and exceeding 90°. Film coatings for which the total thickness equals 90° or 270° are of especial interest in the design of antireflecting coatings. Epstein gives some results for equivalent indices of some symmetric thin film combinations, used in low reflecting coatings. These are shown in Table 4.2.

TABLE 4.2

$\delta = 2\delta_1 + \delta_2$	90°	90°	270°	270°
n_1	1.38	2.30	1.38	2.30
n_2	2.30	1.38	2.30	1.38
δ_2	N	N	N	N
0°	1.380	2.300	1.380	2.300
10°	1.514	2.096	1.258	2.523
20°	1.657	1.916	1.151	2.758

Table 4.2 continued

$\delta = 2\delta_1 + \delta_2$	90°	90°	270°	270°
n_1	1.38	2.30	1.38	2.30
n_2	2.30	1.38	2.30	1.38
30°	1.800	1.763	1.060	2.995
40°	1.938	1.638	0.985	3.222
50°	2.061	1.540	0.926	3.426
60°	2.162	1.468	0.882	3.598
70°	2.238	1.418	0.852	3.726
80°	2.283	1.390	0.834	3.806
90°	2.300	1.380	0.828	3.833

The values obtained from $\delta = 270°$ are very interesting because they give values of N lower than air (1.0) and much higher than that of the high index layer.

We know from (1.5.13) that for a symmetric filter

$$N = \frac{a_{21}}{(1 - a_{11}^2)^{\frac{1}{2}}} \qquad (4.3.3)$$

So for N to be real, $|a_{11}| < 1$. This condition occurs in the pass-band. Inside the stopband $|a_{11}| > 1$. The edge of the stopband occurs when $a_{11} = 1$. Band-pass filters are required to have low reflectance in one spectral region (the pass-band) and high reflectance in the adjacent region

(the stop band). The point of transition is known as the
'cut-off' point. A normal multilayer stack would fulfil
these conditions with the edge of the high reflectance zone
being the 'cut off' if the subsidiary reflectance maxima
were suppressed (Fig.3.1). Now a stack can be considered as
a three-layer film combination ($\frac{L}{2}$ H $\frac{L}{2}$) repeated q times.
This differs from the normal type of stack in that it con-
tains layers of an eighth-wave optical thickness at each
end. This total stack is therefore equivalent to a single
layer whose equivalent index is that of the basic period
and whose equivalent thickness is q times that of the basic
period. Thus, one can estimate the Herpin equivalent index
for the stack at the points where the unwanted reflectances
occur and apply a coating which "matches" the stack and the
substrate at the stack/substrate interface and another which
matches the stack and air at the air/stack interface. As
the dispersion of equivalent index is usually large at
these points, a solution which attempts to suppress more
than one subsidiary reflectance maximum is necessarily a
compromise.

§4.4. Application of Circuit Theory Methods

In recent years, much independent development in the theory of filter design has taken place in the fields of linear circuit theory and microwave quarter-wave transformer theory. Some of the results of this work may be applied to the design of optical filters. Many of the methods used are the outcome of years of research on filter synthesis. A fairly sophisticated theory has evolved from this research and many of the techniques are unlike those used for optical filter design, so it would be impossible to give a complete account of the methods here. Instead, some of the basic concepts of network synthesis will be mentioned and a brief outline of a method of filter synthesis which could well be modified to be directly applicable for multilayer filter design will be given. Full details of electrical filter synthesis are given in Van Valkenburg (1960).

The characteristic impedance of a medium is inversely proportional to the refractive index and the characteristic admittance is defined as the reciprocal of the impedance. We thus have

$$\frac{Y_1}{Y_2} = \frac{Z_2}{Z_1} = \frac{n_1}{n_2} \qquad (4.4.1)$$

For normal incidence, the amplitude reflection coefficient at the boundary between two media is given by

$$\Gamma = \frac{Z_2 - Z_1}{Z_2 + Z_1} = \frac{Y_1 - Y_2}{Y_1 + Y_2} = \frac{n_1 - n_2}{n_1 + n_2} \qquad (4.4.2)$$

There are two important types of response of a lumped constant network. These are the time-domain response, represented by f(t) and the frequency-domain response, $F(i\omega)$. These are related by means of a Fourier transformation

$$F(i\omega) = \int_{-\infty}^{+\infty} f(t) e^{-i\omega t} dt$$

$$f(t) = \frac{1}{2\pi} \int_{-\infty}^{+\infty} F(i\omega) e^{i\omega t} d\omega \qquad (4.4.3)$$

It is usually more convenient in circuit theory to work in terms of a complex frequency s defined by

$$s = \sigma + i\omega \qquad (4.4.4)$$

where F(s) is related to f(t) by a Laplace transformation

$$F(s) = \int_{-\infty}^{+\infty} f(t) e^{-st} dt$$

$$f(t) = \frac{1}{2\pi i} \int_{-i\infty}^{+i\infty} F(s) e^{st} ds \qquad (4.4.5)$$

The response of the network is generally given in

terms of the insertion loss function, P_L, which is defined
as the ratio of the available (or incident) power to the
transmitted power. Thus

$$P_L = \frac{1}{T}$$
(4.4.7)

and it is related to the amplitude reflection coefficient by

$$|\Gamma|^2 = \frac{P_L - 1}{P_L}$$
(4.4.8)

The expression for the impedance of the network is given by

$$\Gamma(s) = \frac{Z(s) - Z_L(s)}{Z(s) + Z_L(s)}$$
(4.4.9)

where Z_L is the load impedance. Thus, if Z_L is known, the
expression for Z(s) may be obtained from P_L(s). Brune
(1931) showed that for Z(s) to represent a physically
realizable L C R circuit, it must be a 'positive real'
function. Full details of the mathematical properties of
these functions are given by Van Valkenburg.

The procedure for circuit filter synthesis is as
follows:- The specification is given as a function of
frequency. For a finite number of circuit elements, the
specification will not, in general, be exactly realisable.
Thus a permissable degree of tolerance will also need to
be given. This tolerance is allowed for by employing a
curve-fitting procedure, using Tschebyscheff polynomials

of the first kind. The higher the degree of the polynomial, the better will be the fit to the specified curve. This type of polynomial is a realizable response function for some network which may be found using a method such as the classical procedure of Darlington (1939). Darlington's method is essentially a means of constructing lossless transmission circuits with a resistive termination to obtain the optimum realizable performance.

The Tschebyscheff polynomials may be defined by

$$T_n(\bar{\omega}) = \begin{cases} \cos(n\arccos\bar{\omega}), & \text{for } |\bar{\omega}| \leqslant 1 \\ \cosh(n\operatorname{arccosh}\bar{\omega}), & \text{for } |\bar{\omega}| > 1 \end{cases} \qquad (4.4.10)$$

Graphs of these polynomials for n = 2,3,4,5,6 are shown in Fig.4.6. They have the following properties:-

(1) $T_n(\bar{\omega})$ oscillates between ± 1 in the interval $-1 \leqslant \bar{\omega} \leqslant + 1$

(2) The zeros are all located in the interval $-1 \leqslant \bar{\omega} \leqslant + 1$ with intervening maxima and minima with values ± 1 respectively

(3) Outside the interval $-1 \leqslant \bar{\omega} \leqslant + 1$ the polynomial becomes very large in comparison with unity. For large values of $\bar{\omega}$

$$T_n(\bar{\omega}) \to 2^{n-1}(\bar{\omega})^n$$

The application may be extended to include transmission line theory by use of the transformation (Richards,

$T_2 (\bar{\omega})$

$T_3 (\bar{\omega})$

$T_4 (\bar{\omega})$

$T_5 (\bar{\omega})$

$T_6 (\bar{\omega})$
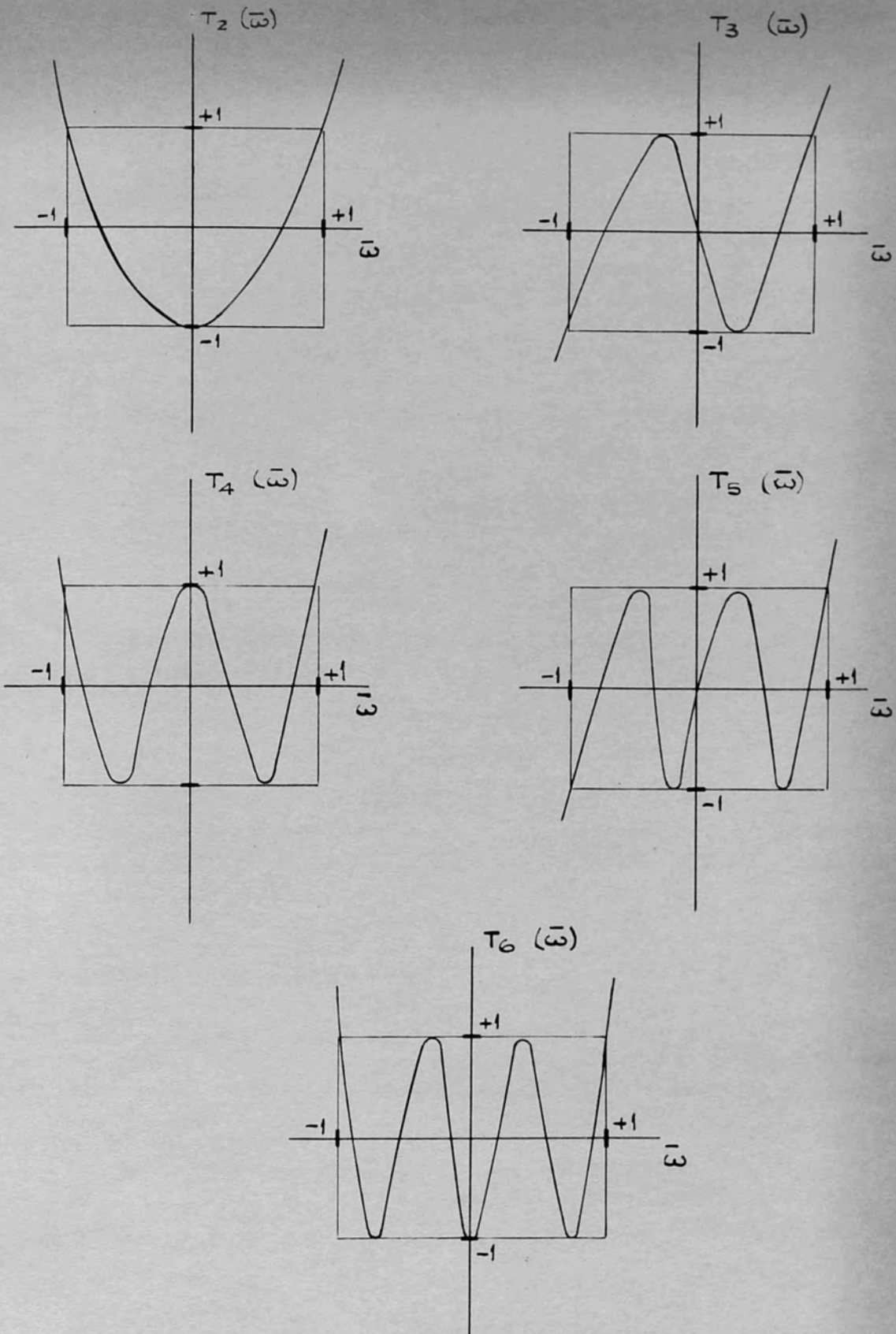
FIG. 4.6 TSCHEBYSCHEFF POLYNOMIALS FOR SMALL VALUES OF $\bar{\omega}$

1948)

$$s = i \tan \theta$$

where θ is the electrical length of a section of trans-
mission line. This is based on the following assumptions:
(1) The elements of the transmission line are lossless;
(2) the elements are commensurate. Because of the similarity
between transmission lines and multilayers, the transforma-
tion effectively extends applications of network theory
into the optical region. In general, for multilayer design,
the configuration is fixed and some of the design data
(e.g. the refractive indices) may also be fixed. In this
case, the circuit prototype must be manipulated to accept
these restrictions on data.

Young (1961) and Seeley (1961) apply the method
of exact synthesis to multilayer design; the former designs
antireflecting coatings, while the latter considers the
synthesis of interference filters. Seeley's transmittance
function is of the form

$$T(\bar{\omega}) = \frac{1}{1 + [h T_n (\bar{\omega})]^2} \qquad (4.4.11)$$

h^2 gives the amplitude of the 'ripple' - its value is
obtained from the allowed tolerance of the specified func-
tion. Another form of response used by Seeley is the
'maximally flat' (Butterworth) function of the form

$$T = \frac{1}{1 + [h(\omega)^n]^2} \qquad (4.4.12)$$

A comparison of the two types of function when h = 1 is given in Figure 4.7.

Both Seeley and Young considered fixed thicknesses for the layers and used the method of synthesis to obtain values for the refractive indices in order that the desired transmission function be obtained. However, only a few dielectric materials are available for use in optical filters, so the synthesised design almost certainly will not be realisable. In this case, it may be more advantageous to have the layer thicknesses as design variables and fix the values of the refractive indices. This problem has been discussed by Chen, Seeley and Williams (1964), who suggest that the optimum multilayer design may be obtained (a) by varying the phase thicknesses (b) by varying the impedances (refractive indices) (c) by any combination of (a) and (b). They also suggest a method for design by relaxation in which the matrix product of the filter is equated directly to the specified insertion loss function and the resulting algebraic equations are solved by a relaxation calculation. This is somewhat similar to the method suggested by Pohlack (1960), except that the latter

$h^2 = 1$

(a) $n = 2$

(b) $n = 3$

(c) $n = 4$
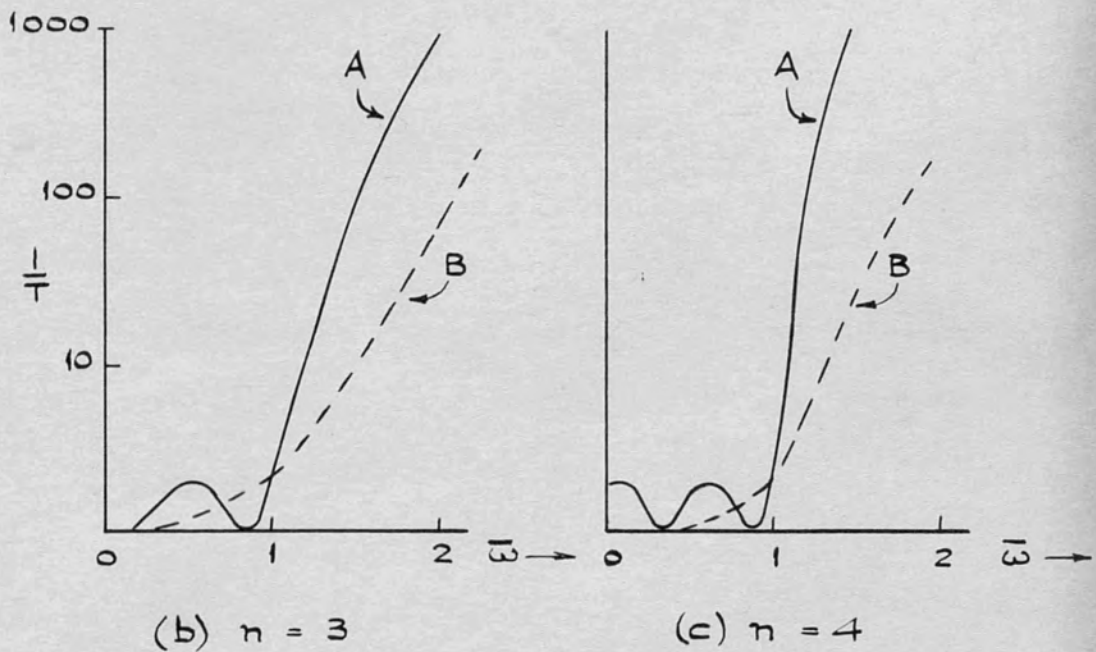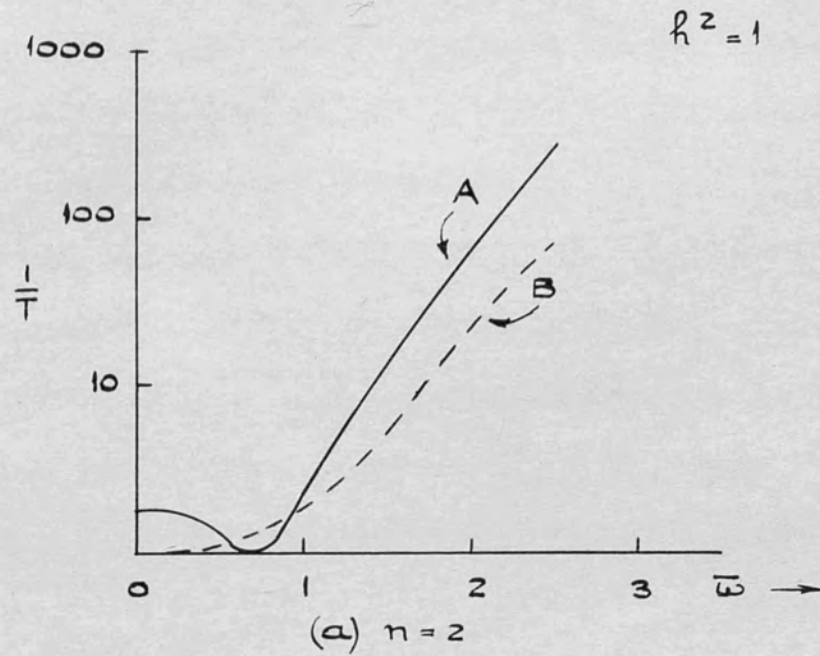
A - EQUIRIPPLE FUNCTION (TSCHEBYSCHEFF)

B - MAXIMALLY FLAT FUNCTION (BUTTERWORTH)

FIG. 4.7. COMPARISON OF TSCHEBYSCHEFF AND BUTTERWORTH RESPONSE FUNCTIONS

fixes the values of the thicknesses so the only design variables are the refractive indices. The types of filter discussed by Pohlack are antireflecting filters requiring only a few layers, so the solution of the resulting algebraic equations is fairly straightforward.

For multilayer filters with varying thicknesses, the multilayer-circuit analogue will hold for only one frequency. However, this frequency may be chosen at a fairly critical point (e.g. the point of cut-off for a band-pass filter) so the method can still be extremely useful.

§4.5. The method of successive iterations

The method of successive iterations (Baumeister, 1958) is a 'relaxation' multilayer design procedure. Small changes are made in the design variables in order to produce a better approximation to the desired result than that given by the initial design. The process may be repeated as many times as necessary to produce the required improvement in performance. Usually, the specified function takes the form of a given transmission or reflection curve, although the method has been generalised to include modifications of Δ , γ , the phase changes on reflection and

transmission or sometimes $\frac{\partial R}{\partial \sigma}$, $\frac{\partial T}{\partial \sigma}$, $\frac{\partial \Delta}{\partial \sigma}$, $\frac{\partial \gamma}{\partial \sigma}$, or if non-normal incidence is to be included values for both states of polarisation of $\frac{\partial R}{\partial \theta}$, $\frac{\partial T}{\partial \theta}$, $\frac{\partial \Delta}{\partial \theta}$, $\frac{\partial \gamma}{\partial \theta}$ are included (Dobrowolski, 1965).

The transmittance or reflectance of an **N**-layer combination of thin films depends on the optical thickness $t_i = n_i d_i$, the refractive index n_i, and the wavenumber σ of the incident light. Then, for some wavenumber σ_j, the change in transmission δT_j, or reflection δR_j, caused by alterations δt_i in the optical thicknesses of the layers, is given by

$$\delta R_j = -\delta T_j = \sum_{i=1}^{N} \frac{\partial R_j}{\partial t_i} \delta t_i + O(\delta t_i)^2 \qquad (4.5.1)$$

if the indices of the layers remain constant. Then if a known combination of layers has a spectral reflectance which is approximately such that it differs from the required design at a finite number, m, of points only, this combination may be used for the initial design. We may estimate the changes in reflectance δR_j required to produce the required spectral curve at these m points and the $\frac{\partial R_j}{\partial t_i}$ may be calculated. This calculation may be done either by using a finite difference approximation or by an exact method (Baumeister, 1962). Thus a set of m simultaneous equations with N unknowns is obtained, and a subsidiary condition that $\sum_{i=1}^{N} (t_i)^2$ be a minimum is also specified. The equa-

tions may be solved for the δt_i and the cycle repeated. In order that the second order terms in (4.5.1) may be neglected, the changes δR_j should be small, so many itera- tions are often necessary to produce the required result.

In Chapter III details were given of the broad- band reflector Baumeister and Stone designed using this method. The starting design for this coating was obtained by combining two 'mismatched' stacks. Baumeister (1958) gives another example - a high-pass filter design. The initial design is a 17-layer classical stack and Baumeister uses the method of successive iterations to remove the sub- sidiary reflectance bands. The initial and final designs are shown in Figure 4.8.

Three conditions are necessary for the method to be successful; first, the initial design must bear some resemblance to the desired curve; second, the $\frac{\partial R}{\partial t_i}$ must exist and be of sufficient magnitude for second order terms to be neglected; finally, the system of simultaneous equations must possess a solution. In many cases, it is not always easy to see if the third condition will hold in a particular case, and it becomes increasingly difficult when factors other than reflectance and transmittance are taken into account.

Baumeister (1962) has also applied the method of successive iterations to the problem of improving the
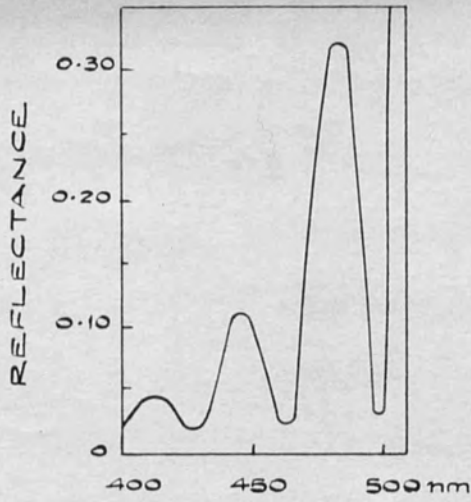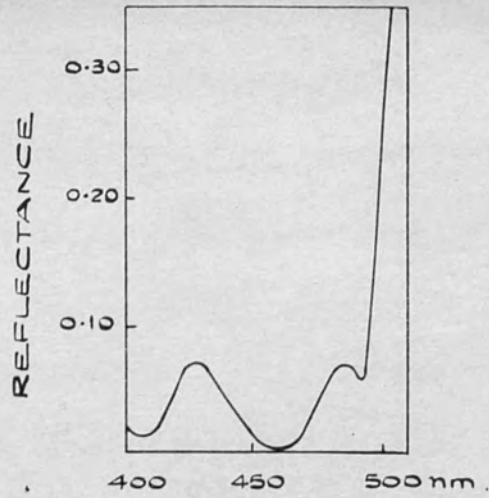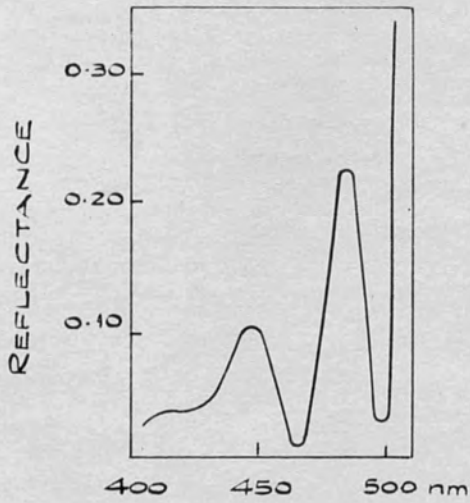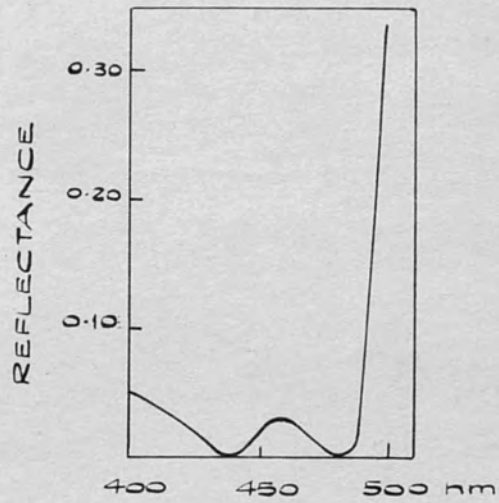
FIG. 4.8 HIGH-PASS FILTER DESIGN

PRODUCED BY METHOD OF SUCCESSIVE ITERATIONS

design of a multilayer containing some absorbing films. For absorbing films, the resulting equations for the multilayer are very much more complicated and analytic methods of synthesis would be extremely difficult to apply.

The problem of choosing a suitable initial design may be fairly difficult and this is a severe limitation of the method of successive iterations. In the next section, we shall discuss methods by which the problem may be overcome.

§4.6. Automatic Design Methods

In order to design a multilayer, which has a specified performance, without providing an initial design which itself gives a fairly good approximation to this performance, values of the reflectance (or one of the other spectral characteristics mentioned above) must be obtained for a range of values of the design variables. The best approximation may then be selected. One must define a function which will measure the performance of the multilayer. Dobrowolski calls this the 'merit function'. This function will depend on all the design variables of the multilayer. It will become more and more complicated as the number of layers increases and will have an increasing number of minima so it becomes very difficult to find the lowest

minimum. However, actually obtaining the lowest minimum
(i.e. the best approximation to the required curve) is not
always important in thin film design; the design will be
acceptable as long as the final multilayer performance is
within the limit of the allowable tolerance.

In order to obtain the lowest minimum for an
N-layer filter (i.e. 2N design variables) when each of the
variables may take p different values (this defines the
'mesh' of the search net) one must calculate the merit
function $(p)^{2N}$ times. It is easy to see that as N increases,
the machine time needed for the search would soon become
formidable even on a large computer. A variation of this
design procedure was applied by Elsner (1964), but in order
to keep down the number of calculations, he fixed the values
of the refractive indices and some of the layer thicknesses
and allowed the remaining thicknesses to take the values
$\frac{m\lambda_o}{4}$ where the integer m = 1, ...6. He imposed the following
condition on the transmittance:-

$$F_1(\kappa) \leqslant T(\kappa) \leqslant F_2(\kappa), \quad \kappa_0 \leqslant \kappa \leqslant \kappa_1 \quad (4.6.1)$$

where $\kappa = \sigma/\sigma_o$. Every time a value of the design variables
satisfying (4.6.1) was obtained, the region of permissable
values of $T(\kappa)$ was increased. The final region of acceptable
values of $T(\kappa)$ is fixed and the optimum value of the
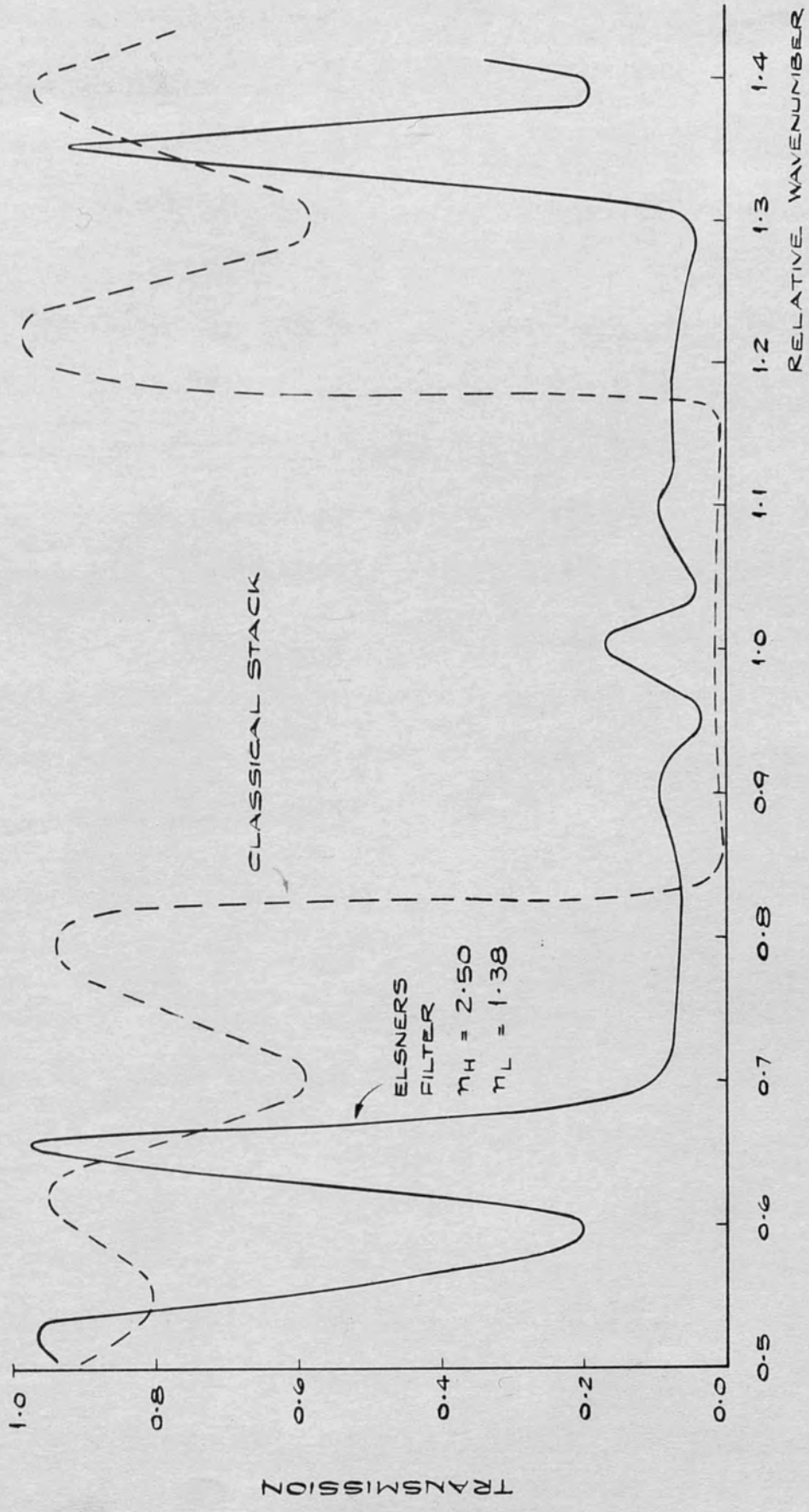
FIG. 4.9 ELSNER'S BROAD BAND REFLECTOR

parameters corresponding to these final boundaries was
determined. Elsner applied the method to the design of a
broad-band reflector. His results for an eleven-layer
system are given in Fig.4.9. The computation time required
for the calculations was 3½ hours. (The Moscow State
University Computer was used.) However, in general a
refractive index/thickness net of this type will not be fine
enough to give the best solution.

Shatilov and Tyutikova (1963) employed a method
which does not use such an exhaustive search procedure. To
simplify the problem, the refractive indices of the layers
were again fixed. The desired curve was given by $R(\omega)$ and
the curve for an N-layer system by $Rm(\omega, t_1, \ldots t_N)$. The
merit function was defined to be

$$\Delta m^2 = \int |R(\omega) - R_m(\omega, t_1 \cdot \cdot t_N)|^2 d\omega \qquad (4.6.2)$$

the integration being taken over the spectral range of the
design. In order to find the final values of t_1, the syn-
thesis of the system took place in stages; at each stage
only one additional layer was added to the multilayer and
Δm^2 was minimised. The value of the integral Δm^2 was
obtained, using Simpson's rule, for eleven values of t_i
for each layer and the value which gave the minimum value
of Δm^2 was chosen as the thickness of the layer. In this
way, systems of up to eight layers were designed, without
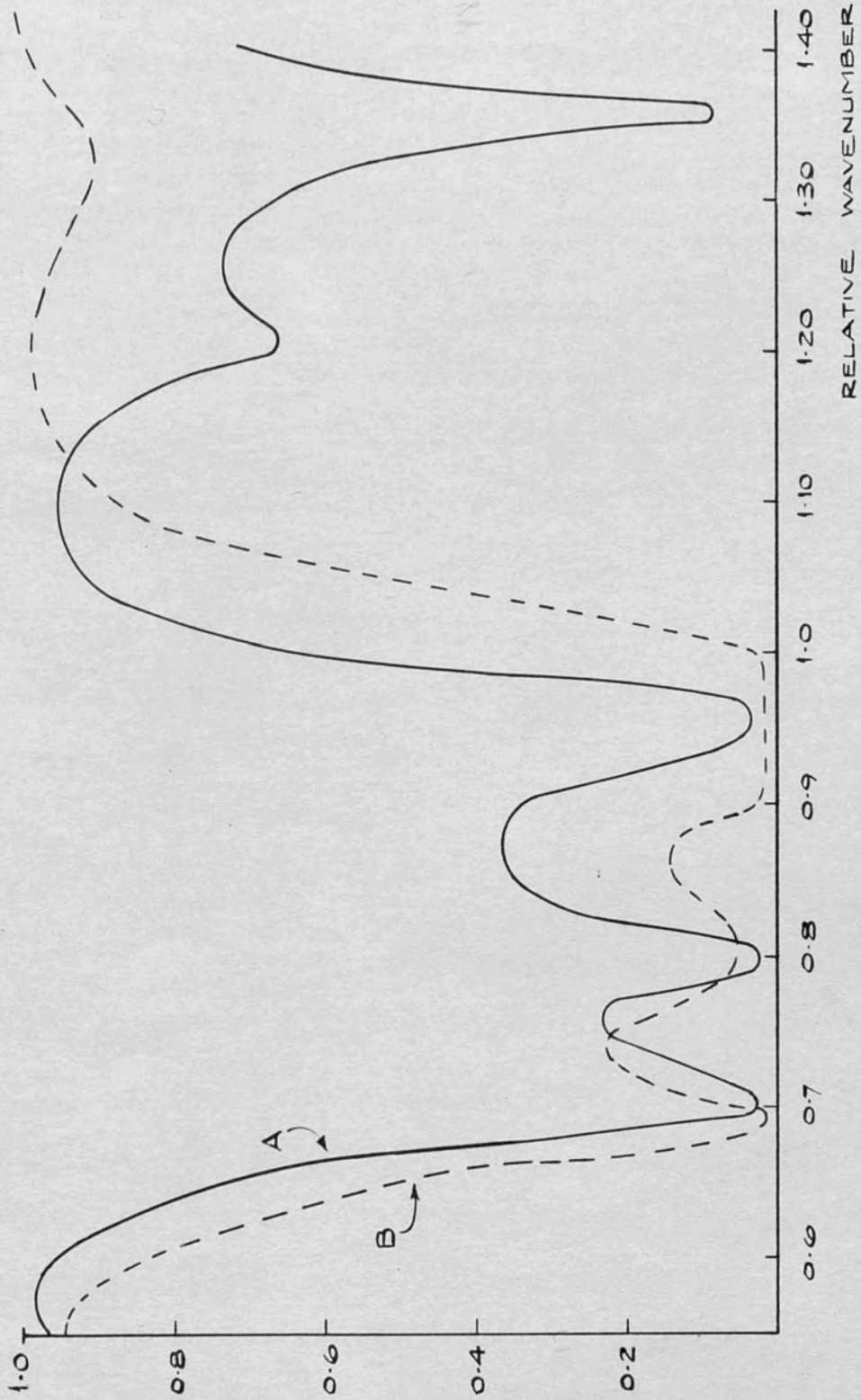
FIG. 4.10   SHATILOV AND TYUTIKOVA'S PROBLEM

the use of electronic computers. Their design for an eight-
layer low reflectance coating is given in Fig.4.10 (Curve A).
The method gives a fairly good result in this instance, but
there are other problems where the method breaks down. One
of the most obvious examples is the design of a thin film
system with the properties of a quarter-wave stack.

Dobrowolski (1965) manages to overcome the diffi-
culty by adding a group of two or more layers at a time to
the existing design. In each group both the refractive
indices and the thicknesses may take several values and the
most favourable combination is then added to the previous
layers. After the addition of each group of layers, the
combination is refined further using the method of successive
iterations. The merit function used in the method is

$$M = \left[\frac{1}{m} \sum_{j=1}^{m} \left(\frac{|P_j^D - P_j|}{T_j} \right)^K \right]^{1/K} \tag{4.6.3}$$

where P_j^D, P_j and T_j are the desired value, the actual value
and the tolerance of the desired property at the point σ_j.
Thus when all the functions are just within tolerance of
their desired values, M = 1. K may take any of the values
1,2,4 or 16. The results for five and six-layer achromatic
beam-splitters with fixed indices are shown in Fig.4.11
(Curves A and B respectively). Curve C represents a four-
layer beam splitter with variable indices. Dobrowolski
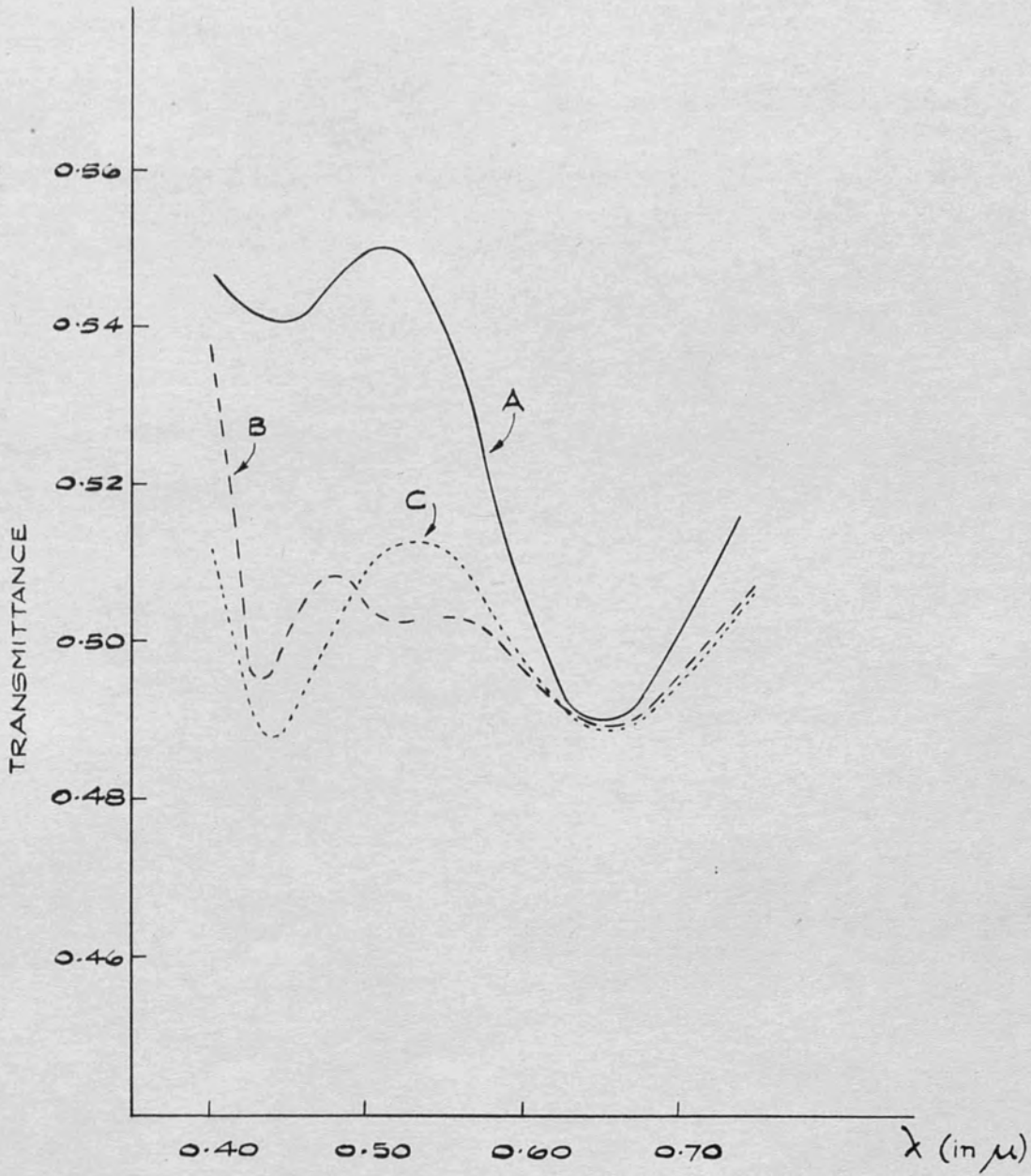
Fig. 4.11   Dobrowolski's Beam Splitter Designs

also applied the method to the examples given by Shatilov
and Tyutikova. This final result after nine iterations is
shown in Curve B of Figure 4.10.

Clearly, this method is a very powerful one, but
there may still be problems where it will not find the
solution. However, it is certainly a very useful method of
automatic synthesis which does not rely on an exhaustive
search procedure. Much of its power lies in its adaptability
for all kinds of design conditions.

CHAPTER V. LEAST SQUARES METHOD OF FILTER DESIGN

§5.1. Discussion of Design Considerations

In Chapter IV, an account was given of the various design methods used at present for producing optical filters. In general, no single method will be suitable for all problems, but a knowledge of the various approaches enables the designer to choose the most suitable method or combination of methods for his particular problem.

One must therefore consider several important criteria for the design of optical filters before presenting a new method. First, one must consider the realities of the problem; if only one or two materials are available, one must obtain the best possible design using only these materials; if the monitoring system used is fairly primitive, one may have to consider designs in which the thicknesses may only take certain values. Finally, one must consider economy of computing time, both in developing the design program and in production of results once the program has been tested. In the method to be reported in this Chapter, use was made of a facility of modern large computers - the existence of library subroutines. These subroutines have

not only been already tested, thus economising on development time, but they have been written by programming experts and are therefore economical to use in production runs. The method of least squares is basically very straightforward; its usefulness lies in its adaptability to different design conditions. It may be used either to improve existing designs by a 'refining' technique or to design a filter automatically when no initial design is given.

§5.2. Theory of the least squares method

One way of specifying the design for a particular filter is to require that the reflectance $R'(\lambda)$ take certain values at wavelengths λ_K, $K = 1, \ldots m$. A multilayer configuration may then be chosen which has a particular number (N) of design variables. The most general configuration for non-absorbing media is that given in Fig.5.1(a) in which all the refractive indices and all the thicknesses (measured at the central wavenumber) are design variables. Because of the difficulty of obtaining suitable materials, a more practical approach is to consider the type of configuration shown in Fig.5.1(b) in which the indices are fixed and the only design variables are the layer thicknesses. Alternative types of configuration are possible if more than two
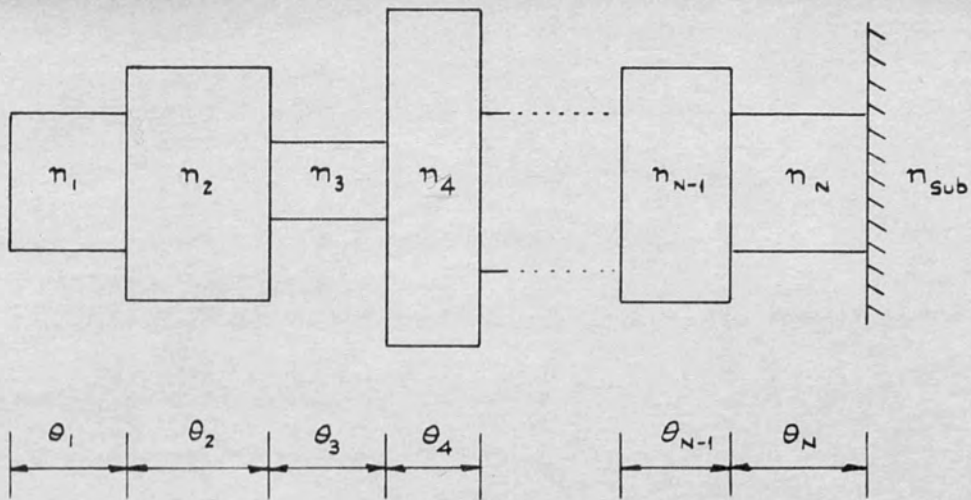
(a) GENERAL CONFIGURATION
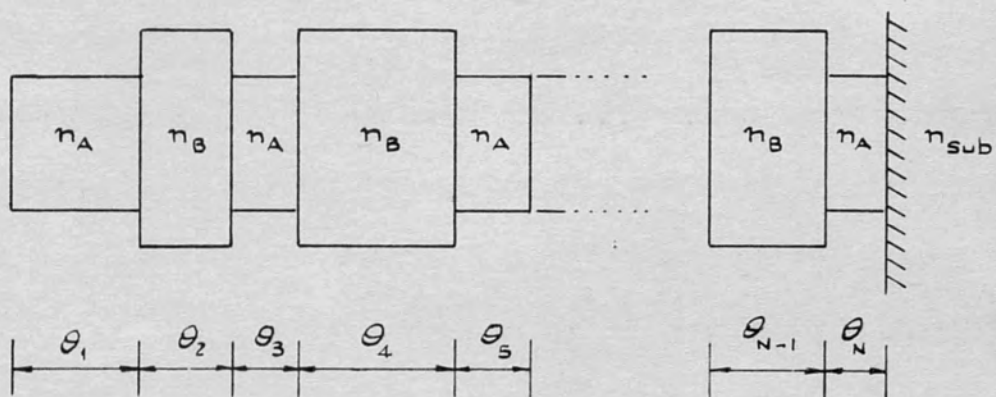
(b) CONFIGURATION WITH FIXED INDICES

FIG. 5.1. MULTILAYER CONFIGURATIONS FOR
NON-ABSORBING MEDIA.

materials are available, but for simplicity of calculation
and manufacture, designs containing only two materials were
considered.

Suppose the design variables have values
x_1, x_2, ... x_N, represented by the vector $\underline{x}$ in the N-
dimensional parameter space of the variables. The reflec-
tance $R(\lambda_K, \underline{x})$ of the multilayer at the wavelength λ_K may
be obtained using the matrix method. We therefore require

$$| R'(\lambda_K) - R(\lambda_K, \underline{x}) | = 0 \qquad (5.2.1)$$

for all λ_K, K = 1, ... m. If the set of simultaneous equa-
tions given by (5.2.1) is to possess a unique solution, one
must have m = N. However, for many design problems it may
be preferable to consider the problem where m > N so that
condition (5.2.1) is replaced by the condition that the
function

$$\sum_{k=1}^{m} \left[R'(\lambda_k) - R(\lambda_k, \underline{x}) \right]^p \qquad \text{where m} \geqslant \text{N} \quad (5.2.2)$$

should be minimised. In order that the terms in the summa-
tion are all positive, p must be an even integer.

Powell (1965) has described a method for minimising
a sum of squares of functions of several variables, and has
written a Fortran library subroutine ($VA_{02}A$) based on the
method. The subroutine will minimise a function of N

variables of the form

$$F(x_1, x_2, \cdots x_N) = \sum_{k=1}^{m} \left\{ f_k(x_1, x_2, \cdots x_N) \right\}^2, \quad m \geqslant N \quad (5.2.3)$$

In principle, the only limitation to the number of variables is set by the size of the computer. Clearly, this method may be applied directly to the problem of filter design by setting

$$f_k(\underline{x}) = \left[R'(\lambda_k) - R(\underline{x}, \lambda_k) \right] \quad (5.2.4)$$

and performing the summation over a range of wavenumbers. The function $F(\underline{x})$ will become very complex as N increases and the subroutine will not always find the lowest minimum, but will converge to the nearest minimum to its starting point. Thus, for use in automatic design methods an initial scan must be incorporated in the program. For filters with only a small number of layers, a complete scan of all possible combinations of layer thicknesses is possible if the mesh of the scan is fairly large (a maximum of five different values of layer thickness were considered for each layer). For more than five layers, another type of scan must be used. Each layer is given an initial thickness value, then the thickness of each layer in turn, starting with the first is allowed to vary through a fixed range of values (these values specify the mesh of the scan). The thickness of the layer is then fixed as that value for which F is least. The

process is repeated a further N-1 times, the second time the second layer is varied first, working through to the Nth and finally the first, and so on. This type of scan will be referred to as the 'N^2-scan'. Thus if each layer is allowed to take q values of thickness, the total number of times F is calculated during the initial scan is q x N^2 in the latter case. This may be compared with the number of calculations, q^N, which is required for a complete scan.

For some design problems, a good approximation to the desired curve may be known, so in this case the scan may be omitted and the initial thicknesses are set as the values corresponding to those in the known design. The subroutine will then 'refine' the thicknesses until the performance of the filter approaches the specified curve.

Later in the chapter, results will be given of designs obtained by the least squares method using

(a) A complete initial scan

(b) the N^2-scan method

(c) the refining method.

First, however, a description of the program will be given since its structure is fairly complex.

§5.3. The Program

A flow diagram and a copy of the program used for

Automatic design, incorporating an N^2-type scan, will be given in the appendix. However, it will not be out of place to mention some features of the program here.

The program was written in the Fortran language for two reasons; (1) it may then be used on many different computers as most of the world's large computers have a Fortran compiler. (This is not the case for most other programming languages); (2) the library minimisation routine was written in Fortran, so it could immediately be incorporated into the program. This routine appeared to be the best available for least squares minimisation and curve fitting.

The program consists of the main program, a subroutine CALFUN which calculates the f_K for a particular value of $\underline{x}$ and the library subroutine $VA_{02}A$, which calls another library subroutine $VD_{01}A$. The subroutine CALFUN calls a subroutine CHMAMP to perform the matrix multiplications. The complete scan main program also calls a subroutine VALTRS which calculates $F(\underline{x})$ and decides whether it is the minimum of the values obtained in the initial scan. Fig.5.2 shows the link between the main program and the various subroutines. The main program consists of the format statements for data input and output and if necessary, the initial scan procedure. The following data is read in:
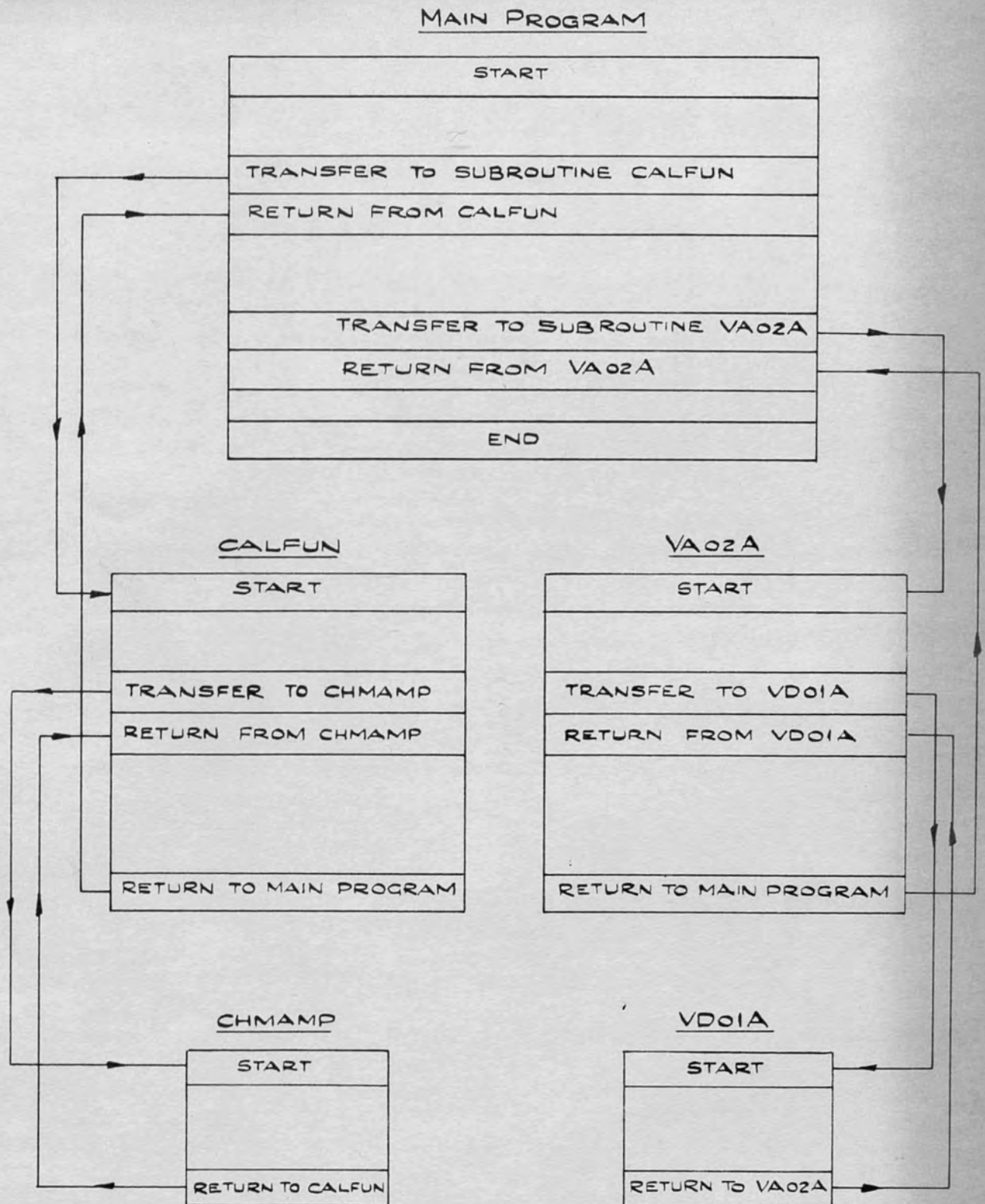
FIG. 5.2. LINK BETWEEN MAIN PROGRAM
AND THE SUBROUTINES

(i)   Information about refractive indices.

(ii)   The number of layers, N, in the filter and the number of wavenumbers, M, considered.

(iii) The specification of the desired curve.

(iv)   Information about the limits and mesh of the initial scan; if no scan is employed, the initial thicknesses are read in instead.

(v)   The absolute accuracy parameters for each design variable.

(vi)   The maximum number of times the minimisation routine should call the routine CALFUN - this sets a time limit for the procedure.

(vii) The frequency at which a print-out of the variables should occur during execution of $VA_{02}A$.

        The last three items are required by the library subroutine specifications.

        The output consists of the heading for the filter, a list of the refractive indices, and a list of the wave-number $(\frac{1}{\lambda_K})$, the given reflectivity $R'(\lambda_K)$ and the calcula-ted reflectivity $R(\lambda_K, \underline{x})$ for all values of λ_K. The latter is given before and after the minimisation subroutine is called. The values of the design variables $x_1 \ldots x_N$ and the functions f_K at the beginning and end and at several points during the execution of the minimisation procedure

are also given. An example of the form of output obtained
is given in the Appendix.

§5.4. Results

Although the least squares method may in principle
be used to design a filter with any given spectral charac-
teristics, the results given here will show its application
to several standard types of filter, as these designs are in
demand at the present time. In all cases, indices corres-
ponding to available materials are used. The designs are to
serve merely as examples to illustrate the method, so the
number of iterations of the subroutine was limited in order
to economise on computing time.

Obviously, if one were designing a filter for mass-
production, it would be profitable to obtain the best pos-
sible design by decreasing the mesh of the scan and by
increasing the number of iterations of the subroutine, so
that a minimum is reached in each case. This is most
important for filters with many layers because then the
reflectance may become a very complex function in the
parameter space of the design variables and in order to
locate a suitable minimum, one needs a scan with a relatively
fine mesh, compared to that needed for filters with fewer
layers.

The results reported here were obtained using the London University Atlas Computer and the Atlas at the S.R.C. Atlas Computer Laboratory at Chilton. A table showing the thicknesses of the layers at the beginning and end of the minimisation procedure will be given for each design. The initial thicknesses for the refining method will be those corresponding to the approximate design, whereas in the automatic design methods, the optimum set of values obtained from the initial scan provide these initial thicknesses. The values of the function F, defined by equation (5.2.3) will be given in each case and also the number of iterations needed to obtain the final result. The graphs were obtained by computing the spectral characteristics of the final design over a given wavelength range at intervals of $\sigma / \sigma_o = 0.02$. The specified values of $R'(\lambda_K)$ and the values of $R(\lambda_K, \underline{x})$ obtained by the design method for wavelengths λ_K will be shown on the graphs by the symbols X and $\odot$ respectively.

(1) Antireflection coatings

For this type of design, the aim was to produce as low a reflectance as possible over the wavenumber range 0.60 to 1.40 using alternate layers of MgF_2 (n = ∼ 1.38) and ZnS (n = ∼ 2.30). This corresponds to a wavelength range from 320 nm. to 750 nm. if λ_o = 450 nm. For both

the three layer and five layer coatings, the designs produced by the complete scan method and the N^2-scan method were the same. They are shown by curves A (Three-layer coating) and B (Five-layer coating) in Fig.5.3. The reflectance of the uncoated substrate is also shown. In both cases, during the initial scan, the phase thicknesses (at λ_o) were allowed to assume the values 30°, 60°, 90°, 120°, 150°, 180°. (A phase thickness of 90° corresponds to an optical thickness of $\lambda_o/4$). It is seen that even by using fixed indices, one may obtain a design which will lessen considerably the reflectance over a wide spectral range.

Table 5.1. Low Reflectance Coatings

Layer	3-layer-coating(Curve A)		5-layer-coating(Curve B)	
	Initial Thicknesses (Degrees)	Final Thicknesses (Degrees)	Initial Thicknesses (Degrees)	Final Thicknesses (Degrees)
1	90	110.44	90	89.25
2	30	10.96	180	191.91
3	30	28.26	30	26.87
4			30	30.57
5			180	187.57
No. of design wavenos. (M)	9		9	
Initial value of F	1.72×10^{-2}		3.63×10^{-3}	
Final value of F	2.28×10^{-3}		2.37×10^{-3}	
No. of iterations	10		8	
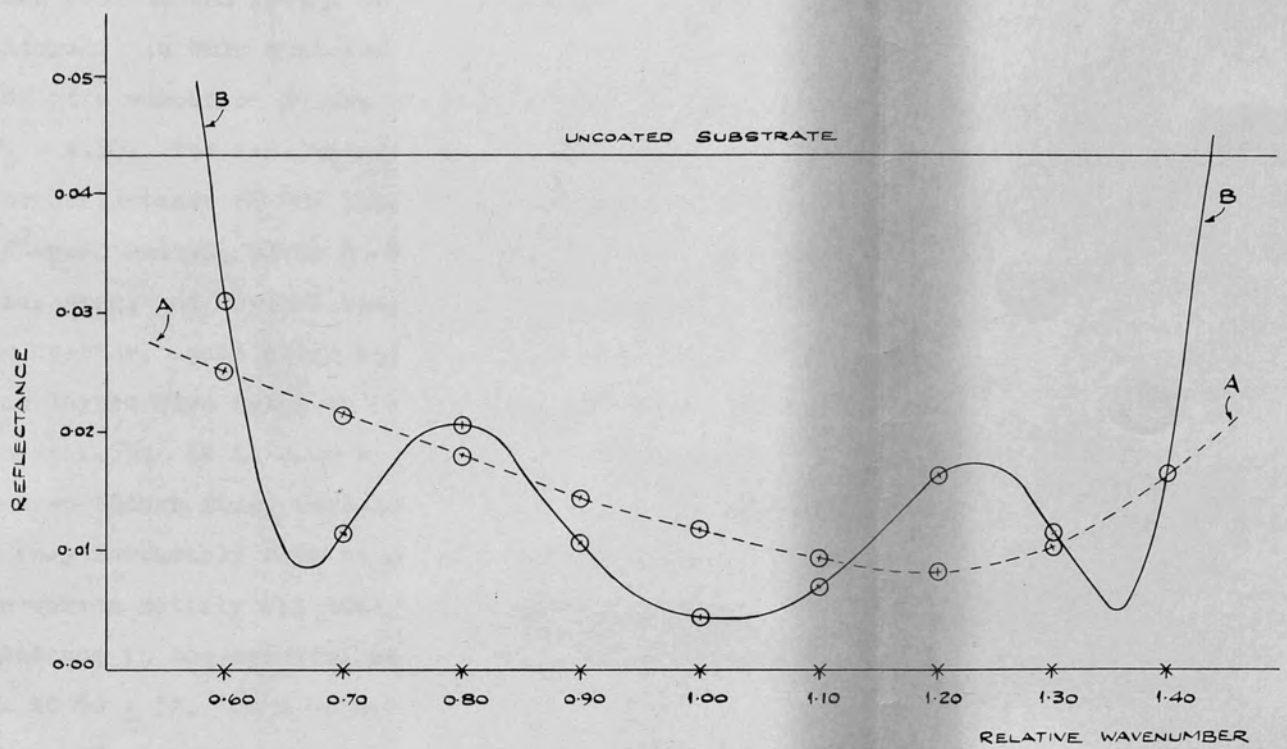
FIG. 5.3.   ANTIREFLECTION COATINGS.

(2) Achromatic beam splitters with 50% reflectance

for normal incidence

As a second example to illustrate the least squares method, the design of achromatic beam splitters was considered. In this case the given reflectance was equal to 50% at a number of points over the range $\sigma/\sigma_0 = 0.70$ to $\sigma/\sigma_0 = 1.30$. The results are shown in Figure 5.4. Curve A is the reflectance of the five-layer coating obtained using the N^2-scan method, Curve B is that obtained with a complete initial scan, and Curve C shows the performance of a seven-layer coating, again using the N^2-scan method. The indices of the layers were taken to be 2.36 and 1.39 on a substrate of index 1.53. It is seen by comparison with Fig.4.11, that even though fixed indices are used, these results compare very favourably with those given by Dobrowolski. All three curves satisfy his design requirements that the reflectance in the spectral region 400 to 700 nm. should be equal to 50 $\pm$ 3%, for a suitable choice of $\sigma_0 = \frac{1}{\lambda_0}$.

The computing time on Atlas for the five-layer complete scan was approximately 3.5 mins., whereas the N^2-scan method was much shorter. In the latter case, the five-layer design took 45 seconds and the seven-layer one 75 seconds. The thicknesses corresponding to these designs are given in Table 5.2.
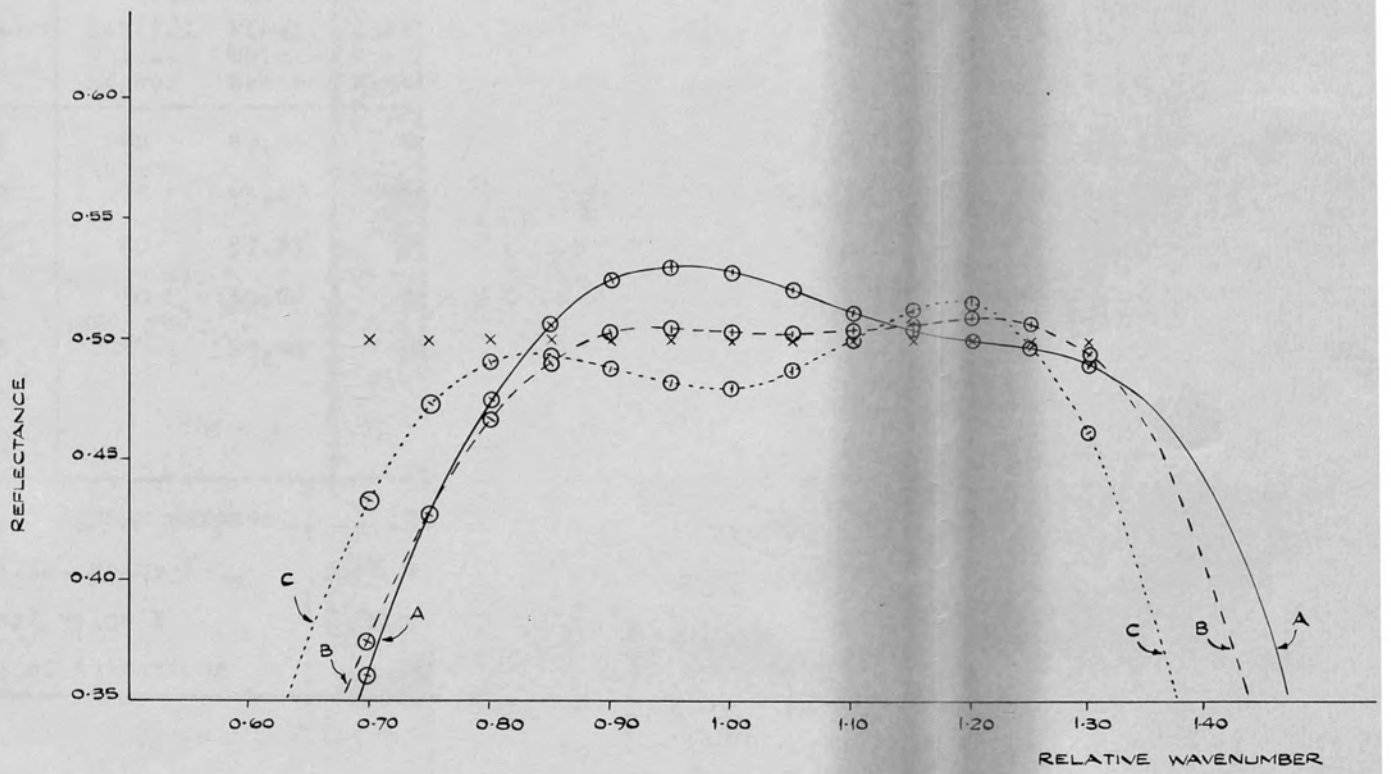
FIG. 5.4.   BEAM SPLITTERS

Table 5.2. Beam splitters

| Layer | 5-layer coatings | | | | 7-layer coatings | |
| | N^2 Scan (Curve A) | | Complete Scan (Curve B) | | Curve C | |
	Initial Thicknesses	Final Thicknesses	Initial Thicknesses	Final Thicknesses	Initial Thicknesses	Final Thicknesses
1	90	87.93	70	92.57	90	99.42
2	90	93.47	110	97.11	90	99.70
3	60	57.87	70	52.61	30	57.47
4	30	30.72	30	38.42	30	34.42
5	30	29.66	30	28.05	30	16.65
6					30	5.64
7					30	20.91
No.of design wavenos.	13		13		13	
Initial value F	2.96×10^{-2}		3.27×10^{-2}		9.64×10^{-2}	
Final value F	2.88×10^{-2}		2.29×10^{-2}		7.99×10^{-3}	
No. of iterations	20		20		21	

(3) Double-Half-Wave Interference filters

In order to test the design program, the spectral characteristics of one or two well-known filter designs were given as the specified curve. The first of this type of 'test' design was the production of a three-layer Double Half-Wave interference filter. The design was first sugges-

ted by Smith (1958) as a means of producing interference
filters with a rectangular shape transmission band rather
than the Airy shape shown by a conventional Fabry-Perot
type interference filter. Both the complete scan and the
N^2-scan methods were used. The values of the allowed thick-
nesses in the initial scan for the former method were 50°,
80°, 110°, 140°, 170°. The values 90°, 180° were
deliberately omitted in order to test the minimisation sub-
routine. In the N^2-scan method, the thicknesses took the
values 60°, 80°, 100°, 120°, 140°, 160°, 180° during the
initial scan. The final designs obtained are shown in Fig.
5.5 (Curves A and B represent the N^2-scan and the complete
scan respectively), and the corresponding thicknesses are
given in Table 5.3. The values of reflectance for the
specified curve were estimated approximately from the pub-
lished curve, so the final values of the thicknesses
obtained by the least squares method are correct to within
the accuracy one might reasonably expect.

Table 5.3. Double Half-Wave filters

Layer	N^2 Scan		Complete Scan	
	Initial Thicknesses	Final Thicknesses	Initial Thicknesses	Final Thicknesses
1	180	182.5	170	177.65
2	120	92.9	110	92.49
3	160	175.5	170	181.22
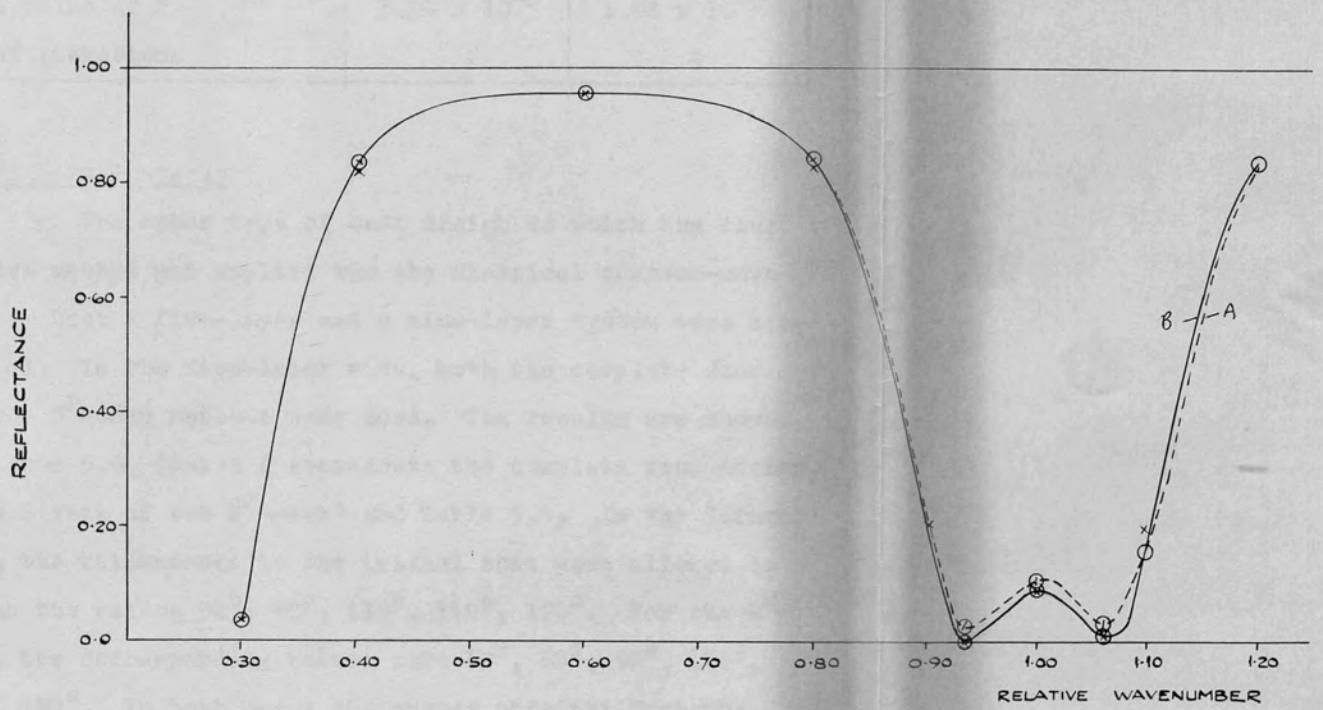
FIG. 5.5. DOUBLE HALF WAVE FILTERS

Table 5.3. continued

No. of design wavenos. (M)	10	10
Initial value of F	2.02×10^{-1}	9.48×10^{-2}
Final value of F	3.94×10^{-3}	1.98×10^{-3}
No. of iterations	2	4

(4) Classical stacks

The other type of test design to which the least
squares method was applied was the classical quarter-wave
stack. Both a five-layer and a nine-layer system were con-
sidered. In the five-layer case, both the complete scan
and the N^2-scan methods were used. The results are shown
in figure 5.6, (Curve A represents the complete scan design,
Curve B that of the N^2-scan) and Table 5.4. In the former
case, the thicknesses in the initial scan were allowed to
assume the values 50°, 80°, 110°, 140°, 170°. For the N^2-
scan, the corresponding values were 30°, 60°, 90°, 120°,
150°, 180°. In both cases the curves obtained from the
design are very close to the given curve, although in the
N^2-scan case, the thicknesses of the layers have not
attained their quarter-wave values. The result for the
nine-layer filter is shown by Curve A of Fig.5.7. Curve B
represents the reflectance of a nine-layer classical stack.
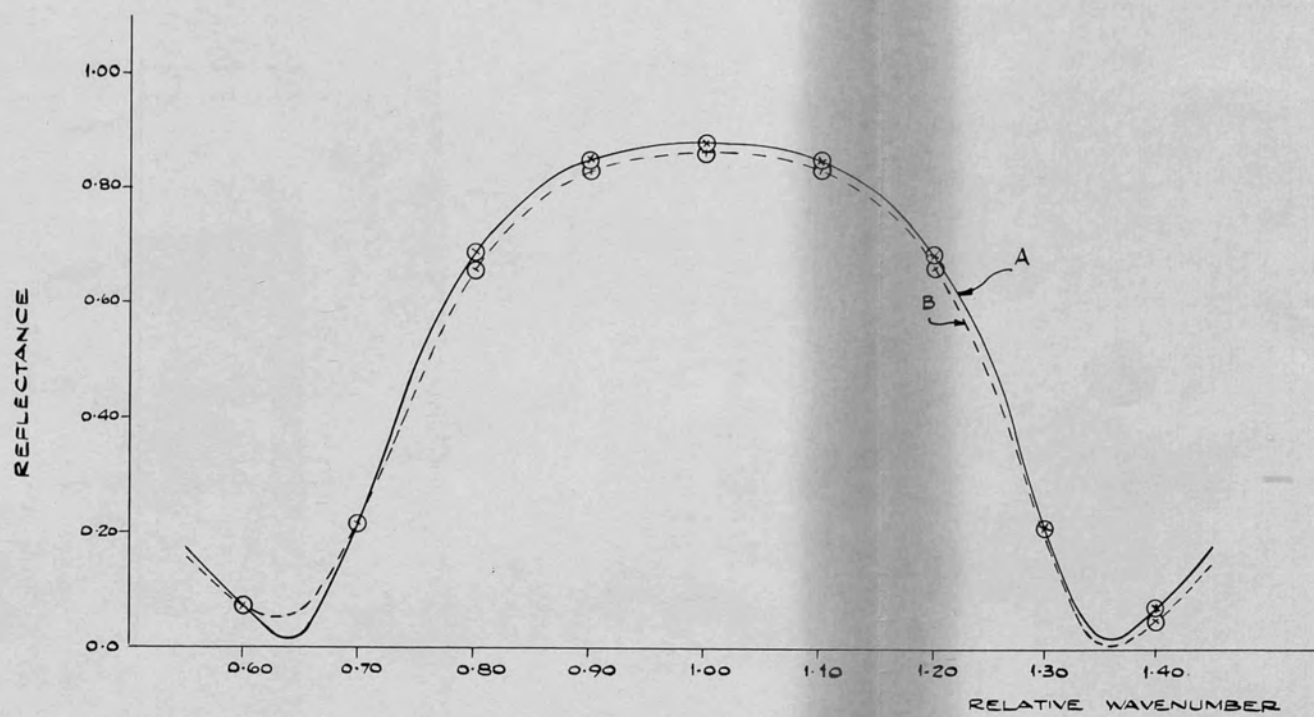
FIG. 5.6. FIVE-LAYER CLASSICAL FILTER
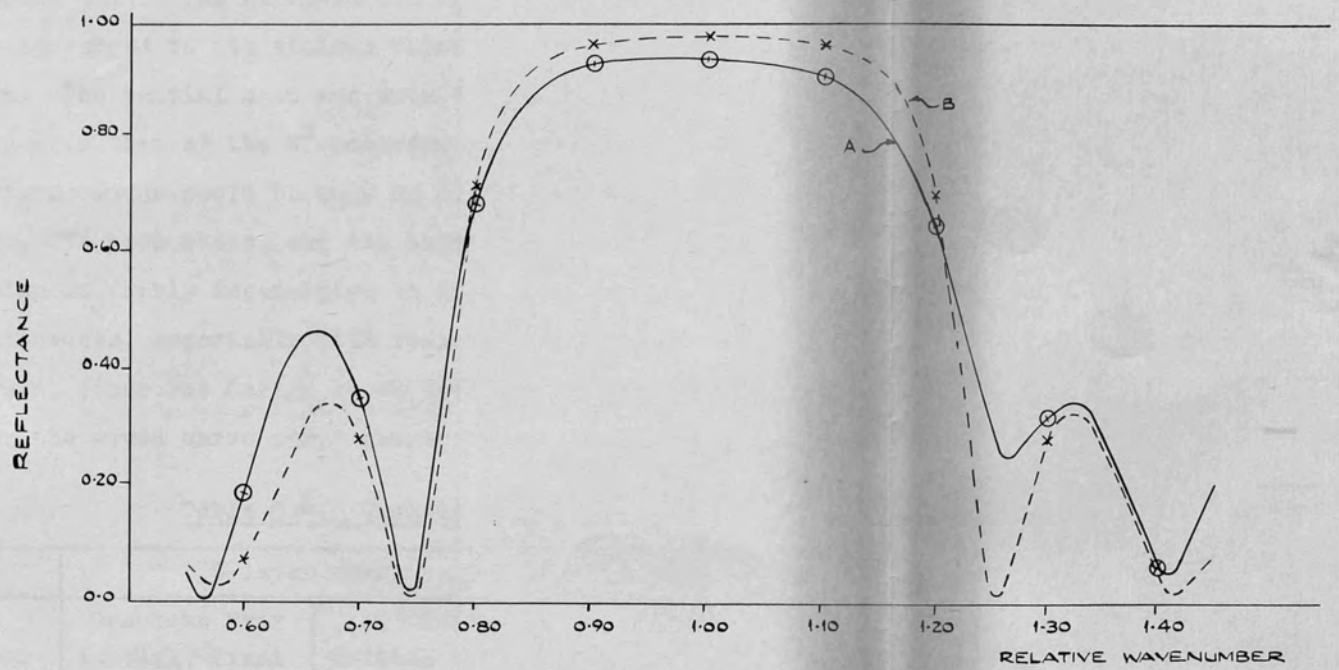
FIG. 5.7. NINE-LAYER CLASSICAL FILTER.

Again the curve obtained from the design method is reasonably close to the given curve, although from Table 5.4 it is seen that the thicknesses deviate considerably from the quarter-wave values. However, in this case, the system is fairly complex and in the minimisation subroutine the function had not converged to its minimum value because of time limitation. The initial scan was over the same range of thickness values as that of the N^2-scan for the five-layer filter, but an improvement could be made by decreasing the mesh of this scan. In both cases, one can easily see that this type of design is fairly insensitive to deviations in the layer thicknesses, especially with respect to the outermost layers, since the design curve does not differ markedly from the given curve for a quarter-wave stack.

Table 5.4. Classical stacks

| Layer | 5-layer stack | | | | 9-layer stack | |
| | Complete Scan | | N^2-Scan | | N^2-Scan | |
	Initial Thicknesses	Final Thicknesses	Initial Thicknesses	Final Thicknesses	Initial Thicknesses	Final Thicknesses
1	80	89.21	120	101.92	120	128.98
2	110	90.61	60	81.20	60	41.34
3	80	91.07	90	89.86	120	117.38
4	80	87.49	120	100.15	60	84.08
5	110	92.58	30	66.34	90	78.67

Table 5.4. continued

6			120	102.24
7			60	86.10
8			90	82.34
9			180	179.00
No. of design wavenos.	9	9	9	
Initial value of F	1.37×10^{-2}	8.38×10^{-2}	6.78×10^{-2}	
Final value of F	9.75×10^{-6}	2.06×10^{-3}	2.90×10^{-2}	
No. of iterations	12	24	24	

(5) High- and Low-Pass Filters

The next type of design to which this method was
applied - namely, the design of low- and high-pass filters -
was very much more complex than the designs given in the
previous examples. The criteria one must consider for this
type of filter are generally (1) very good rejection proper-
ties (R > 99.9%) in the stopping region; this is usually of
maximum importance, (2) steepness of cut-off, and (3) good
passing performance. The automatic least squares method
with the N^2-scan was used to design thirteen layers low- and
high-pass filters. The results are shown in Figs. 5.8 and
5.9 (Curves A). In the low-pass case, the rejection proper-
ties and steepness of cut-off are very reasonable, but the

passing properties are not particularly good. This is partly due to the high index of the substrate and an improvement could be made by the application of an anti-reflection coating. However, the latter would affect the steepness of cut-off. The design points around the point of cut-off give quite a large contribution to the function F if the steepness is reduced, and in this case this is greater than the effect of poor passing performances at one or two design points in the pass-band. The relative sensitivity of the method to passing performance and steepness of out-off may be altered by applying some kind of weighting procedure. The passing performance is better in the high-pass case (there are more design points in the pass-band) with a resultant lessening of the cut-off steepness.

An alternative way of approaching this design problem is to use a refining method. The initial approximate design was obtained by Seeley (1965) using a multilayer/circuit analogy method. The components of the electric filter whose performance corresponds to a Tschebyscheff response may be obtained (Microwave Engineers Handbook, p.92 (1964)). At the point of cut-off, the thicknesses of a multilayer with fixed refractive indices may be found approximately, using Seeley's method, so the multilayer/circuit analogy is established. The refined results for

fifteen layer filters are shown by Curves B of Figs. 5.8,
5.9. In both cases an antireflection coating was applied
in order to improve the passing performance of the filters.
In the low-pass case this was applied at $\sigma/\sigma_0 = 0.65$, in
the high-pass case at $\sigma/\sigma_0 = 1.70$. Much of the cut-off
steepness is lost by using this antireflection coating - the
effect is more apparent in the low-pass case. Thus, in the
latter case, the value of $F(\underline{x})$ is much larger than one would
perhaps expect for a minimum - most of the contribution to F
comes from the design points around cut-off. The refining
program has little effect on the low-pass design; obviously,
the approximation is good in this instance. However, the
multilayer-circuit approximation is only applicable over a
limited range and in the high-pass case this range of
applicability is much smaller than that for the low-pass
design. Thus, the initial approximation used for the high-
pass filter is not so well justified as that for the other
case, and the design is considerably changed by the refining
method.

The indices used were 2.2 and 5.1, corresponding
to ZnS and PbTe respectively, on a substrate of Germanium
(index 4.0). The filters were designed for Infra-red work.
The initial and final thicknesses for all the high- and
low-pass filters are shown in Table 5.5.
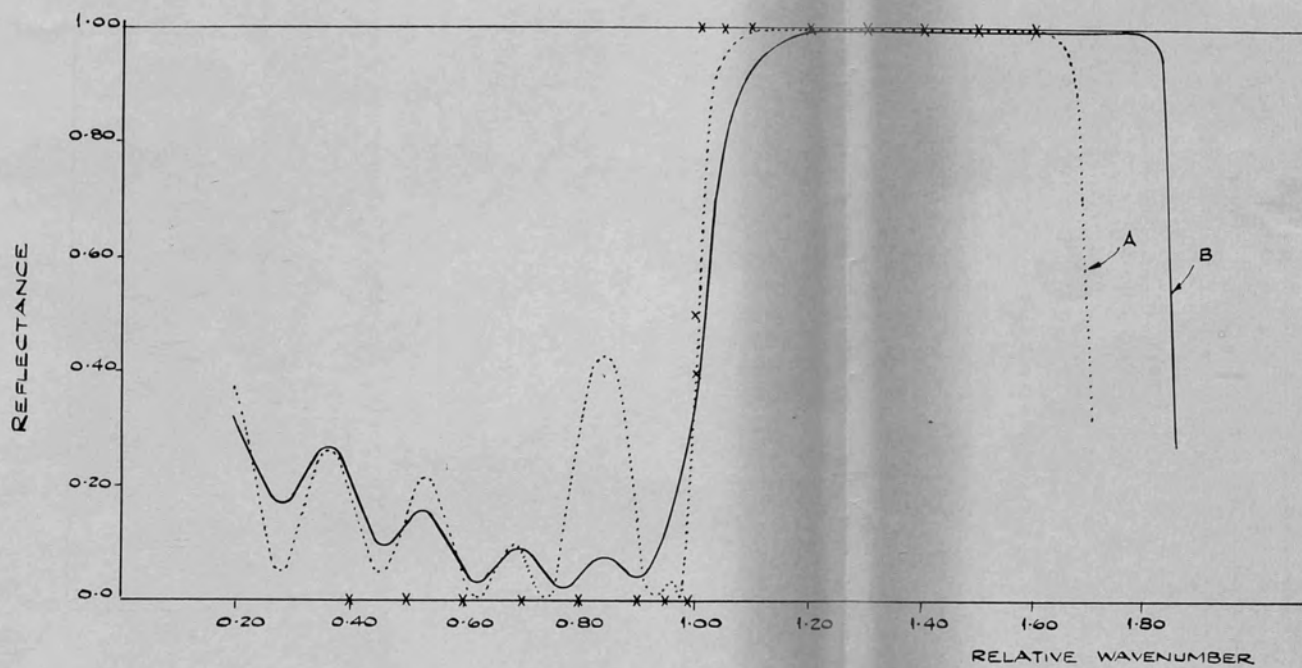
FIG. 5.8. LOW - PASS FILTERS
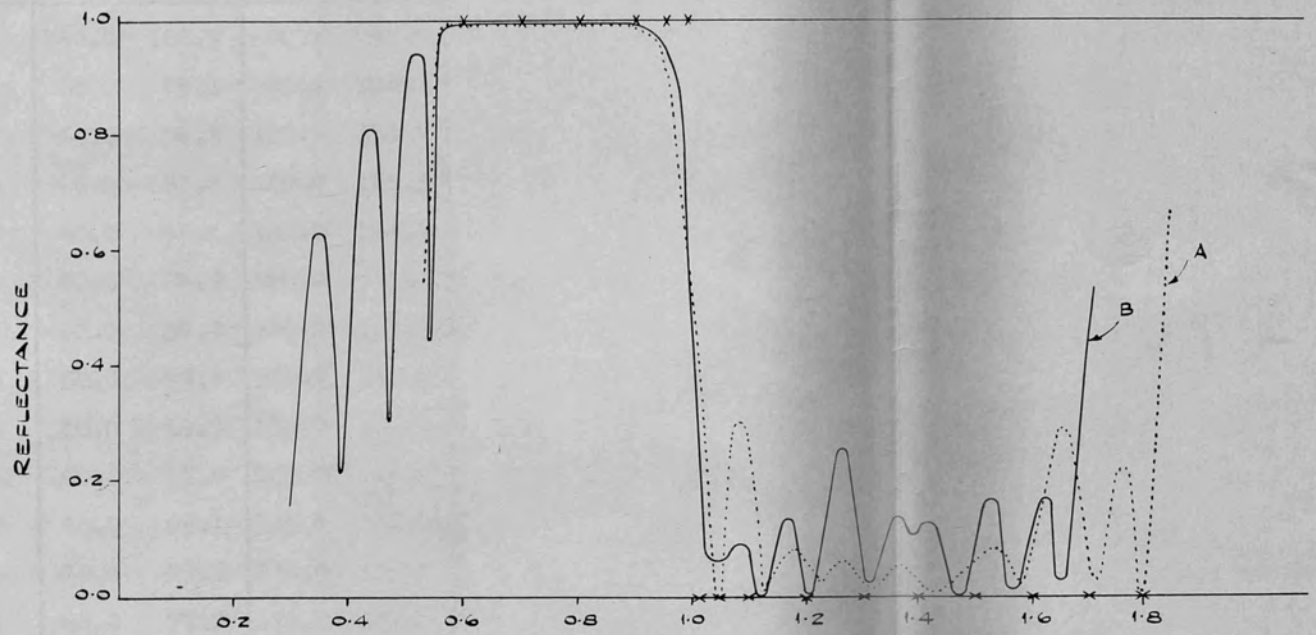
FIG. 5.9.   HIGH - PASS   FILTERS

Table 5.5. Low- and High-Pass Filters

Layer	N^2-scan method				Refined design			
	Low-Pass		High-pass		Low-pass		High-pass	
	Initial Thickness	Final Thickness	Initial Thickness	Final Thickness	Initial Thickness	Final Thickness	Initial Thickness	Final Thickness
1	160.0	162.7	60.0	54.5	128.0	127.9	58.0	56.2
2	60.0	55.1	100.0	102.5	36.0	36.1	144.0	137.2
3	60.0	58.9	120.0	119.8	53.1	52.8	126.9	133.8
4	60.0	63.8	120.0	109.3	58.5	58.9	121.5	131.6
5	60.0	55.1	120.0	118.5	62.4	61.9	117.6	115.4
6	80.0	94.9	120.0	113.9	62.6	62.0	117.4	117.6
7	60.0	50.8	120.0	125.5	64.4	65.3	115.6	116.5
8	80.0	79.5	120.0	114.1	64.0	64.2	116.0	114.9
9	60.0	60.7	120.0	113.9	64.4	64.0	115.6	115.8
10	60.0	57.4	120.0	124.7	63.0	63.1	117.0	113.9
11	60.0	69.1	120.0	128.9	63.4	63.9	116.6	120.6
12	60.0	47.5	120.0	130.1	61.3	60.1	118.7	109.2
13	60.0	71.2	120.0	130.0	58.6	59.8	121.4	116.8
14					52.2	51.6	127.8	130.9
15					35.4	35.4	144.6	135.2
No.design points	17		17		17		17	
Initial value of F	3.36x10^{-1}		6.75x10^{-1}		4.810x10^{-1}		4.27x10^{-1}	
Final value of F	2.96x10^{-1}		4.55x10^{-1}		4.730x10^{-1}		1.96x10^{-1}	
No.of iterations	46		49		152		122	

(6) Broad-band reflecting multilayers

The final design problem which was considered was
that of obtaining broad-band reflecting multilayers. In
Chapter III, a method for producing reflecting multilayers
with fixed indices was given. In this case, it was seen
that the bandwidth increased with increasing number of
layers. The least squares method was applied to the problem
of designing a broad-band reflector with fixed indices and a
fixed number of layers. Again, this is a fairly complex
problem for automatic design, as there are fifteen indepen-
dent variables in a fifteen-layer filter - the type con-
sidered here. The method was again applied in two ways;
(1) the N^2-scan method was used for automatic design, in
which the thicknesses were allowed to take the values 60°,
80°, 100°, 120°, 140°, 160°, 180° in the initial scan;
(2) a mismatched stack was fed in as the initial design for
the minimisation routine and the least squares program was
used to refine this design. The results are shown in Fig.
5.10. Curve A represents the automatic design, curve B
shows the performance of the refined design. The limiting
width of a classical stack with materials of the same
indices (2.36 and 1.39) is also shown. The thicknesses of
the designs are given in Table 5.6. These results show that
a marked improvement in bandwidth over that obtainable for a
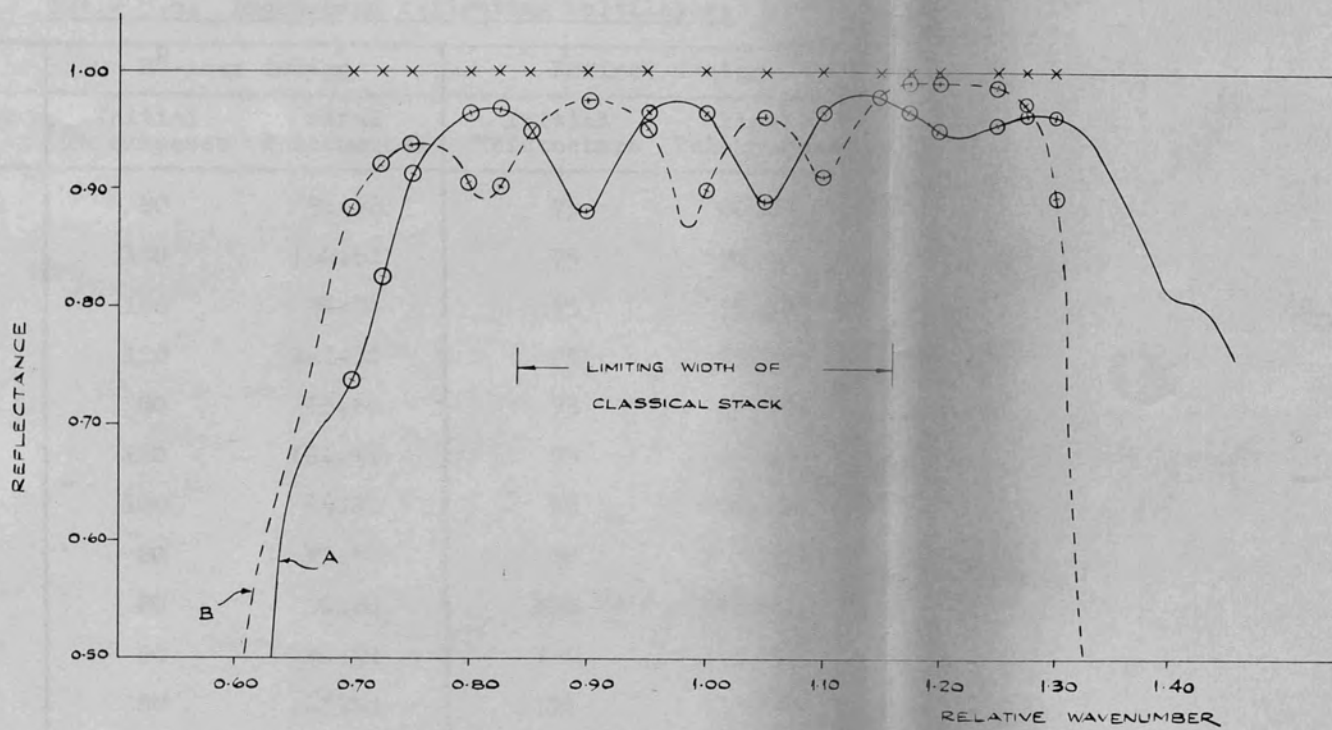
FIG. 5.10   BROAD-BAND REFLECTING MULTILAYERS

classical stack may be produced, using this method. The computing time on Atlas was 7 minutes for the automatic design and two minutes for the refined design.

Table 5.6. Broad-band reflecting multilayers

| Layer | N^2-scan design | | Refined design | |
	Initial Thicknesses	Final Thicknesses	Initial Thicknesses	Final Thicknesses
1	80	91.50	75	60.29
2	160	156.81	75	76.70
3	100	94.74	75	75.39
4	120	121.60	75	77.82
5	80	83.86	75	74.59
6	160	162.62	75	65.34
7	100	89.21	75	72.95
8	80	82.45	90	100.15
9	80	80.38	110	102.38
10	80	80.50	110	110.62
11	80	83.62	110	116.46
12	80	76.77	110	99.96
13	100	95.91	110	117.85
14	60	67.47	110	107.32
15	80	72.60	110	109.28

Table 5.6. continued

No. design points	17	15
Initial value F	8.91×10^{-2}	1.68×10^{-1}
Final value F	8.18×10^{-2}	1.39×10^{-1}
No. of iterations	65	132

CHAPTER VI. CONCLUSIONS AND SUGGESTIONS
FOR FUTURE WORK

§6.1. The Abelès Condition Work

The results reported in Chapter II show that even a small amount of absorption can cause a considerable change in the measurement of refractive index, using the Abelès method. For the film considered, it was found that values of K greater than 0.005 cause an error in measurement which is greater than the experimental inaccuracy, so a correction must be applied if absorption is present in the film. For a film whose index differs from that of the substrate by less than 0.03, the experimental error in measurement is much smaller than that for the film considered in this work, and it may well be that a value of K smaller than 0.005 will cause an error in measurement outside the expected experimental error.

Two methods for determining the error in the film measurement were outlined. The graphical method is suitable for use if only a discrete number of values of K are considered for several films, and if a digital computer is available. However if one wishes to obtain a general expression for the variation of θ_A with K for a particular

film, the power series method should be used. The results
from both methods were seen to be in very good agreement.

§6.2. Broad-band reflecting filters

The results in Chapter III show that really broad
reflectance bands may be obtained using two materials of
fixed indices and staggering the thicknesses of the layers.
The bandwidth of such filters is not limited by the ratio
of the refractive indices of the layer materials, as in the
case of classical stacks, but can be seen to increase with
increasing number of layers.

For materials of refractive indices 2.36 and 1.39,
symmetric staggered layers exhibit broad reflectance bands
over a range of σ/σ_0 which extends from 1.03 to 2.30 for
the 35-layer stacks. Throughout the range narrow-band
transmission peaks occur approaching 100% transmission in
value. Asymmetric filters exhibit considerably wider
reflectance bands than the symmetric systems and show only
slight variations in reflectance. Both the narrow band
transmission peaks in the symmetric filters and the fluc-
tuations in reflectance in the asymmetric case have been
explained by reducing the multilayers to two effective

interfaces and performing a Fabry-Perot-type of analysis.

These staggered stacks exhibit a very large dispersion of phase change on reflection. One result of this is that when the stacks are used as the reflecting elements of an interference filter, the transmission bands of the filters should be extremely narrow. Another consequence of the high dispersion of phase change is that the filters are stabilized so that the reflectance properties are not seriously modified by the presence of small errors in layer thickness.

Finally, a closed form expression was obtained for the matrix product of the layers in a staggered stack, if the difference in thicknesses of the layers is small. This expression has been checked numerically with the computed values for a nine-layer asymmetric arithmetic filter, using a common difference $K = 0.005$. It may well be possible to explain reflectance characteristics of the staggered stacks, using this expression, in a similar manner to that used for classical stacks.

§6.3. The least squares design method

In Chapter V a fairly simple method of general filter design has been developed. This method makes use of

a particularly suitable Fortran library subroutine and is
therefore economical on computing time. Many of the best
results obtained by other methods were produced by varying
the refractive indices of the materials in the filter. In
this work a more practical approach has been made in that
the indices of the materials are regarded as fixed and
instead the thicknesses of the layers have been allowed to
vary.

The method has been applied both to automatic
filter design and to the problem of 'refining' existing
designs. Results were given for several types of filter
including anti-reflection coatings, achromatic beam splitters,
low and high-pass filters and broad-band reflectance filters.
The method is also tested for the design of classical stacks
and double-half-wave transmission filters. The results show
that this type of design procedure can be very useful,
especially for the design of filters with only a few layers,
where a complete initial scan may be used to locate a suit-
able minimum. Filters with many layers present a more com-
plex problem, but the method can produce some useful results
in these cases too; striking examples are the designs
produced for broad-band reflectance filters. It may also
be used to check approximate designs and to refine them if
necessary. This was illustrated by the low- and high-pass

filter design examples. The least squares method was also shown to produce good results for the test filter designs, although the time limitation in the minimisation subroutine prevented the minimum being attained in one or two instances.

§6.4. Suggestions for Future Work

The results of the Abelès condition work reported in Chapter II show that absorption can have considerable effect on the performance of a single film. It may therefore be important to include the effect of even a small amount of absorption in a general multilayer system. Another phenomenon for which allowance should be made is that of dispersion of refractive index. Apart from analysing the result of absorption and dispersion, it may be possible to use these effects constructively in the design of a multilayer filter. Very little work has been done on this subject, although Baumeister (1962) has mentioned the possibility of allowing for absorption, and Seeley and Smith (to be published) have considered the use of semi-conductor absorption edges in Infra-red blocking filters.

It is seen from the results reported in Chapter V that design methods are generally most successful if a good approximation to the required design is known initially. In

order to provide more information about the initial approximation, much more analytic work needs to be done so that details of the general behaviour of any multilayer system may be obtained. A certain amount of analysis has been done for the classical stack, but there is still a lot to be learnt even about this fairly simple system. One way of tackling the problem is to consider the behaviour of the equivalent index of the filter; the formulae derived in Chapter I should extend the application of this concept to the case of a general multilayer system, rather than restricting its use to symmetric multilayers. Another method which may well prove extremely useful is one used by Electrical Engineers for the analysis of electrical filters; namely, the analysis of the behaviour of a system in terms of the poles and zeros of the insertion loss function in the complex frequency plane. This technique has proved to be very useful in electrical filter synthesis problems.

There are various ways in which improvements may be made in the least squares design method. A weighting procedure may be used in the summation $\sum f_K^2$. i.e. f_K may instead be represented by

$$f_k(\underline{x}) = \frac{\left[R'(\lambda_k) - R(\lambda_k, \underline{x}) \right]}{W_k} \qquad (6.4.1)$$

where W_K is the weighting for the point λ_K. This method could be employed to improve the fit to the desired curve at certain critical points. An initial scan of the type suggested by Dobrowolski, where more than one layer is added at a time, could be incorporated into the automatic design method before the minimisation subroutine is called. More than two materials may be used in the design; ideally, one might provide a list of the indices of available materials and program the computer to choose the best combination of materials. However, these refinements will obviously increase the complexity of the method and the amount of computing time required; the resulting improvement in design may not justify the additional expense.

One factor which is of great importance in the manufacture of filters, especially for designs containing unequal thicknesses of the layers, is the effect of monitoring errors on the performance of the system. If these are detected during manufacture, it may be possible to compensate for them in later layers. For this reason, from the practical point of view, there is an urgent need for an investigation to be made into a general analysis of errors and their correction.

APPENDIX

Example to illustrate the use of Tschebyscheff polynomials in multilayer calculations

The reflectance of several quarter-wave multilayer stacks was computed at $\lambda = \lambda_o$, the monitoring wavelength, for the cases of normal incidence and 10° angle of incidence. The high index material was CeO_2 ($n_H = 2.36$) and the low index material was MgF_2 ($n_L = 1.39$). The films were deposited on a substrate of index 1.53. The calculations for the 13-layer stack are shown below and the results for other stacks are also given. These agree with the results obtained by the computer.

a) Normal incidence

Using (1.4.16), $X = 2 - \dfrac{(2.36 + 1.39)^2}{2.36 \times 1.39} = 2.286824$

$$S_6(X) = X^6 - 5X^4 + 6X^2 - 1 = 36.65494$$

$$S_5(X) = X^5 - 4X^3 + 3X = -21.56463$$

$$(M_H M_L)^6 M_H = S_6(X)M_H - S_5(X)M_L^{-1}$$

Hence

$$\begin{pmatrix} E_o \\ H_o \end{pmatrix} = \begin{pmatrix} 0 & i\dfrac{36.65494}{2.36} - \dfrac{21.56463}{1.39} \\ i(2.36 \times 36.65494 - 1.39 \times 21.56463) & 0 \end{pmatrix}\begin{pmatrix} 1 \\ 1.53 \end{pmatrix} E_S^+$$

$$R = \left| \frac{n_o E_o - H_o}{n_o E_o + H_o} \right|^2 = 99.810$$

b) 10° angle of incidence

(i) S-component of polarisation

Using Snells law, $\theta_H = 4^\circ 13.177'$, $\theta_L = 7^\circ 10.592'$,

$\theta_S = 6^\circ 31.001'$

$\mu_H = 2.353603$, $\mu_L = 1.379097$, $\mu_S = 1.520115$, $\mu_o = 0.984808$

$$X = -2.292277$$

$$S_5(X) = -21.9875$$

$$S_4(X) = 12.846525$$

$$(M_H M_L) = \begin{pmatrix} -0.585850 & 0.008318i \\ 0.034847i & -1.706429 \end{pmatrix}$$

$$\begin{pmatrix} E_o \\ H_o \end{pmatrix} = \begin{pmatrix} -0.585850\, S_5(X) - S_4(X) & 0.008318\, S_5(X)i \\ 0.034847i\, S_5(X) & -1.706429\, S_5(X) - S_4(X) \end{pmatrix} M_H \begin{pmatrix} 1 \\ 1.520115 \end{pmatrix} E_S^+$$

$$= \begin{pmatrix} 0.430599 & 0.014029i \\ 58.068039i & 0.4316 \end{pmatrix} \begin{pmatrix} 1 \\ 1.520115 \end{pmatrix} E_S^+$$

$$R = 99.825\ \%$$

(ii) p-component of polarisation

$\mu_H = 2.366414$, $\mu_L = 1.400989$, $\mu_S = 1.539949$, $\mu_o = 1.015427$

$$X = -2.280834$$

$$S_5(X) = -21.107084$$

$$S_4(X) = 12.456312$$

$$(M_H M_L) = \begin{pmatrix} -0.591928 & 0.008246i \\ 0.035121i & -1.688906 \end{pmatrix}$$

$$\begin{pmatrix} \mu_o E_o \\ H_o \end{pmatrix} = \begin{pmatrix} 0.418384 & + & 0.023662i \\ 0.634468 & + & 54.877187i \end{pmatrix}$$

$$R = 99.7925\ \%$$

Other results:-

Table A.1

No.of layers	Normal incidence $R\%$	10° Angle of incidence	
		$R_S\ \%$	$R_p\ \%$
1	32.375	33.004	31.745
3	68.226	68.914	67.514
7	95.517	95.714	95.299
11	99.450	99.504	99.410
13	99.810	99.825	99.793
17	99.978	99.981	99.974

Program for Abelès condition work

TITLE

ABELES CONDITION MEASUREMENT OF REFRACTIVE INDEX

CHAPTER 0

U → 10

C → 10

D → 10

G → 10

H → 10

V → 10

X → 10

Y → 10

Z → 10

B → 10

F → 10

1) I = 0(1)2

    READ (UI)

    REPEAT

    READ (L)

    J = 1(1)L

    READ (BJ)

    REPEAT

```
READ (B)

READ (M)

I = 1(1)M

READ (A)

NEWLINE

NEWLINE

CAPTION

K =

PRINT (A)0,3


J = 1(1)L

DO = Ψ SIN (BJ π/180)

D2 = UODO/U2

D2 = 1 - D2D2

D  = 1/D2

D2 = D2 - 1

D2 = Ψ SQRT (D2)
F = Ψ  ARCTAN (I, D2)
CO = Ψ COS (BJ π/180)

C2 = Ψ COS (F)


E = U1U1 - UOUODODO

E = Ψ SQRT (E)

E = 1/E

E = 0.5 π E
```

G1 = U1U1 - UOUODODO - AA

G2 = G1G1 + 4U1U1AA

G2 = ψ SQRT (G2)

G3 = G1 + G2

G3 = 0.5 G3

G1 = G2 - G1

G1 = 0.5 G1

G2 = ψ SQRT (G1)

H1 = U1U1 - AA

H1 = H1C0

H2 = U0G4

H3 = H1 - H2

H4 = H1 + H2

H3 = H3H3

H4 = H4H4

H5 = 2U1AC0

H6 = U0G2

H7 = H5 - H6

H7 = H7H7

H8 = H5 + H6

H8 = H8H8

H7 = H3 + H7

H8 = H4 + H8

H = H7/H8

Hn = ψ SQRT (H)

V1 = U1U1 - AA

V1 = V1C2

V2 = U2G4

V3 = V1 - V2

V4 = V1 + V2

V3 = V3V3

V4 = V4V4

V5 = 2U1AC2

V6 = U2G2

V7 = V5 - V6

V8 = V5 + V6

V7 = V7V7

V8 = V8V8

V7 = V3 + V7

V8 = V4 + V8

V = V7/V8

Vn = γ SQRT (V)

X1 = 2U1AG4 - U1U1G2 + AAG2

X2 = 2UOCOX1

X3 = U1U1CO + AACO

X3 = X3X3 - UOUOG3 - UOUOG1

X = X2/X3

Xn = γ ARCTAN (1,X)

```
        Y1 = 2U2C2X1

        Y2 = U1U1C2 + AAC2

        Y2 = Y2Y2 - U2U2G3 - U2U2G1

        Y  = Y1/Y2

        Yn = Ɣ ARCTAN (1,Y)


        Z1 = Yn - Xn + 2G4E

        Z1 = Ɣ COS (Z1)

        Z1 = 2HnVnZ1

        Z2 = Yn + Xn + 2G4E

        Z2 = Ɣ COS (Z2)

        Z2 = 2HnVnZ2

        Z3 = Ɣ EXP (2G2E)

        Z4 = 1/Z3

        D  = B - BJ

        JUMP 3, D > 0

        JUMP 4

3)      FJ = -1.0

        JUMP 5

4)      FJ = +1.0

        JUMP 5

5)      Z5 = HZ3 + VZ4 + FJZ1

        Z6 = Z3 + HVZ4 + FJZ2

        Z  = Z5/Z6
```

```
NEWLINE

NEWLINE

CAPTION

ANG. OF INC. =

PRINT (BJ) 0,6

NEWLINE

NEWLINE

PRINT (Z) 0,6

REPEAT

REPEAT

PSA

γ SIN

γ SQRT

γ EXP

γ ARCTAN

PSA

CLOSE
```

Program for computing reflectance and phase
of staggered multilayers

TITLE

MULTILAYER OPTICAL FILTER CALCULATIONS

ROUTINE 50

AO = XOYO - X1Y2

A1 = XOY1 + X1Y3

A2 = X2YO + X3Y2

A3 = X3Y3 - X2Y1

T = 1(1)4

X(T-1) = A(T-1)

REPEAT

RETURN

※ ※

CHAPTER O

A $\rightarrow$ 3

X $\rightarrow$ 3

Y $\rightarrow$ 3

C $\rightarrow$ 50

W $\rightarrow$ 200

U $\rightarrow$ 3

```
B → 3
H → 1
V → 1
D → 2


READ (U0)

READ (U1)

READ (U2)

READ (U3)

9)  READ (N)

    READ (Q)

10) NEWLINE

    PRINT (N) 2,0

    READ (L)

    READ (Z)

    Ln = L + 4

    S) = Ln)

    JUMP (S)


11) NEWLINE

    NEWLINE

    CAPTION

    K =

    PRINT (Z) 0,3

    READ (P)
```

```
        In = 1(1)P
        I = In - 1
        READ (WI)
        Sn) = L)
        JUMP (Sn)


12) X0 = ᵧ COS (CO)
        X3 = ᵧ SIN (CO)
        X2 = X3U2
        X1 = X3/U2
        X3 = XO
        Nn = N - 1
        J = 2(2)Nn
        Jn = J - 1
        YO = ᵧ COS (CJn)
        Y3 = ᵧ SIN (CJn)
        Y1 = Y3/U3
        Y2 = Y3U3
        Y3 = YO
        JUMPDOWN (R50)
        YO = ᵧ COS (CJ)
        Y3 = ᵧ SIN (CJ)
        Y1 = Y3/U2
        Y2 = Y3U2
        Y3 = YO
```

```
JUMPDOWN (R50)

REPEAT

NEWLINE

NEWLINE

PRINT (X0) 0,6

PRINT (X1) 0,6

PRINT (X2) 0,6

PRINT (X3) 0,6

B0 = X0U0 - U1X3

B0 = B0B0

B1 = X0U0 + U1X3

B1 = B1B1

B2 = X1U1U0 - X2

B2 = B2B2

B3 = X1U1U0 + X2

B3 = B3B3

B0 = B0 + B2

B1 = B1 + B3

B  = B0/B1

NEWLINE

NEWLINE

PRINT (WI) 0,3

PRINT (B) 0,6

V0 = U1U1X3X1 - X0X2

V0 = 2U0V0
```

```
.V1 = UOUOU1U1X1X1 + UOUOXOXO - U1U1X3X3 - X2X2

V  = ɣ ARCTAN (V1, VO)

V  = 180V/π

PRINT (V) 0,6

REPEAT


Q = Q - 1

JUMP 10, Q > 0

JUMP 9


1)  CO = 0.5π WI

    K = 2(1)N

    C(K-1) = ZC(K-2)

    REPEAT

    JUMP 12


2)  CO = 0.5π WI

    K = 2(1)N

    C(K-1) = CO + KZCO - ZCO

    REPEAT

    JUMP 12


3)  Vn = 0.5N + 1.5

    R = ɣ INTPT (Vn + 0.01)

    C(R-2) = 0.5π WI
```

K = 3(1)R

Tn = R - K

Rn = R + K

CTn = C(R-2) + KZC(R-2) - 2ZC(R-2)

C(Rn-4) = CTn

REPEAT

JUMP 12

4) Vn = 0.5N + 1.5

R = γ INTPT (Vn + 0.01)

C(R-2) = 0.5πWI

K = 3(1)R

Tn = R - K

Rn = R + K

CTn = ZC(Tn+1)

C(Rn-4) = CTn

REPEAT

JUMP 12

5) CAPTION

-LAYER ASYMMETRIC GEOMETRIC FILTER. REFLECTANCE AND PHASE.

JUMP 11

6) CAPTION

-LAYER ASYMMETRIC ARITHMETIC FILTER. REFLECTANCE AND PHASE.

JUMP 11

7) CAPTION

   -LAYER SYMMETRIC ARITHMETIC FILTER. REFLECTANCE AND PHASE.

   JUMP 11

8) CAPTION

   -LAYER SYMMETRIC GEOMETRIC FILTER. REFLECTANCE AND PHASE.

   JUMP 11

   PSA

   γ COS

   γ SQRT

   γ ARCTAN

   PSA

   CLOSE

12 -LAYER ASYMMETRIC GEOMETRIC FILTER, REFLECTANCE AND PHASE.

K= 9.500, -1

```
1.044670        -4.884423,  -1  -1.814714         1.087588,  -1
8.000,  -1  3.882874,  -1  6.474931,   1
1.254244        -3.236579,  -1  -1.586750         3.878319,  -1
8.200,  -1  4.358562,  -1  5.281437,   1
1.351238     *  -1.118189,  -1  -1.236517         6.377369,  -1
8.400,  -1  4.412395,  -1  4.227890,   1
1.316277         1.326966,  -1  -7.934081,  -1  8.397034,  -1
8.600,  -1  4.026255,  -1  3.295969,   1
1.139536         3.918652,  -1  -2.946637,  -1  9.788794,  -1
8.800,  -1  3.185421,  -1  2.573996,   1
8.220809,  -1  6.451470,  -1  2.176953,  -1  1.045584
9.000,  -1  2.095667,  -1  2.533164,   1
3.764475,  -1  8.708365,  -1  7.003982,  -1  1.036181
9.200,  -1  1.643986,  -1  4.115654,   1
-1.736295,  -1  1.047543         1.112658         9.535038,  -1
9.400,  -1  2.819579,  -1  5.370308,   1
-7.943437,  -1  1.155699         1.419808         8.067919,  -1
9.600,  -1  4.852798,  -1  4.956402,   1
-1.443748         1.178992         1.596557         6.111367,  -1
9.800,  -1  6.502883,  -1  4.099871,   1
-2.074378         1.105616         1.629580         3.864723,  -1
1.000    7.535205,  -1  3.272321,   1
-2.636400         9.292509,  -1  1.519233         1.561784,  -1
```
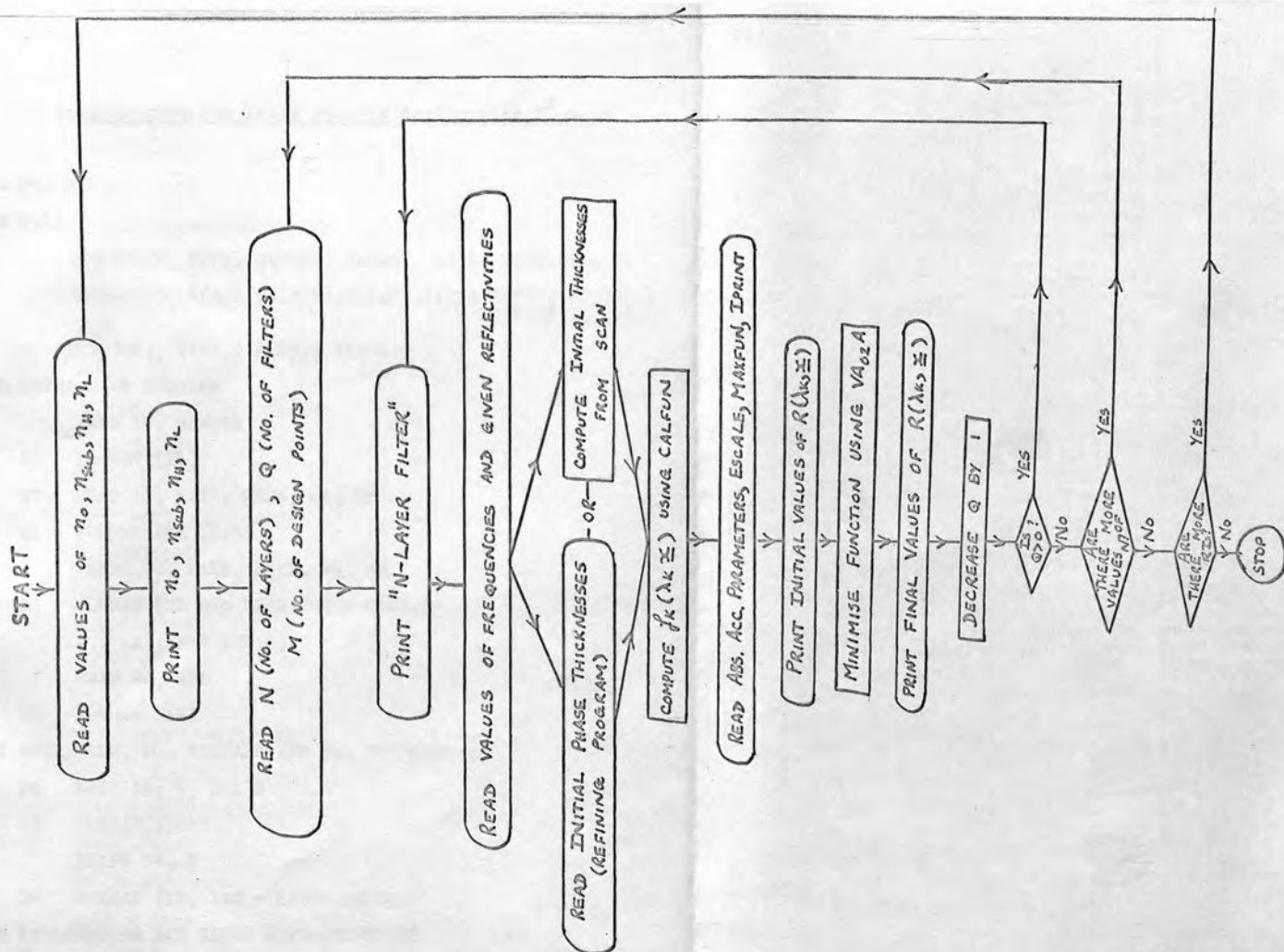
FIG A.1   FLOW DIAGRAM   FOR LEAST   SQUARES   DESIGN   PROGRAM

The flow diagram shows the following sequence of boxes:

START

READ VALUES OF n_0, n_{sub}, n_H, n_L

PRINT n_0, n_{sub}, n_H, n_L

READ N (No. OF LAYERS), Q (No. OF FILTERS) M (No. OF DESIGN POINTS)

PRINT "N-LAYER FILTER"

READ VALUES OF FREQUENCIES AND GIVEN REFLECTIVITIES

READ INITIAL PHASE THICKNESSES (REFINING PROGRAM) — OR — COMPUTE INITIAL THICKNESSES FROM SCAN

COMPUTE $f_k(\lambda_k, \Sigma)$ USING CALFUN

READ ASS. ACC. PARAMETERS, ESCALE, MAXFUN, IPRINT

PRINT INITIAL VALUES OF $R(\lambda_k, \Sigma)$

MINIMISE FUNCTION USING VA05A

PRINT FINAL VALUES OF $R(\lambda_k, \Sigma)$

DECREASE Q BY 1

IS Q > 0 ?   YES / No

ARE THERE MORE VALUES OF Q?   YES / No

ARE THERE MORE R'S?   YES / No

STOP

Main Program for least squares design with N^2-scan

```
⋇ FORTRAN
C MAIN
      COMMON W, FREQ, GIVREF, CALREF, RAIR, RSUB, RA, RB
      DIMENSION A(2,2),B(2,2),C(2,2),X(25),F(25),FREQ(25),
                                  GIVREF(25),CAL
      1REF(25), Y(25), E(25), W(1000)
C REFRACTIVE INDICES
      READ 10, NSETSR
10    FORMAT (I4)
27    READ 11, RAIR, RSUB, RA, RB
11    FORMAT (4E 12.4)
      PRINT 12, RAIR, RSUB, RA, RB
12    FORMAT (22 H④ REFRACTIVE INDICES,/40 H⑤ RAIR ⑥RSUB.⑦RA
      1. ⑦ RB., /4E 12E.4)
      READ 28, NDL
28    FORMAT (I4)
C NO.LAYERS, NO. FILTERS AND NO. FREQUENCIES
26    READ 13, N, IQ, M
13    FORMAT (3I4)
      PRINT 14, N
14    FORMAT (I4, 13H - LAYER FILTER)
C FREQUENCIES AND GIVEN REFLECTIVITIES
17    READ 15, (FREQ (I), GIVREF (I), I = 1,M)
```

```
15    FORMAT ((6E 12.6))

      READ 31, IXIN, IXINC, IXMAX, IXBEG

31    FORMAT (4I6)

C ABSOLUTE ACCURACY PARAMETERS

      READ 19, (E(I), I = 1,N)

19    FORMAT ((6E 12.6))

      READ 21, ESCALE

21    FORMAT (E 12.6)

      READ 22, IPRINT, MAXFUN

22    FORMAT (2I4)

      DO 71 I = 1,N

      X(I) = FLOATF (IXBEG)

      Y(I) = X(I)

71    CONTINUE

      TRSUM = 10.0

      DO 76 J = 1,N

      DO 72 I = J,N

      DO 73 ITH = IXIN, IXMAX, IXINC

      X(I) = FLOATF (ITH)

      CALL CALFUN (M,N,F,X)

      RSUM = 0.0

      DO 74 IK = 1,M

      RSUM = RSUM + F(IK) + F(IK)

74    CONTINUE

      IF (RSUM - TRSUM) 75, 73, 73
```

```
 75    Y(I) = FLOATF (ITH)

       TRSUM = RSUM

 73    CONTINUE

       X(I) = Y(I)

 72    CONTINUE

       IF (J-2) 76, 79, 79

 79    JM1 = J - 1

       DO 77 I = 1, JM1

       DO 78 ITH = IXIN, IXMAX, IXINC

       X(I) = FLOATF (ITH)

       CALL CALFUN (M, N, F, X)

       RSUM = 0.0

       DO 81 IK = 1,M

       RSUM = RSUM + F(IK) * F(IK)

 81    CONTINUE

       IF (RSUM - TRSUM) 82, 82, 78

 82    Y(I) = FLOATF (ITH)

       TRSUM = RSUM

 78    CONTINUE

       X(I) = Y(I)

 77    CONTINUE

 76    CONTINUE

C CALCULATION OF REFLECTIVITIES

       CALL CALFUN (M, N, F, X)

       PRINT 20, (FREQ(K), GIVREF(K), CALREF(K), K = 1,M)
```

```
20      FORMAT (51 H 5 FREQ 16   GIVREF 14   CALREF, /(3E
        120.6))
        CALL VAO2A (M, N, F, X, E, ESCALE, IPRINT, MAXFUN)
        CALL CALFUN (M, N, F, X)
        PRINT 23, (FREQ(K), GIVREF(K), CALREF(K), K = 1,M)
23      FORMAT (14 H FINAL VALUES, /(3E20.6))
        IQ = IQ - 1
        IF(IQ) 18, 18, 17
18      NDL = NDL - 1
        IF (NDL) 24, 24, 26
24      NSETSR = NSETSR - 1
        IF (NSETSR) 25, 25, 27
25      CONTINUE
        END
```

REFRACTIVE INDICES
```
 RAIR.      RSUB.       RA.       RB.
1.0000E+00  1.0800E+00  4.0000E+00  1.3500E+00
```
3-LAYER FILTER

FREQ	GIVREF	CALREF
1.200000E+00	8.300000E-01	6.754059E-01
1.100000E+00	2.000000E-01	1.178465E-01
1.060000E+00	0.000000E+00	2.256116E-01
1.000000E+00	9.000000E-02	3.217640E-01
9.400000E-01	0.000000E+00	1.636004E-01
9.000000E-01	2.000000E-01	2.028339E-01
8.000000E-01	8.300000E-01	8.511296E-01
6.000000E-01	9.600000E-01	9.682816E-01
4.000000E-01	8.300000E-01	8.895888E-01
3.000000E-01	3.000000E-02	2.200142E-01

```
 ITERATION    0      4 CALLS OF CALFUN    F =   2.02208028799034E-01
 VARIABLES
1.80000000000000E+02   1.20000000000000E+02   1.60000000000000E+02
 FUNCTIONS
1.54594083756992E-01   8.21535126054478E-02  -2.25611565254059E-01  -2.31763957335335E-01  -1.63600375415802E-
-2.83386883166598E-03  -2.11296338493604E-02  -8.28162528345001E-03  -5.95888035496132E-02  -1.90014215890314E-
```

VA02A FINAL VALUES OF FUNCTIONS AND VARIABLES

```
 ITERATION    2     11 CALLS OF CALFUN    F =   3.93736224012559E-03
 VARIABLES
1.82535712501406E+02   9.29325018050149E+01   1.75513501720875E+02
 FUNCTIONS
-1.09516188967740E-03   3.41710497669138E-02  -3.04492630660028E-02  -2.68848466917251E-02  -2.32764834384154E-
1.65822617418749E-02  -1.31862993221543E-02  -1.57847197987840E-03  -9.44153446474073E-03   6.02253211540056E-
```
FINAL VALUES.

1.200000E+00	8.300000E-01	8.310952E-01
1.100000E+00	2.000000E-01	1.658290E-01
1.060000E+00	0.000000E+00	3.044926E-02
1.000000E+00	9.000000E-02	1.168848E-01
9.400000E-01	0.000000E+00	2.327648E-02
9.000000E-01	2.000000E-01	1.834177E-01
8.000000E-01	8.300000E-01	8.431863E-01
6.000000E-01	9.600000E-01	9.615785E-01
4.000000E-01	8.300000E-01	8.594415E-01
3.000000E-01	3.000000E-02	2.397747E-02

REFRACTIVE INDICES
```
 RAIR.      RSUB.       RA.       RB.
1.0000E+00  1.5300E+00  2.3600E+00  1.3900E+00
```

BIBLIOGRAPHY

Abelès F., "Sur la propagation des ondes électromagnétiques dans les milieux stratifiés". Ann. de Physique, 3, 504 (1948a).

Abelès F., "Transmission de la lumière à travers un système des lames minces alternées". Compt. Rend., 226, 1808 (1948b).

Abelès F., "Sur la determination des indices et des epaisseurs des couches minces". Compt. Rend., 228, 553 (1949).

Abelès F., "La determination de l'indice et de l'epaisseur des couches minces transparentes". J.de Physique et le Rad., 11, 310 (1950).

Abelès F., "Methods for determining optical parameters of thin films". 'Progress in Optics' Vol.II, 251 (1963).

Baumeister P.W., "Design of multilayer filters by successive approximations". J.Opt.Soc.Amer., 48, 955 (1958).

Baumeister P.W., "Methods of altering the characteristics of a multilayer stack". J.Opt.Soc.Amer., 52, 1149 (1962).

Baumeister P.W., "Notes on multilayer optical filters". Summer course on modern methods of optical design, Institute of Optics, University of Rochester (1963).

Baumeister P.W. and Jenkins F.A., "Dispersion of the phase change for dielectric multilayers. Application to the interference filter". J.Opt.Soc.Amer., 47, 57 (1959).

Baumeister P.W., Jenkins F.A. and Jeppesen M.A., "Characteristics of the phase-dispersion interference filter". J.Opt.Soc.Amer., 49, 1188 (1959).

Baumeister P.W. and Stone J.M., "Broad-band multilayer film for Fabry-Perot interferometers". J.Opt.Soc.Amer., 46, 228 (1956).

Berning P.H., "Use of equivalent films in the design of infrared multilayer antireflection coatings". J.Opt. Soc.Amer., 52, 431 (1962).

Berning P.H., "Theory and calculations of Optical Thin Films". 'Physics of Thin Films' Vol.I, pp.69-121. (Academic Press, 1963.)

Born M. and Wolf E., "Principles of Optics". (Pergamon, 1959.)

Brune O., "Synthesis of a finite two-terminal network whose driving-point impedance is a prescribed function of frequency". J.Maths. and Physics, 10, 191 (1931).

Catalan L., "Conditions d'égalité des facteurs de réflexion d'une couche mince et son support mi en incidence oblique". Rev.d'Optique, 43, 499 (1964).

Chen J.C., Seeley J.S. and Williams J.C., "Filter synthesis at microwave and optical frequencies under practical constraints". From a summary of a colloquium on 'Microwave Circuit Synthesis', I.E.E., London (1964).

Crook A.W., "Reflection and transmission of light by any system of parallel isotropic films". J.Opt.Soc.Amer., 38, 954 (1948).

Darlington S., "Synthesis of reactance 4-poles which produce prescribed insertion loss characteristics". J.Maths. and Physics, 18, 257 (1939).

Ditchburn R.W., "Light", (Blackie, 1963).

Dobrowolski J.A., "Completely automatic synthesis of optical thin film systems". Applied Optics, 4, 937 (1965).

Elsner Z.N., "On the calculation of multilayer interference coatings with given spectral characteristics". Optika i Spektroskopiya, 17, 446 (1964).

Epstein L.I., "The design of optical filters". J.Opt.Soc. Amer., 42, 806 (1952).

Giacomo P., Baumeister P.W. and Jenkins F.A., "On the limiting band width of interference filters". Proc. Phys.Soc., 73, 480 (1959).

Heavens O.S., "Optical properties of thin solid films". (Butterworth Scientific publications, 1955.)

Heavens O.S., "Optical properties of thin films". Repts on prog.in Physics, 23, 1 (1960).

Heavens O.S., "Measurement of optical constants of thin films". 'Physics of Thin Films' Vol.II, 193 (Academic Press, 1964).

Heavens O.S. and Liddell H.M., "Influence of absorption on measurement of refractive index of films". Applied Optics, $\underline{4}$, 629 (1965).

Heavens O.S. and Liddell H.M., "Staggered broad-band reflecting multilayers". (to be published)

Herpin A., "Calcul du pouvoir réflecteur d'un système stratifié quelconque". Compt.Rend., $\underline{225}$, 182 (1947a).

Herpin A., "Sur une nouvelle méthode d'introduction des polynomes de Lucas". Compt.Rend., $\underline{225}$, 17 (1947b).

Jenkins F.A., "Extension du domaine spectral de pouvoir réflecteur élevé des couches multiples dielectriques". J.de Phys.et le Rad., $\underline{19}$, 301 (1958).

Kard P.G., "A graphical method of calculation for multilayer films". Soviet Physics Doklady, $\underline{1}$, 256 (1956).

Lockhart L.B. and King P., "Experimental and theoretical results in two-layer low reflecting coatings for glass". J.Opt.Soc.Amer., $\underline{36}$, 513 (1946).

The Microwave Engineers Handbook p.92 (Horizon House, 1964).

Mielenz K.D., "Use of Tschebyscheff polynomials in thin film computations". Jour.Res.of N.B.S., $\underline{63A}$, 297 (1959).

Mooney R.L., "An exact theoretical treatment of reflection-reducing coatings". J.Opt.Soc.Amer., $\underline{35}$, 574 (1945).

Penselin S. and Steudel A., "Fabry-Perot-Interferometerver-
spiegelunglen aus dielektrischen vielfachachichten".
Z.fur Physik, 142, 21 (1955).

Pohlack H., "Synthesis of system of thin films with given
spectral transmissivity". 'Optics of Thin Films' by
Vasicek, p.275, (North Holland, 1960).

Potter J.I. and Fich S., "Theory of networks and lines".
(Prentice Hall Electrical Engineering Series, 1963.)

Powell M.J.D., "An efficient method for finding the minimum
of a function of several variables without calculating
derivatives". Computer Journal 7, 155 (1964).

Powell M.J.D., "A method for minimising a sum of squares of
non-linear functions without calculating derivatives".
Computer Journal 7, 303 (1965).

Richards P.I., "Resistor-Transmission-Line Circuits".
Proc.I.R.E., 36, 217 (1948).

Rouard P., "Etude des propriétés optiques des lames
metalliques très minces". Ann.de Physique, 7, 291 (1937).

Seeley J.S., "Synthesis of Interference filters". Proc.
Phys.Soc., 78, 998 (1961).

Seeley J.S., "LC ladder used as broadband prototype for dis-
tributed components". Electronics letters, 1, 265 (1965).

Seeley J.S. and Smith S.D., "High performance blocking
filters for the region 1 to 20 microns". Applied Optics,

Shatilov A.V. and Tyutikova L.P., "Example of the calculation
of an interference filter using the method of successive
synthesis". Optika i Spektroskopiya, 14, 426 (1963).

Smith S.D., "Design of multilayer filters by considering two
effective interfaces". J.Opt.Soc.Amer., 48, 43 (1958).

Traub A.C. and Osterberg H., "Brewster angle apparatus for
thin film index measurements". J.Opt.Soc.Amer., 47,
62 (1951).

Turner A.F., "Some current developments in multilayer optical
films". J.de Phys.et le Rad., 11, 444 (1950).

Van Valkenburg M.E., "Introduction to modern network syn-
thesis". (John Wiley, 1960)

Vašíček A., "Sur la réflexion de la lumière sur des verres
supportant des couches minces multiples". J.de Phys.et
le Rad., 11, 342 (1950).

Vašíček A., "On achromatising of two and three thin films".
Czech J.of Phys., 2, 72 (1952).

Vašíček A., "Optics of Thin Films". (North Holland, 1960.)

Weinstein W. (now Welford W.), "Computations in thin film
optics". Vacuum 4, 3 (1954).

Young L., "Synthesis of multiple antireflection films over
a prescribed frequency band". J.Opt.Soc.Amer., 51,
967 (1961).

Influence of Absorption on Measurement of Refractive Index of Films

O. S. Heavens and H. M. Liddell

Royal Holloway College, University of London, London, England.

One of the simplest methods of determining refractive indices of thin films is the now classic method due to Abelès.[1] Light polarized with the electric vector in the plane of incidence is directed onto a surface (refractive index n_2) partly covered with a film (index n). At an angle of incidence $\theta_B = \arctan(n/n_0)$, the reflectance of the filmed and uncoated parts of the substrate are equal. n/n_0 is the refractive index of the medium of incidence. The angle θ_B is readily determined experimentally. The condition is independent of film thickness, but the sensitivity of detection is greatest for films whose phase thickness (in the direction of the beams) is in the neighborhood of $\pi/2$.

If the material of the film shows absorption at the wavelength used, the results given above no longer apply. It is important, therefore, to determine the extent to which the presence of absorption may introduce errors in the measurement of refractive index by this method. This note gives expressions enabling this determination to be made and illustrate the results by considering typical slightly absorbing films.

The reflectance of the substrate for the p component is simply given by

$$R_p = \frac{\tan^2(\theta_2 - \theta_0)}{\tan^2(\theta_2 + \theta_0)}, \tag{1}$$

where θ_0 is the angle of incidence and θ_2 is the angle of refraction. With the help of Snell's law, the value of R_p may be determined readily for any value of θ_0, given the values of n_0 and n_2. For the case of an absorbing film of index $n - ik$, the expression for the reflectance R_f is cumbersome, but may be written[2]

$$R_f = \frac{l^2 e^{2v\eta} + m^2 e^{-2v\eta} + 2lm \cos(\phi_{12} - \phi_{01} + 2u\eta)}{e^{2v\eta} + l^2 m^2 e^{-2v\eta} + 2lm \cos(\phi_{12} + \phi_{01} + 2u\eta)}, \tag{2}$$

where

$$l^2 = \frac{[(n^2 - k^2)\cos\theta_0 - n_0 u]^2 + [2nk\cos\theta_0 - n_0 v]^2}{[(n^2 - k^2)\cos\theta_0 + n_0 u]^2 + [2nk\cos\theta_0 + n_0 v]^2}, \tag{3}$$

$$m^2 = \frac{[(n^2 - k^2)(n_2^2 - n_0^2\sin^2\theta_0)^{1/2} - n_2^2 u]^2 + [2nk(n_2^2 - n_0^2\sin^2\theta_0)^{1/2} - n_2^2 v]^2}{[(n^2 - k^2)(n_2^2 - n_0^2\sin^2\theta_0)^{1/2} + n_2^2 u]^2 + [2nk(n_2^2 - n_0^2\sin^2\theta_0)^{1/2} + n_2^2 v]^2}, \tag{4}$$

$$\eta = \frac{\pi}{2(n^2 - n_0^2\sin^2\theta_0)^{1/2}}, \tag{5}$$

$$\tan\phi_{01} = \frac{2n_0\cos\theta_0[2nku - (n^2 - k^2)v]}{(n^2 + k^2)^2\cos^2\theta_0 - n_0^2(u^2 + v^2)}, \tag{6}$$

$$\tan\phi_{12} = \frac{2n_2^2(n_2^2 - n_0^2\sin^2\theta_0)^{1/2}[2nku - (n^2 - k^2)v]}{(n^2 + k^2)^2(n_2^2 - n_0^2\sin^2\theta_0) - n_2^4(u^2 + v^2)}, \tag{7}$$

and u, v are obtained from the relations

$$\left. \begin{array}{l} u^2 - v^2 = n^2 - k^2 - n_0^2\sin^2\theta_0 \\ uv = nk \end{array} \right\} \tag{8}$$

For values of $k \ll 1$, these expressions may be conveniently expanded as a power series in k.

At the Abelès angle θ_B, $R_f = R_p$. Hence, for variation of k and θ_0 to preserve equality of reflectance

$$\frac{\partial\theta_0}{\partial k} = -\frac{\partial R_f}{\partial k} \bigg/ \left(\frac{\partial R_f}{\partial\theta_0} - \frac{\partial R_p}{\partial\theta_0}\right) \tag{9}$$

which also may be expressed, with the help of Eqs. (1) to (8) as a power series in k. For values of k up to 0.05 it is unnecessary to include terms of the order of (k^4).

We may illustrate these results by considering a film of index $n = 2.30$ on a substrate of index $n_2 = 1.46$. This corresponds to cerium dioxide deposited on quartz at 50°C for a wavelength of 0.440 μm. The change in the Abelès angle corresponding to values of k of 0.005, 0.01, 0.02, 0.03, and 0.05 are given in Table I, which also gives the error in the derived refractive index if the effect of absorption is neglected.

Table I. Error in Derived Refractive Index if Absorption is Ignored

K	Change in θ_B (min.)	Error in derived refractive index
0.005	−1.82	−0.004
0.01	−3.59	−0.007
0.02	−6.95	−0.013
0.03	−10.1	−0.020
0.05	−15.7	−0.029

References

1. P. Abelès, J. Phys. Rad. **11**, 310 (1950).
2. M. Born and E. Wolf, *Principles of Optics* (Pergamon, New York, 1959).